MECHANICS OF HYDROGEN - DISLOCATION - IMPURITY INTERACTIONS: PART I - INCREASING SHEAR MODULUS

P. Sofronis and H. K. Birnbaum*
Department of Theoretical and Applied Mechanics
*Department of Materials Science and Engineering
University of Illinois at Urbana-Champaign

October 1993

ABSTRACT

The effect of hydrogen on dislocation-dislocation and dislocation-impurity atom interactions is studied under conditions where hydrogen is in equilibrium with local stresses and in systems where hydrogen increases the shear modulus. In the case of two edge dislocations (plane strain) the effect of hydrogen is modeled through a continuous distribution of dilatation lines whose strength depends on the local hydrogen concentration. The hydrogen distribution in the atmospheres is adjusted to minimize the energy of the system as the dislocations approach each other. The iterative finite element analysis used to calculate the hydrogen distribution accounts for the stress relaxation associated with the hydrogen induced volume and the elastic moduli changes due to hydrogen. The interactions between the dislocations are calculated accounting for all the stress fields due to dislocations and hydrogen atmospheres. An analytical formula is suggested for the hydrogen induced reduction in the magnitude of the shear stress exerted between the dislocations along the slip system. Modeling of the hydrogen effect on the edge dislocation-interstitial solute atom interaction is discussed using a finite element analysis and a formula is developed for the calculation of the dislocation-solute atom interaction energy in the presence of hydrogen.

In this paper the numerical results are presented for the case where hydrogen increases the shear modulus of the metallic system. A significant decrease of the edge dislocation-interstitial solute atom interaction energy was observed when the dislocation-solute distance is approximately less than 2 Burgers vectors. This can be attributed almost entirely to the modulus change due to hydrogen. The effect of hydrogen on the screw dislocation-interstitial solute interaction was investigated. Numerical results indicate that, depending on the orientation of the tetragonal axis of the carbon distortion field, hydrogen may strengthen or weaken the interaction.

The present model provides strong support for the hydrogen shielding mechanism whereby hydrogen diminishes the local stress fields from dislocation and solutes which act as barriers to the dislocation motion.

1. INTRODUCTION

Direct observations of the effects of hydrogen on dislocations under stress (TABATA and BIRNBAUM, 1984; ROBERTSON and BIRNBAUM, 1986; BOND, ROBERTSON and BIRNBAUM, 1988a, b; ROZENAK, ROBERTSON and BIRNBAUM, 1990; SHIH, ROBERTSON and BIRNBAUM, 1988) have shown that the dislocation velocities are increased by the presence of hydrogen in solid solution. This hydrogen enhanced dislocation mobility was observed for edge, screw and mixed dislocations and was observed in FCC, BCC, and HCP crystal structures in relatively pure metals and alloys. The generality of the effect suggests it derives from the elastic interactions between dislocations and barriers to their motion. Hydrogen enhanced dislocation velocity under stress is the physical basis of the hydrogen enhanced localized plasticity (HELP) model of hydrogen embrittlement (SIROIS, SOFRONIS and BIRNBAUM, 1992; SIROIS and BIRNBAUM, 1992). Hydrogen "shielding" of the elastic interactions between dislocations and short range stress fields has been suggested as the mechanism responsible for HELP (BIRNBAUM and SOFRONIS, 1993). The underlying principle of the hydrogen shielding mechanism is that hydrogen diminishes the local stress fields from dislocations and solutes which act as barriers to the dislocation motion.

In this paper the micromechanics of the shielding mechanism is investigated from a continuum mechanics viewpoint and illustrative calculations are carried out for a few important cases. The material is considered linearly elastic, isotropic, and local constitutive moduli changes due to hydrogen are allowed for. In the present

paper the calculations are carried out for the case where the shear modulus <u>increases</u> with the addition of hydrogen to solid solution. In a subsequent paper the calculations will be presented for the case where hydrogen <u>decreases</u> the shear modulus of the solid. Hydrogen concentrations in the stress fields of microstructural defects are studied under steady state, equilibrium migration conditions. The mechanical effect of hydrogen is modeled through the stress field of a continuous distribution of dilatation centers in space with the strength of a center taken proportional to the local hydrogen concentration. Transient effects or solute drag on moving dislocations of the type calculated by FUENTES-SAMANIEGO, GASCA-NERI and HIRTH (1984) are not accounted for.

In Section 2 the stress effect on hydrogen solubility is described and the Fermi-Dirac form for the hydrogen concentration in the lattice as affected by hydrostatic stress is given. A description of the hydrogen effect on the interaction between two edge dislocations is presented in Section 3.1 with a treatment in which the elastic moduli are treated as unaffected by hydrogen. The stress fields of the hydrogen atmospheres which vary pointwise are integrated to estimate the hydrogen effect on the interaction between the dislocations. Stress relaxation and modulus change effects (for the case of the <u>increase</u> of the shear modulus with solute hydrogen) on the interaction between two edge dislocations are assessed in Section 3.2 with an iterative finite element analysis. The same finite element methodology is used to study the hydrogen effect on the interaction between an interstitial impurity atom with (a) an edge dislocation in Section 4.1, and (b) a screw dislocation in Section 4.2. The implications of the numerical computation results for hydrogen enhanced dislocation mobility and embrittlement are summarized in Section 5.

Numerical calculations for the systems in which hydrogen decreases the shear modulus will be presented in a subsequent paper. It will be shown that while

the general behavior is similar to that discussed in the present paper, the magnitudes of the effects are larger.

2.   STRESS EFFECT ON HYDROGEN SOLUBILITY

The effect of solute atoms on the behavior of dislocations, and their equilibrium distribution at a dislocation, have been studied by COTTRELL (1948), COTTRELL and JAWSON (1949), COTTRELL and BILBY (1949), BILBY (1950), HIRTH and LOTHE (1982). The local concentration of solutes is increased or decreased by diffusion to minimize the free energy of the system and to remove local chemical potential gradients. In order to understand and measure the interaction of the solute atoms with the host metal matrix, ESHELBY (1951, 1954, 1955, 1956) proposed a continuum model of the elastic behavior of a solute atom on the assumption that the impurity acts as a center of dilation or contraction.

According to COTTRELL (1948) the first order elastic interaction energy (ESHELBY, 1957) associated with a hydrogen atom introduced against the stress field, σ_{ij}^a, of a defect is given by $W_{int}^{(1)} = -\sigma_{kk}^a \Delta v'/3$ where $\Delta v'$ is the unconstrained volume dilatation and the repeated index summation convention is used. (Cartesian tensors and vectors are denoted by bold-face roman letters ($\mathbf{A}, \mathbf{a}$) and their scalar components by the corresponding light-face italic letters (A_{ij}, a_i). Indices are understood generally to range over 1, 2, and 3). Parameter $\Delta v'$ denotes the difference in volume of the hydrogen atom before its introduction into the lattice and that of the interstitial lattice space available to host the hydrogen atom. The solution of hydrogen into the lattice is also characterized by the volume change, Δv, of the host metal lattice per hydrogen atom. A relationship between these two parameters may be established as $\Delta v = \Delta v'$ (HIRTH and LOTHE, 1982). The

interaction energy per hydrogen atom, based on this first order elastic interaction, may then be written as

$$W_{int}^{(1)} = -\frac{1}{3}\sigma_{kk}^a \Delta v.$$ (1)

The volume change, Δv, is directly related to the partial molar volume of hydrogen $V_H = \Delta v N_A$ where N_A is Avogadro's number. It is assumed in eq. (1) that the solution is dilute and the hydrogen induced strains are approximately spherically symmetric, i.e. purely hydrostatic. The interaction energy, $W_{int}^{(1)}$, represents the change in the potential energy, that is, work done by external forces and change in the elastic energy of the crystal, which accompanies the introduction of the solute into the lattice against the stress field of the defect.

In the case of a hydrogen atom introduced in the stress field of an edge dislocation the first order interaction energy is given by

$$W_{int}^{(1)} = \frac{\mu b}{3\pi} \frac{(1+v)}{(1-v)} \frac{\sin\phi}{r} \Delta v$$ (2)

where r and ϕ are position polar coordinates relative to the dislocation, μ and v are the shear modulus and Poisson's ratio respectively, and b is the magnitude of the dislocation Burgers vector. Equation (2) implies that solute hydrogen atoms in the region of tensile stress lower the potential energy of the system, resulting in an increased concentration of hydrogen in the region of tension and a depletion in the region of compression stress.

In addition to the first order elastic interaction which arises from the volume change associated with the solute atom, there is a second order elastic interaction caused by the change of the local elastic moduli associated with the solute atoms (ESHELBY, 1955, 1956; HIRTH AND LOTHE, 1982). This interaction arises from the additional change in the potential energy resulting from the change of the moduli upon the introduction of the stress center (solute atom) in the lattice while the

external loads, σ_{ij}^a, are held fixed. This second order elastic interaction can be written as

$$W_{int}^{(2)} = \frac{1}{2}\left(C'_{ijkl} - C_{ijkl}\right)\varepsilon'_{ij}\varepsilon_{kl}^a v_s \tag{3}$$

where v_s is the volume over which the solute atom alters the elastic stiffnesses, C_{ijkl}, strains ε_{ij}^a are those caused by the external stress, σ_{ij}^a, in the absence of the solute atom, and strains ε'_{ij} are the elastic strains inside the volume v_s after the solute atom has been introduced in the lattice in the presence of the external stresses σ_{ij}^a which are held constant. The primed stiffnesses correspond to those characteristic of the local stiffnesses in the presence of the solute atom, and the value of v_s is usually taken as the volume of the solute atom. In general, the second order interaction energy is much smaller than the first order interaction energy and, in the case of a solute introduced in the stress field of a dislocation, it decreases with distance from the dislocation as $1/r^2$ in contrast to the $1/r$ dependence of the first order interaction energy. In the case of an isotropic solid the second order elastic interaction is manifest primarily through the dependence of the shear modulus and bulk modulus on the solute concentration. The first order interaction dominates the solute interactions with edge dislocations. In the case of solutes interacting with screw dislocations, the dominant interaction term is the second order interaction for those solutes having isotropic distortion fields (e.g. H interstitials), and the first order interaction for solutes having distortion fields with symmetries lower than cubic (e.g. C interstitials).

In discussing the interaction of hydrogen with screw dislocations (and the screw dislocation - C solute interaction) the significant effect of hydrogen on the moduli (MAZZOLAI AND BIRNBAUM, 1985a, 1985b) should be taken into account. For the hydrogen - screw dislocation interaction the first order interaction energy is zero, as hydrogen has a spherical distortion field (PEISL, 1978) while this second

order interaction energy is non-zero. However, in the case where hydrogen increases the shear modulus, the case discussed in the present paper, the second order interaction energy is positive and hence it decreases the local hydrogen concentration around the screw dislocation. Since these calculations are carried out for the low hydrogen concentration case, the effects on the hydrogen concentration are small and may be neglected. In a subsequent publication the results will be presented for the case where hydrogen decreases the shear modulus.

The hydrogen concentration C, measured in atoms of hydrogen per unit lattice volume, is given by

$$C = \theta \beta N_L \qquad (4)$$

where θ denotes the occupancy of the available interstitial sites, i.e the ratio of occupied sites to the total available, β denotes the number of interstitial sites per solvent atom and N_L denotes the number of solvent lattice atoms per unit lattice volume. In cases where the ratio of the interaction energy, W_{int}, over the absolute temperature, T, is large, as in dislocation cores, the equilibrium occupancy of interstitial sites in the region of the stress field of a defect is calculated with use of the Fermi-Dirac form (HIRTH and CARNAHAN, 1978)

$$\frac{\theta}{1-\theta} = \frac{\theta_0}{1-\theta_0} \exp\left(-\frac{W_{int}}{kT}\right) \qquad (5)$$

where θ_0 denotes the occupancy of remote sites, effectively at zero stress, from the defect and k is Boltzmann's constant. Occupancy θ_0 is related to the hydrogen concentration C_0 in the remote unstressed lattice through eq. (4)

$$C_0 = \theta_0 \beta N_L. \qquad (6)$$

For the numerical calculations, the H/M ratio was taken as a maximum of 1 corresponding to $\beta = 6$ and $\theta = 1/6$ for the tetrahedral interstitial site occupancy of the Nb-H system. Equations (4), (5) and (6) combined yield the equilibrium hydrogen concentration in terms of the remote lattice concentration as

$$C = \frac{C_0}{\frac{C_0}{\beta N_L} + \left(1 - \frac{C_0}{\beta N_L}\right)\exp\left(\frac{W_{int}}{KT}\right)}. \qquad (7)$$

3. HYDROGEN EFFECT ON THE INTERACTION BETWEEN TWO EDGE DISLOCATIONS

3.1 Analytical calculation

In the absence of hydrogen, the interaction force per unit length between two parallel dislocations is given (HIRTH and LOTHE, 1982) by

$$\mathbf{F} = \sigma_1 \mathbf{b}_2 \times \xi \qquad (8)$$

where σ_1 is the stress tensor of dislocation 1, $\mathbf{b}_i$, $i = 1,2$, are the Burgers vectors, and ξ is the unit vector along the dislocation lines. In component form, equation (8) is written as $F_i = \varepsilon_{ijk}(\sigma_1)_{jm}(b_2)_m \xi_k$, where ε_{ijk} is the alternating symbol. In the case to be discussed, parallel edge dislocations, equation (8) results in a repulsive force if the dislocations are of the same sign and on the same slip system. In this case, the force on dislocation 2 due to dislocation 1 is $\tau_D b_2$, where τ_D is the stress of dislocation 1 resolved along the slip plane and Burgers vector.

The hydrogen effect on the interaction between the dislocations 1 and 2 is assessed by calculating the hydrogen induced change to the shear stress τ_D due to interactions between the hydrogen atmospheres surrounding the two dislocations. These hydrogen atmospheres are modeled by a continuous distribution of dilatation lines parallel to the dislocation lines. Each dilatation line is viewed as a stress source which affects the shear stress, τ_D. This model for the hydrogen effect is consistent with the plane strain assumption for the dislocation strain field when the hydrogen concentration does not vary in the direction of the dislocation lines. In that case the

in-plane concentration of the dilatation lines, n, is directly related to the hydrogen concentration per unit volume, C, through

$$n = Ch \qquad (9)$$

where h is the distance between two successive hydrogen atoms along the dilatation line and the concentration n denotes the number of hydrogen atoms per unit area in the plane normal to the dilatation line. In the following subsection hydrogen effects on the constitutive moduli are neglected. They are discussed in a later section.

(i) *The stress field of a single hydrogen dilatation line*

　　　Consider a line of dilatation associated with hydrogen atoms introduced into a stress free lattice. The dilatation line is produced in a continuum sense by replacing a cylindrical hole of infinite length and radius r_0 in an infinite lattice with a cylinder of the same material and radius $r_0 + \varepsilon r_0$. Parameter ε is a small positive number related to the volume of solution of hydrogen. The region round the dilatation line experiences a plane strain stress field having axial symmetry. Relative to a polar cylindrical coordinate system r, ϕ and x_3, whose the x_3 axis coincides with the dilatation line, one may write the nonzero stress components σ_{ij} at distance r from the dilatation line as

$$\sigma_{rr} = -\frac{\mu \Delta a}{\pi r^2} \quad , \qquad \sigma_{\phi\phi} = \frac{\mu \Delta a}{\pi r^2} \qquad (10)$$

where

$$\Delta a = \frac{\Delta a'}{2(1-\nu)} \qquad (11)$$

denotes the strength of the dilatation line, and $\Delta a' = 2\pi r_0 \varepsilon$ is the "unconstrained area of expansion." Due to combined axial symmetry and plane strain, only the displacement, u, in the r direction in the x_3 plane is non-zero and is given by

$$u = \frac{\Delta a}{2\pi r}. \tag{12}$$

The strain field associated with u is incompressible and the area flux in the x_3 plane through a circular boundary enclosing the dilatation line is $\Delta A = \Delta a$. The unconstrained area of expansion, $\Delta a'$, can be evaluated in terms of the unconstrained volume change, $\Delta v'$, of a hydrogen atom. Consistent with the plane strain assumption of the model, the unconstrained volume of the unit length cylinder, $\Delta a'$, used to produce the dilatation line is equal to the total unconstrained volume $\Delta v'/h$ of the $1/h$ hydrogen atoms which make the unit length of the cylinder. Therefore $\Delta a' = \Delta v'/h$. In view of the fact that $\Delta v = \Delta v'$ one may write $\Delta a' = \Delta v/h$. Since the volume change, Δv, is related to the partial molar volume of hydrogen in solution, V_H,

$$\Delta a' = \frac{V_H}{N_A h}. \tag{13}$$

(ii) *Interaction of a single dilatation line with an applied stress*

Assume that a dilatation line is introduced in an infinite elastic solid subject to stresses, σ_{ij}^a, with corresponding displacements, u_i^a, caused by externally applied loads. The interaction energy per unit length between the stress field, σ_{ij}, of the dilatation line and the stress field, σ_{ij}^a, due to the external loads is given by ESHELBY (1956) as

$$E_{\text{int}} = \oint_s \left(\sigma_{ij} u_i^a - \sigma_{ij}^a u_i \right) n_j ds \tag{14}$$

where s is any arbitrary curve on the x_3 plane encircling the dilatation line and $\mathbf{n}$ is the outward unit normal vector to the curve. Using eqs. (10), (11) and (12) one may calculate the interaction energy from eq. (14) as

$$E_{\text{int}} = -\frac{\sigma_{11}^a + \sigma_{22}^a}{2}\Delta a' \tag{15}$$

where the stress components of σ_{ij}^a are measured in a Cartesian coordinate system whose axis, x_3, coincides with the hydrogen dilatation line. Equation (15), which is the plane version of eq. (1), remains valid in the case of a finite body as well, because the contribution of the image forces to the line integral of eq. (14) vanishes. This is a direct result of the nonsingular nature of the displacement field due to the image forces (ESHELBY, 1956). Dividing E_{int} by the total number of hydrogen atoms, $1/h$, in the unit length of the dilatation line, one finds the interaction energy per hydrogen atom as $W_{\text{int}} = E_{\text{int}}h$. Therefore, with use of eqs. (13), and (15), one obtains W_{int} as

$$W_{\text{int}} = -\frac{\sigma_{11}^a + \sigma_{22}^a}{2}\frac{V_H}{N_A}. \tag{16}$$

Equation (16) is used in eq. (7) to calculate the hydrogen concentration C in equilibrium with an applied stress field, σ_{ij}^a, and eq. (9) provides the density n of the dilatation lines in the plane normal the dislocation lines. Since the stress field, σ_{ij}^a, varies with position, so also do the fields C and n.

(iii) *Integrated shear stress effect of the hydrogen dilatation lines on a dislocation*

Consider a Cartesian coordinate system of axes x_1 and x_2 centered at the core of the dislocation 2 as is shown in Fig. 1, and a single hydrogen dilatation line at a point with polar coordinates r and ϕ. The shear stress exerted at the core of dislocation 2 along the slip plane by the hydrogen dilatation line can be found from eqs. (10) as

$$\frac{\sigma_{rr} - \sigma_{\phi\phi}}{\pi r^2}\sin 2\phi = -\frac{\mu\Delta a}{\pi r^2}\sin 2\phi \tag{17}$$

Using the principle of linear superposition and eq. (17), one may calculate the shear stress, $d\tau_H$, due to the dilatation lines of an infinitesimal area, dS, at r, ϕ (see Fig. 1) as

$$d\tau_H = ndS\left(-\frac{\mu\Delta a}{\pi r^2}\right)\sin 2\phi. \tag{18}$$

Substitution of eqs. (9), (11) and (13) into eq. (18) yields

$$d\tau_H = -C\frac{\mu}{2\pi(1-\nu)}\frac{V_H}{N_A}\frac{\sin 2\phi}{r^2}dS. \tag{19}$$

The net shear stress, τ_H, induced by the hydrogen atmosphere is found by integrating eq. (19) over the entire area S occupied by the atmosphere as

$$\tau_H = -\frac{\mu}{2\pi(1-\nu)}\frac{V_H}{N_A}\int_A C\frac{\sin 2\phi}{r^2}dS \tag{20}$$

and in polar coordinates as

$$\tau_H = -\frac{\mu}{2\pi(1-\nu)}\frac{V_H}{N_A}\int_0^{2\pi}\int_{r_2}^{R}C(r,\phi)\frac{\sin 2\phi}{r}dr\,d\phi \tag{21}$$

where r_2 is the inner cutoff radius of dislocation 2 and R is the outer cutoff radius of the atmosphere centered at dislocation 2. The core of dislocation 1 with cutoff radius r_1 is also excluded from the integration. A similar expression can be written for the resolved shear stress on dislocation 1 due to hydrogen.

According to eqs. (10) the stress field of a hydrogen dilatation line is purely deviatoric. Consequently, the interaction energy, as calculated from eq. (16), between the hydrogen dilatation lines is zero, i.e., the introduction of a dilatation line into the lattice is energetically independent of the presence of the neighboring lines. Therefore the hydrogen concentration $C(r,\phi)$ at any position (r, ϕ) is determined solely by the corresponding stress due to dislocations 1 and 2. Superposition of the singular linear elastic stress fields of the two dislocations (HIRTH and LOTHE, 1982) yields the in-plane hydrostatic stress as

$$\frac{\sigma_{11}^a + \sigma_{22}^a}{2} = -\frac{\mu}{2\pi(1-\nu)}\left(b_2\frac{\sin\phi}{r} + b_1\frac{r\sin\phi - l\sin\omega}{r^2 + l^2 - 2rl\cos(\phi-\omega)}\right) \qquad (22)$$

where l and ω are the polar coordinates of the position of dislocation 1 (see Fig. 1). Then concentration $C(r,\phi)$ in eq. (21) is calculated by combining eqs. (7), (16) and (22).

Equations (10) indicates that the stress field of a hydrogen dilatation line decays as $1/r^2$ with distance, r. It is expected that the magnitude of the shear stress, τ_H, due to hydrogen on dislocation 2 will depend mainly on the dilatation lines close to the core of dislocation 2 and less on those which are remote from the core. This effect is seen in the integrand of eq. (21) which diminishes as r increases and becomes zero at $r = \infty$ where $C(r,\phi) = C_0$. In the calculations for the hydrogen distribution and stresses on the dislocation, for fixed relative dislocation positions, (l, ω), the integral of eq. (21) is computed numerically for an arithmetic progression of outer cutoff radii, R, deffering by $20b_2$. The calculation is regarded as convergent when the relative error in the calculated shear stress for two successive radii is less than 10^{-3}. The details of the numerical integration are given in Appendix A.

Lastly, the corresponding shear stress, τ_D, resolved along the slip plane at the core of dislocation 2 due to dislocation 1 is given by

$$\tau_D = -\frac{\mu b_1}{2\pi(1-\nu)}\frac{\cos\omega\cos2\omega}{l}. \qquad (23)$$

The net shear stress exerted on dislocation 2 is equal to $\tau_D + \tau_H$.

(iii) *Numerical integration results*

All parameters, mechanical and hydrogen related, were chosen for the BCC niobium system whose lattice parameter is $a = 3.301\text{Å}$ with a corresponding Burgers vector magnitude, $b = 0.285\,10^{-9}m$. The elastic behavior of the niobium was assumed to be isotropic with a shear modulus of 30.8 GPa and a Poisson's ratio of 0.415, values which correspond to the hydrogen free material. Given the ratio of volume

expansion per hydrogen atom to volume of the host lattice atom is 0.174 (PEISL, 1975), one can calculate the partial molar volume of hydrogen as $V_H = 0.188 \, 10^{-5} m^3 / mol$. The molar volume of the metal was $V_M = 0.108 \, 10^{-4} m^3 / mol$ which corresponds to $N_L = 0.555 \, 10^{29}$ solvent lattice atoms per m^3 of host metal lattice. The parameter β was chosen equal to 6 interstitial lattice atoms per solvent atom corresponding to tetrahedral site occupancy, thus allowing for local hydrogen concentrations capable of forming the NbH structure at $\theta = 1/6$. The system's temperature was 300K.

The hydrogen atmosphere in equilibrium with the stress field of a single dislocation in an infinite medium is shown in the form of normalized iso-concentration lines, c / c_0, in Fig. 2 at a nominal concentration $c_0 = 0.1$ hydrogen atoms per solvent atom. The atmosphere is symmetric with respect to the dislocation plane because of the corresponding symmetry in the hydrostatic stress field of the dislocation. Under the same temperature and nominal hydrogen concentration, Figs. 3 and 4 show the hydrogen atmosphere for dislocations 1 and 2 on the same slip system and at respective relative positions of 10, 8 and 6 Burgers vectors apart. In Fig. 4, the Burgers vector of dislocation 2 is negative. The portion of the hydrogen atmosphere around each dislocation is non-symmetric when compared with the atmosphere of the single dislocation shown in Fig. 2. This is a direct result of the linear superposition in the stress field of the two dislocations. For dislocations of the same sign, the hydrostatic stress field is reinforced positively below the slip plane and negatively above the slip plane. For any given point in the area between the dislocations, this reinforcement increases as the dislocations approach each other. Consequently the hydrogen concentration increases in the regions of positive stress enhancement and its value becomes larger than the

concentration of the corresponding region in the atmosphere of a single dislocation. In contrast, the positive hydrostatic stress field of each dislocation is weakened in the case of dislocations of opposite sign. As a result, the level of hydrogen accumulation in the tensile regions of the two dislocations is below that of a single dislocation alone. Figures 3a to 3c and 4a to 4c indicate that as the dislocations come closer, the iso-concentration curves become increasingly unsymmetrical.

In Figs. 5 and 6 the hydrogen induced shear stress, τ_H, resolved on the slip plane and along the Burgers vector at the core of dislocation 2 is plotted against distance l between the dislocations for nominal concentrations equal to 0.1, 0.01 and 0.001 hydrogen atoms per solvent atom, a temperature of 300K and at an angle ω equal to 180^0 (see Fig. 1). In Fig. 6, dislocation 2 has a negative Burgers vector. The shear stress is normalized by the shear modulus μ and the distance by the Burgers vector magnitude, b. In the same figures the normalized shear stress, τ_D / μ, due to dislocation 1 in the absence of hydrogen (eq. (23)) and the total normalized shear stress, $(\tau_D + \tau_H) / \mu$, are also plotted. Results for l/b less than 3 were not calculated because they correspond to dislocation positions with very close or overlapping core regions.

The shear stress due to hydrogen is negative and its absolute value increases as the nominal concentration becomes larger, consistent with concentration dependence of the hydrogen dilatation line density, n, on C_0. The sign of the hydrogen induced shear stress is understood by looking at the sign of the function $f(r,\phi) = -C(r,\phi)\sin(2\phi)/r$ in the integrand of eq. (21). In both cases, the effect of hydrogen is to decrease the force exerted on dislocation 2 by dislocation 1.

3.2. Finite element calculation

In the preceding section it was assumed that the nature of each source of stress was unaffected by the presence of the others; i.e. that each dilatation line and

dislocation produced stresses in the surrounding medium which were combined by the principle of linear superposition. The strength, and therefore the stress field, of each dilatation line was computed directly from the local hydrogen concentration as determined by the standard dislocation stress fields. However, the region close to dislocation can become saturated with solute atoms and the dilatation caused by the dislocation may be replaced by the solute dilatation. This effect was not implicit in the treatment of the preceding section because of the approximation made, when expanding the lattice, that the consequent change in the forces exerted by the stress field on the dilating lattice may be neglected. In other words, the hydrogen dilatation line produced only a deviatoric stress field because the stresses arising from the lattice accommodation of the finite hydrogen volume were not considered. According to COTTRELL (1948) and BILBY (1950) this approximation is reasonable for a single solute atom but cannot be extended to the case where several solute atoms gather in the same region since their contributions to the relaxation of the hydrostatic stresses are additive.

In this section, the relaxed elastic stress field associated with the introduction of hydrogen into the lattice is calculated and the elastic moduli of the lattice are allowed to vary pointwise according to the local hydrogen concentration. Relaxation of the standard singular dislocation elastic stress field is not accounted for, even though it may be substantial in the region close to the core. Hydrogen from regions further afield is incapable of relaxing the dislocation singular stress field because the stresses due to hydrogen decay rapidly, as $(1/r^2)$. The total stress field in the lattice is found by superposition of the relaxed elastic stress due to hydrogen and that of the standard singular elastic dislocation stress field (HIRTH and LOTHE, 1982). The latter is calculated at a given position by using elastic moduli modified accordingly to the corresponding local hydrogen concentration. The hydrogen constitutive effect

on the dislocation stress field is modeled by perturbing the modulus in the standard elastic solution for the hydrogen free material.

(i) *Hydrogen induced transformation strain*

Assume that n_H moles of hydrogen are introduced in a region of n_M moles of the host metal with the local hydrogen concentration thus being $c = n_H/n_M$. Provided that the solution is dilute, the local unconstrained volume dilatation of the lattice volume, $V = n_M V_M$, is $\Delta V = n_H N_A \Delta v'$ and the corresponding unconstrained dilatational strain is $e^H = c\Delta v'/\Omega$, where Ω is the mean atomic volume of the host metal atom. Using the condition $\Delta v' = \Delta v$, one finds

$$e^H = c\frac{\Delta v}{\Omega}. \tag{24}$$

For a dilute solution, the concentration C which denotes hydrogen atoms per unit lattice volume is related to concentration c by

$$C = c\frac{N_A}{V_M} = \frac{c}{\Omega} = cN_L. \tag{25}$$

Comparing eq. (25) to eq. (4) one finds $c = \theta\beta$ which in the case of a fully saturated lattice, $\theta = 1/6$, gives $c = 1$.

(ii) *Hydrogen effect on the elastic moduli of niobium*

MAZZOLAI and BIRNBAUM (1985a, 1985b) have made high frequency acoustic measurements of constants C', C_{11} and C_L of single crystals of the Nb-H(D) system in the composition range of the $\alpha - \alpha'$ phase. These values were used to calculate the cubic moduli C_{11}, C_{12} and C_{44} from the well known relationships

$$C_L = \frac{1}{2}(C_{11} + C_{12} + 2C_{44}) \quad \text{and} \quad C' = \frac{1}{2}(C_{11} - C_{12}). \tag{26}$$

The results are available over a wide range of hydrogen concentrations and show that the Nb-H system is elastically anisotropic with $C_{44} \neq C'$. This set of data allows

the calculation of the Reuss and Voigt averages of the isotropic elastic moduli and these will be used in the calculations presented in a subsequent paper. In the present paper the elasticity of the material was assumed to be isotropic with bulk modulus, $B = (C_{11} + 2C_{12})/3$, and shear modulus, $\mu = C_{44}$, calculated from

$$B = C_{11} - \frac{4}{3}C' \quad \text{and} \quad \mu = C' + C_L - C_{11}. \tag{27}$$

This choice of $\mu = C_{44}$ is appropriate for this paper which models the behavior in systems in which hydrogen increases the shear modulus. Using this procedure, the hydrogen effects on Young's modulus E, Poisson's ratio, ν, and shear modulus, μ, are modeled through

$$E = E_0(1 + 0.34c), \qquad \nu = \nu_0 - 0.025c, \qquad \mu = \mu_0 \frac{1 + 0.34c}{1 - 0.0177c}. \tag{28}$$

where $E_0 = 87.1 \text{GPa}$, $\nu_0 = 0.415$ and $\mu_0 = 30.8 \text{GPa}$ are Young's modulus, Poisson's ratio and shear modulus respectively for the hydrogen free material. As will be seen, the conclusions about the hydrogen effect on the mechanical behavior of the material are strongly associated with the assumed increase of the shear modulus with increasing hydrogen concentration. The alternative case will be discussed in a subsequent publication.

(iii) *Formulation of the boundary value problem for the hydrogen stress field*

Consider the hydrogen atmosphere associated with two parallel edge dislocations at distance l apart on the same slip plane and of equal Burgers vector magnitude, b. Since hydrogen remote from the core of the dislocations is not expected to affect their interaction, modeling is confined to a finite square region, S, of the atmosphere centered at the midpoint between the dislocations (see Fig. 7). The outer boundary of the area S is placed within the remote region of the atmosphere where the hydrogen equilibrium concentration is essentially equal to C_0. In order to

ensure that the hydrogen composition immediately inside S is exactly the same as that outside S, one has to apply image tractions along the outer boundary. These image tractions arise mainly from the hydrogen close to the remote boundary because the stress field of a hydrogen dilatation center well inside the boundary decays away within short distance from the center, i.e as $1/r^2$. Consequently the contribution of the image tractions to the hydrogen equilibrium concentration close to the dislocation cores may be neglected in comparison to the effect of the singular hydrostatic stresses due to dislocations. Therefore, in the case of a dilute solution, those tractions can approximately be set equal to zero. With regard to the hydrogen residing in a dislocation core, the Fermi-Dirac form of eq. (5) dictates that the region at and very close to the core is saturated with finite amount of hydrogen. This allows the same treatment of the core hydrogen as that of the rest of the atmosphere and consequently no interior holes corresponding to the dislocation cores were excluded from the area S. In conclusion, the domain S over which the hydrogen related boundary value problem is set up consists of a simply connected rectangular region (see Fig. 7) whose outer boundary is free of loads.

The mechanical effect of hydrogen is modeled by a dilatational transformation strain whose components are given by

$$\varepsilon_{ij}^{H} = \frac{1}{3} e^{H} \delta_{ij} \tag{29}$$

where δ_{ij} is the Kronecker delta. Transformation strain ε_{ij}^{H} varies pointwise and its magnitude depends upon the local hydrogen concentration as dictated by eq. (24). The linear elasticity of the hydrogen-metal system accounting for transformation strain is characterized by

$$\sigma_{ij} = C_{ijkl}\left(\varepsilon_{ij} - \varepsilon_{ij}^{T}\right) \tag{30}$$

where σ_{ij} are the components of the elastic stress tensor due to hydrogen, ε_{ij} are the components of the net strain tensor which obey compatibility, $\varepsilon_{ij}^{T} = \varepsilon_{ij}^{H}$, and C_{ijkl} are

the linear elastic moduli of the system which are function of position as dictated by eq. (28) through the hydrogen concentration field. The mechanical equilibrium of the system in the absence of body forces is stated in the form of the principle of virtual work by

$$\int_V \sigma_{ij} \delta \varepsilon_{ij} dV = 0 \qquad (31)$$

where δ indicates an arbitrary virtual variation of the quantity it precedes, and V denotes the volume of the rectangular domain S whose outer boundary is traction free.

The local hydrogen concentration is obtained from eq. (7) with the interaction energy W_{int} furnished by eq. (1) where σ_{ij}^a is the net hydrostatic stress due to all stress sources in the lattice. This procedure ignores the small effect of the second order elastic interaction on the calculation of the hydrogen concentration. Solution of hydrogen into the lattice requires that work be done against both the singular dislocation hydrostatic stress and the relaxed hydrostatic stress of the neighboring solutes. The former is unknown because the local moduli are concentration dependent. Thus the hydrogen concentration as calculated through eqs. (1) and (7) is locally a nonlinear function of the unknown total hydrostatic stress. This implies that the local hydrogen composition needed to characterize the transformation strain in eq. (29) and the local elastic moduli in eq. (30), and required to solve the governing equations (30) and (31) can only be determined after the solution is found. Therefore the problem of calculating the stress fields of the dislocation, the stress field due to hydrogen and the local distribution of hydrogen is coupled in a nonlinear sense and the solution procedure involves iteration. Assuming a solution for the hydrogen concentration field, one determines the transformation strain and the local constitutive moduli pointwise. Next the resulting linear problem arising from eqs. (30) and (31) is solved and the solution for the hydrostatic

stress is used to recalculate the hydrogen concentration through eqs. (1) and (7). The new solution for the concentration field is compared with the assumed one and the process continues until convergence is achieved. The hydrogen concentration in equilibrium with the hydrostatic stress found by superposition of the singular elastic fields of dislocations 1 and 2 can be used to initiate the process.

(iv)*Finite element method*

Let $\{u\}$ denote the array of nodal displacement components in the finite element model used to represent the problem. Using eqs. (30) and (31) in plane strain conditions, the standard interpolation matrices, $[A]$ for the displacement, $[B]$ for the strain and $[C]$ for the constitutive law of an isotropic material, one derives the finite element equations

$$[K]\{u\} = \{F\} \tag{32}$$

where

$$[K] = \int_S [B]^T [C][B] dV, \tag{33}$$

$$[F] = \int_S [B]^T [C]\{\varepsilon^{Tr}\} dV, \tag{34}$$

$$\{\varepsilon^{Tr}\}^T = [\varepsilon_{11}^H \quad \varepsilon_{22}^H \quad \varepsilon_{33}^H \quad 0] \tag{35}$$

and the superscript T stands for array or matrix transpose. The stiffness matrix $[K]$ changes during the iteration process since it involves the elasticity tensor $[C]$ which is concentration dependent through the elastic moduli. Similarly the force vector $\{F\}$ follows the changes in the local transformation strain vector $\{\varepsilon^{Tr}\}$ due to changes in the concentration.

Iterations were performed until the convergence criterion

$$\|\Delta C\| \leq \alpha \|C\| \tag{36}$$

was met where the norm $\|a\|$ is defined for an array $\{a\}$ as

$$\|a\| = \left(\{a\}^T\{a\}\right)^{\frac{1}{2}}, \tag{37}$$

$\{C\}$ is the array for the assumed concentration at the element integration stations at the beginning of the iteration, $\{\Delta C\}$ is the array which denotes the difference between the calculated concentration at the end of the iteration and the assumed one, and the convergence parameter α is a very small fraction taken equal to 0.005. The next iteration was initiated with concentration array $\{C\} + \gamma\{\Delta C\}$ where the constant γ used to relax the difference $\{\Delta C\}$ was taken equal to 0.2. Usually 10 iterations were sufficient for convergence to be achieved.

By symmetry, the solution in the half plane $x_1 > 0$ only was required (see Fig. 7). The surface $x_1 = 0$ was prescribed to have zero normal velocity and to be free of shear traction. To eliminate rigid body motion, the point at the origin of the coordinate axes was constrained from moving along the x_2 direction. The square domain, $0 \le x_1 \le 0.12x10^6 b$, $-0.1x10^6 b \le x_2 \le 0.1x10^6 b$, (see Fig. 7) was discretized into 1422 4-noded quadrilateral isoparametric elements with 4 integration stations and a total number of 1563 nodes. The area $0 \le x_1 \le 36b$, $-20b \le x_2 \le 4b$ close to the origin and containing the dislocation 2 was finely discretized by 864 square elements of side b in order to ensure that the concentration is determined fairly reliably.

(v) *Results*

First, a series of calculations was carried out by gradually moving the outer boundary of the rectangular region modeled further away from its position shown in Fig. 7. No dependence of the hydrogen effect was found upon the finite element mesh used. Therefore the suggested modeling of the hydrogen effect through a rectangular region of finite dimensions is reliable.

Equation (7) was used to calculate the hydrogen concentration in equilibrium with the superposed hydrostatic stress fields of the two edge dislocations at

temperature 300K and nominal concentration of H/M=0.1. The interaction energy was found through eq. (1) with all three components of the normal stress included in the calculation of the hydrostatic stress. No hydrogen effects on stress relaxation and the elastic moduli were considered and therefore no iterations were needed. The estimated hydrogen atmosphere is shown in Fig. 8 in the form of iso-concentration lines. Comparing the atmosphere of Fig. 8 to that of Fig. 3c which is also unrelaxed and calculated by the same method at the same temperature and nominal concentration one notices a slight difference in the location of the same iso-concentration lines relative to the two dislocations. The iso-concentration lines in Fig. 8 are closer to the dislocations than the corresponding ones of Fig. 3c indicating that the hydrostatic stress at a given position is lower in Fig. 8 than in Fig. 3c. This is expected as the hydrostatic stress as calculated in Fig. 8 with all three normal components of the stress, is $2(1+v)/3$ times the hydrostatic stress of Fig. 3c which is calculated only with the two in-plane components (see eq. (15)).

The effect of the volumetric transformation strain that accompanies the introduction of hydrogen into the lattice on stress relaxation, (volumetric effect), was calculated by solving the relevant boundary value problem through iteration. In this calculation the shear modulus, $\mu_0 = 30.8\,GPa$, and Poisson's ratio, $v_0 = 0.415$, were treated as unaffected by hydrogen since only the volumetric effect was to be studied. The hydrogen atmosphere associated with the two edge dislocations at a distance of 6 Burgers vectors apart, and with the same parameters as used for the calculations shown in Figs. 3 and 8 is shown in Fig. 9. The relaxation effect of hydrogen can be seen between the two dislocations, e.g. at a distance of 8 Burgers vectors below the dislocation slip plane where the normalized hydrogen concentration changes from a level close to 3 in Fig. 8 to a level close to 2 in Fig. 9 due to hydrogen relaxation. Also, comparing the iso-concentration levels of Figs. 9 and 3c, one deduces that the 3-D hydrostatic stress in Fig. 9 is relaxed even with

respect to the 2-D hydrostatic stress of Fig. 3c. Therefore it is expected that the hydrogen induced shear stress, τ_H, as estimated by the analytical calculation of the previous section and shown in Fig. 5 for various nominal concentrations, is greater in magnitude than the shear stress associated with the relaxed atmospheres furnished by the finite element calculations. This is demonstrated by comparing the results of Fig. 5 with those of Fig. 10 where the shear stress associated with the relaxed atmospheres at nominal concentrations of H/M=0.1, 0.01 and 0.001 is plotted against normalized distance between the dislocations.

Next the hydrogen volumetric effect was investigated in combination with the hydrogen induced modulus change, (modulus effect), as given by eq. (28) at the same temperature of 300K. The hydrogen atmosphere at nominal concentration H/M=0.1 and dislocation distance $6b$ is shown in Fig. 11. Comparing the iso-concentration curves of Fig. 11, where both volumetric and modulus effects were accounted for, with those of Fig. 9 where only volumetric effects were considered, one sees that the volumetric effect significantly decreases the stresses relative to the unrelaxed solution (Fig. 8) and that the combined volumetric and modulus effect has a smaller influence than the volumetric effect alone. This can be explained by the monotonic increase of shear modulus with hydrogen concentration (see eq. (28)) which causes a hydrostatic stress elevation resulting in an increased hydrogen concentration. The hydrostatic stress elevation due to modulus effect is in opposition to the hydrostatic stress relaxation due to the volumetric effect. Therefore one expects that the combined modulus and volumetric effects result in a hydrogen induced stress, τ_H, larger in magnitude than the one associated with the volumetric field alone. In Fig. 12 the shear stress, τ_H, due to the combined effect is plotted against the normalized distance between the dislocations, l/b, at various nominal hydrogen concentrations. The effects, volumetric alone and combined

modulus and volumetric are compared in Fig. 13 where the percent reduction of the dislocation shear stress, τ_D, due to hydrogen is plotted against distance l/b.

The local values of shear modulus and Poisson's ratio, whose hydrogen dependence is described by eq. (28) are shown in Figs. 14 and 15 respectively at nominal hydrogen concentration of H/M=0.1 and a dislocation separation of 6b. Figure 14 shows that shear modulus decreases with distance from the dislocations whereas Fig. 15 shows the opposite is true for the Poisson's ratio; in agreement with eq. (28) and the hydrogen concentration field shown in Fig. 11.

In reporting the results of Figs. 12 and 13, the modulus effect on the shear stress, τ_D, due to the dislocation stress field was not considered. The dislocation shear stress was calculated using isotropic elasticity and the elastic moduli of the hydrogen free material. One may account for the modulus effect on the dislocation stress field by calculating τ_D as for the hydrogen free material but with the moduli being replaced by those at the nominal hydrogen concentration, an approximation based on the smearing out of the pointwise modulus variation. The results do not also account for the hydrogen volumetric effect on the dislocation stress field which has been neglected altogether as has been discussed in Section 1. The reduction in the total shear stress due to combined modulus and volumetric effects when the dislocation shear stress is calculated with the corresponding moduli at the nominal concentration is shown in Fig. 16. Comparing the reductions due to hydrogen in the net shear stress exerted on the dislocation 2, as shown in Figs. 13 and 16, one sees that the modulus effect becomes weaker when the modified dislocation stress is used. This is a direct result of the increase in the shear modulus as the H/M concentration is increased, relative to the modulus of the hydrogen free material. The former modulus provides a larger shear stress, τ_D, than the latter and consequently the hydrogen induced stress, τ_H, counteracts a larger dislocation shear stress, τ_D. The effects of the opposite dependence (μ decreases as the hydrogen

concentration is increased) of the shear modulus on hydrogen will be discussed in a subsequent publication.

3. 3. Discussion of the results

In the absence of hydrogen, it is well known that two parallel edge dislocations on the same slip system and with Burgers vectors of the same sign repel each other. Both the analytical and finite element results of this work indicate that the hydrogen shielding effect reduces the repulsive force acting on the dislocation glide plane. The reduction is a synergistic effect associated with the volumetric strain produced by the introduction of hydrogen into the lattice, (volumetric effect), and the hydrogen induced changes in the constitutive moduli, (modulus effect). The magnitude of these effects will depend on the nature of the variation of the moduli with hydrogen. In the present paper the case of increasing shear modulus with increased H/M is explored and the opposite dependence will be discussed in a subsequent publication. The hydrogen related decrease of the repulsive interaction depends strongly on the nominal hydrogen concentration as indicated by Figs. 5, 10, 12 and 13. At a fixed nominal hydrogen concentration, Figs. 5, 10 and 12 indicate that both volumetric and modulus effects on the absolute magnitude of the hydrogen induced shear stress become weaker with increased dislocation separation. For dislocation separations greater than about 10 Burgers vectors the percentage net stress reduction, that is, the hydrogen stress normalized by the corresponding repulsive shear stress in the absence of hydrogen is almost independent of the distance between the dislocations (see Fig. 13). At large dislocation separations the hydrogen atmosphere is sufficiently asymmetric to cause a reduction of the interaction force, but the total amount of hydrogen in the dislocation atmospheres responsible for the magnitude of the effect is almost independent of the dislocation

separation as it is determined predominantly by the stress field of each dislocation alone.

Figure 13 shows that the modulus effect is of second order when compared to the volumetric strain effect and it seems to be significant only at nominal hydrogen concentrations larger than 0.01 hydrogen atoms per metal atom. At concentration H/M=0.1 9.3% of the net stress reduction is caused by the modulus effect whereas at H/M=0.001 the contribution due to the modulus effect is almost negligible. The modulus effect decrease of 9.3% decreases to 6.2% when the dislocation shear stress, τ_D, is evaluated (as in the Fig. 16) with the elastic moduli estimated at the nominal hydrogen concentration. In the case of opposite signed dislocations hydrogen reduces the attractive force between the dislocations (see Fig. 6).

Hydrogen shielding of the stress field of the parallel edge dislocations results in a decrease in the magnitude of the shear stress, τ_D, which the dislocation 1 exerts on dislocation 2. As a consequence, the force between parallel dislocations is reduced, both for the repulsive force between two dislocations of the same sign and for the attractive force between two dislocations of opposite signed Burgers vectors. As expected from the hydrogen contribution to these interactions, the effects are greatest at small distances between the dislocations. The consequences of these effects on the dislocation behavior are many and will be discussed in detail in a subsequent publication. In the following only a few examples are cited.

Qualitatively, it is evident that in the presence of hydrogen, the spacing between dislocations in pileups will be decreased, particularly for the closely spaced dislocations at the tip of the pileup. At sufficiently high H/M values and at close enough dislocation spacing, the sign of the force may in fact reverse and opposite signed dislocations can attract. This may cause fracture by the coalescence of edge dislocations at the head of the pileup; a mechanism first proposed by ZENER (1948) and discussed by STROH (1957). The internal stress field of plastically deformed

metals is mainly provided by the stress fields of dislocations and groups of dislocations. The general effect of hydrogen is to reduce these stresses and hence may be expected to reduce the internal stress field and the fluctuations in this field. Since in the deformed metals the mobility of dislocations is determined by the interaction of the moving dislocations with the internal stress field, the effect of a decrease in the internal stresses due to hydrogen is to decrease the barriers to dislocation motion and hence to increase the dislocation mobility. Another consequence of the reduction of attractive interactions between opposite signed Burgers vectors is the decrease in stability of the dislocation dipoles formed during deformation, again resulting in a decrease in the strength of the obstacles to dislocation motion.

4. HYDROGEN EFFECT ON THE INTERACTION BETWEEN A DISLOCATION AND AN IMPURITY ATOM

Interstitial solutes in BCC crystals are known to provide barriers to the motion of dislocation lines as they move through the crystal under the action of an applied stress. Hence, hydrogen effects on the interactions between dislocations and solute impurity atoms are important for the understanding of hydrogen effects on plastic deformation and fracture. COCHARDT et al. (1955) have studied the interaction between dislocations and interstitial solute atoms on the basis of the tetragonal distortion of the BCC lattice caused by carbon interstitials in alpha iron. In this section the effect of hydrogen on the interactions between an interstitial carbon atom and a dislocation will be studied.

Following COCHARDT et al. (1955), one may study the mechanical effect of carbon in the lattice through a transformation strain associated with the unit cell. In the case of alpha iron the components of the transformation strain for a carbon

interstitial having its tetragonal strain axis along the [100] axis of the crystal coordinate system are given by

$$\left[\varepsilon^{TC}\right]_{ij} = \begin{bmatrix} \varepsilon_1 & 0 & 0 \\ 0 & \varepsilon_2 & 0 \\ 0 & 0 & \varepsilon_3 \end{bmatrix} \tag{38}$$

where

$$\varepsilon_1 = 0.38, \qquad \varepsilon_2 = \varepsilon_3 = -0.026 \tag{39}$$

If a is the lattice parameter, equations (38) and (39) indicate extension of the unit cell in the 1-direction by an amount $\varepsilon_1 a$ and compression in the 2- and 3- directions by an amount $-\varepsilon_2 a$ and $-\varepsilon_3 a$ respectively. The transformation strain due to interstitials having their tetragonal axes in directions [010] and [001] can be found by rearranging the components of ε^{TC} so that they are compatible with the corresponding distortion of the lattice.

4. 1. Edge dislocation

(i) *Formulation of the boundary value problem*

The net stress field in the lattice can be found by linear superposition of the fields of the hydrogen atmosphere, σ_H, the carbon atom, σ_C, and the dislocation, σ_D. First the combined stress field of the continuously distributed hydrogen and that of a single carbon interstitial in the absence of the dislocation, $\sigma_H + \sigma_C$, (carbon/hydrogen), is evaluated through the transformation strain model for carbon and hydrogen interstitials by accounting for the hydrogen induced changes in the elastic moduli. The calculation of the combined hydrogen and carbon field is carried out as in section 3.2 with respect to a portion S of the hydrogen atmosphere which in this case is taken to be circular and centered at the dislocation core. The external boundary, s, of area S is located remote from both the dislocation and the carbon

interstitial and is traction free. Hydrogen solutes inside S induce a continuously varying dilatational transformation strain field which depends on the local hydrogen concentration as described by eq. (24). The carbon interstitial induces a transformation strain given by eqs. (38) and (39) which is assigned to the point at which the carbon atom is located. Since hydrogen interacts with the tetragonal distortion of the carbon interstitial, the hydrogen concentration is calculated using an interaction energy based on the hydrostatic stress fields of the other hydrogen solutes, the carbon itself and the dislocation. Solution to this problem requires iteration as has been discussed in Section 3.2. The stress field due to carbon, σ_C, is calculated next by considering the carbon transformation strain fixed at the same position inside the region S in the absence of the dislocation and the hydrogen solutes (carbon/no-hydrogen). The external circular boundary of the region S is again traction free and its elastic moduli vary pointwise as dictated by the distribution of hydrogen in the combined carbon/hydrogen problem. The carbon/no-hydrogen problem is linear and can be solved directly.

Both stress fields of the combined carbon/hydrogen problem, and that of the carbon/no-hydrogen are analyzed in plane strain deformation conditions. Consider a Cartesian coordinate system x_1, x_2, x_3 centered at the dislocation core with the x_3 axis lying along the dislocation line in the [211] direction of the unit cell and the Burgers vector lying along the [$\bar{1}$11]. The domain S is identified with a circular region on the plane x_1, x_2. Using eq. (38) one may find the unit cell components of the carbon transformation strain tensor with respect to the system of axes x_1, x_2, x_3 as

$$[\varepsilon^{CT}]_{ij} = \begin{bmatrix} \frac{1}{3}(\varepsilon_1 + \varepsilon_2 + \varepsilon_3) & \frac{1}{\sqrt{6}}(\varepsilon_3 - \varepsilon_2) & 0 \\ \frac{1}{\sqrt{6}}(\varepsilon_3 - \varepsilon_2) & \frac{1}{2}(\varepsilon_2 + \varepsilon_3) & 0 \\ 0 & 0 & \frac{2}{3}\varepsilon_1 + \frac{1}{6}(\varepsilon_2 + \varepsilon_3) \end{bmatrix} \qquad (40)$$

where strains ε_{13}^{CT} and ε_{23}^{CT} have been set equal to zero, since under plane strain conditions they do not affect the interaction of hydrogen with the stress field of the dislocation nor with the stress field of the hydrogen solutes. In accord with the plane strain deformation, the carbon mechanical effect can be thought of as arising from an infinite sequence of unit cubic cells all containing carbon atoms and aligned along an axis which is parallel to the x_3 axis. It is assumed that this infinitely long parallelepiped of unit cells intersects the x_1, x_2 plane over a plane domain S_c whose area is given by a_c^2 where a_c is a typical length scale of S_c. In the continuum plane strain model of the carbon induced distortion domain S_c is taken to represent an area which undergoes a transformation strain due to carbon. The magnitude of the transformation strain inside S_c can be calculated as follows: The unconstrained volume change of a unit cell in the cylinder-in-hole model equals $\varepsilon_{kk}^{CT} a^3$. Hence, the unit length of the parallelepiped which contains $1/a$ unit cells exhibits an unconstrained volume change equal to $\varepsilon_{kk}^{CT} a^2$. Assuming this volume change, $\varepsilon_{kk}^{CT} a^2$, to be induced by an area expansion in the x_1, x_2 plane, one finds an unconstrained area change per unit length equal to $\varepsilon_{kk}^{CT} a^2$. A volumetric transformation strain, ε^C, consistent with this area change may then be derived by equating $\varepsilon_{kk}^{CT} a^2$ to $\varepsilon_{kk}^C a_c^2$. Thus, under plane strain deformation conditions, the carbon lattice distortion is modeled through the area S_c which undergoes a uniform transformation strain, ε^C, such that

$$\varepsilon_{ij}^C = \left(\frac{a}{a_c}\right)^2 \varepsilon_{ij}^{CT} \tag{41}$$

in the system of x_1, x_2, x_3 axes.

The governing equations for both carbon/hydrogen and carbon/no-hydrogen problems are given in plane strain by eqs. (30) and (31) with volume V replaced by area S,

$$\varepsilon_{ij}^T = \begin{cases} \varepsilon_{ij}^C & \text{in} & S_c \\ \varepsilon_{ij}^H & \text{in} & S - S_c \end{cases} \tag{42}$$

for the carbon-hydrogen problem, and

$$\varepsilon_{ij}^T = \begin{cases} \varepsilon_{ij}^C & \text{in} & S_c \\ 0 & \text{in} & S - S_c \end{cases} \tag{43}$$

for the carbon/no-hydrogen problem.

(ii) *Finite element method*

Solutions to both problems were found by the finite element method. The corresponding equations are (32), (33), (34) and (35) with the transformation strain array $\{\varepsilon^{Tr}\}$ appropriately modified to account for eqs. (42) and (43). The domain S was discretized into 1560 4-noded quadrilateral isoparametric and 24 3-noded triangle elements with a total of 1585 nodes. The dislocation core represents the first node. The rest of the nodes were placed on 66 circles centered at the core node number 1 and of increasing radii. On each circle, 20 nodes were placed at 15^0 apart. The dislocation core elements are triangular and all others are focused isosceles trapezoids. The element sides in the first 46 rings constitute an arithmetic progression with a first term, that is the side of the triangle core element, equal to $\lambda_1 b$ and a common difference equal to $\lambda_2 b$. Constants λ_1 and λ_2 are chosen less than unity in order for the mesh to be fine in the field near the dislocation core and the

carbon region, S_c. The far field mesh was composed of the remaining 20 rings of elements. The ratio of the size of an element in any ring of the far field mesh to the size of the element in the immediately preceding ring was 2. Fine discretization of the near core region was used for accurate modeling of the stress due to both hydrogen and carbon. The carbon atom position was taken always at the centroid of a near field element. The corresponding element area was identified with area S_c which was assigned to undergo a uniform strain transformation ε^c determined through eq. (41) with a_c^2 set equal to the element area. The finite element equations for the combined carbon/hydrogen problem were solved by the iterative technique described in Section 3.2.

(iii) *Results and interaction energy*

The finite element parameters, λ_1 and λ_2, were set equal to 0.02 and 0.08 respectively. In this case the side of the triangle element was $0.02b$ and the common difference in the arithmetic progression of the element sides in the near field mesh was $0.008b$. The radius of the outer boundary of the circular region corresponding to the near field mesh was $9.2b$ and the outer radius of the circular domain S was $796926.2b$.

Finite element solutions were obtained for the carbon/no-hydrogen problem with the moduli taken constant and equal to those of the hydrogen free material. The carbon area S_c was fixed on the x_1, x_2 plane at position (r,ϕ) relative to the origin. By averaging the shear stress σ_{12} over the 24 triangle elements round the origin, one finds the shear stress, τ, an edge dislocation would undergo on its slip system if it were introduced at the origin in the absence of hydrogen. The interaction energy per unit length between the dislocation and the carbon atom can be found through

$$W = -\int_{S_c} (\sigma_D)_{ij} \varepsilon_{ij}^C dS \tag{44}$$

where $(\sigma_D)_{ij}$ are the components of the singular dislocation stress field, σ_D, (HIRTH and LOTHE, 1982). Using eqs. (40) and (41) one can evaluate the surface integral in eq. (44) numerically. The results are shown in Figs. 17 and 18 where the shear stress and the interaction energy per slab of thickness a respectively are plotted against normalized distance r/b of the carbon atom from the dislocation core at an angle $\phi = -37.5^0$. Figures 19 and 20 show the same results at fixed distance $r/b = 1.2$ and angle $0 \le \phi \le 2\pi$. The analytic solution (COCHARDT et al., 1955)

$$\tau = -\frac{Da^2}{r^2 b} \left\{ \frac{1}{3}(\varepsilon_1 + \varepsilon_2 + \varepsilon_3)[(1+v)\sin 2\phi + \sin 4\phi] \right.$$
$$-(\varepsilon_2 + \varepsilon_3)\sin\phi\cos 3\phi - \frac{\sqrt{6}}{3}(\varepsilon_3 - \varepsilon_2)\cos 4\phi$$
$$\left. + v\varepsilon_1 \sin 2\phi \right\}, \tag{45}$$

$$W = -\frac{Da^2}{r} \left\{ \frac{1}{3}\sin\phi(1 + v + 2\cos^2\phi)(\varepsilon_1 + \varepsilon_2 + \varepsilon_3) \right.$$
$$-\frac{1}{2}(\varepsilon_2 + \varepsilon_3)\sin\phi\cos 2\phi$$
$$\left. -\frac{\sqrt{6}}{3}\cos\phi\cos 2\phi(\varepsilon_3 - \varepsilon_2) + v\varepsilon_1\sin\phi \right\} \tag{46}$$

where $D = \mu b / [2\pi(1-v)]$, is shown in Figs. 17 through 20 as the lines for comparison with the finite element calculations which are the plotted points. Figures 17 through 20 show that the finite element solutions are very accurate, thereby implying that the plane strain model used for the carbon distortion field simulates the mechanical behavior of the carbon interstitial reliably.

The finite element solutions for the carbon/hydrogen problem provide the distribution of the hydrogen atoms round the dislocation and the carbon atom.

Representative situations are shown in Fig. 21 where the solution for the iso-concentration lines was obtained without accounting for the hydrogen induced modulus change, and in Fig. 22 where the modulus effect taken into consideration. Both calculations were carried out at nominal concentration of H/M=0.1, with the carbon interstitial at position $r/b = 1.2$, $\phi = -37.5^0$, the carbon tetragonal axis in the [001] direction and the edge dislocation line along the [211] direction with its Burgers vector in the [$\bar{1}$11]. In agreement with the discussion in Section 3.2, iso-concentration curves (Fig. 22) are found to be located at a greater distance from the dislocation relative to the corresponding ones in Fig. 21 because the hydrogen effect on the moduli increases the hydrostatic stress of the dislocation at any particular radial distance resulting in an increased hydrogen concentration below the dislocation slip plane. Averaging the calculated shear stress, $\left(\sigma_H + \sigma_C\right)_{12}$, in the carbon/hydrogen problem over the 24 triangle elements around the origin, one finds the shear stress exerted on the dislocation resolved along the slip plane and in the direction of the Burgers vector for a dislocation introduced at the origin against the stress fields of the hydrogen and carbon interstitials. This stress, normalized by the shear modulus of the hydrogen free material, is plotted in Figs. 23 through 25 as a function of the carbon atom position along the x_1 direction on a plane parallel to and below the dislocation slip plane at $x_2 = -0.505b$, for carbon tetragonal axes along [100], [010] and [001] respectively. The results of Figs. 23 to 25 may also be interpreted by considering the carbon atom fixed at the origin while the dislocation moves from position $x_1/b = -4$ to $x_1/b = 4$ with the resolved shear stresses being those required to hold the dislocation at equilibrium at each point. A positive stress corresponds to a force which pushes the dislocation in the positive x_1 direction. Results of Figs. 23 to 25 do not demonstrate any significant hydrogen effect on the dislocation/carbon interaction stress.

Another way to study the hydrogen effect is by calculating the change in the interaction energy W between the dislocation and the carbon atom caused by the presence of hydrogen. According to eq. (46), the stress fields of the edge dislocation and the carbon atom do not interact when the defects are at a sufficiently large distance apart. In that case the atmospheres which form round the edge dislocation and the carbon atom, upon the introduction of hydrogen into the lattice, can be considered effectively identical to those that would form round each of the defects in the absence of the other. Upon the action of an external stress, the dislocation and its symmetric atmosphere (configuration A) can be brought close to the carbon atom and its hydrogen atmosphere (configuration B) so that the constituents of the configurations A and B begin to interact among one another. The result of this interaction is a configuration AB characterized by hydrogen redistribution round the two defects. The corresponding hydrogen atmosphere of configuration AB is furnished by a solution of the carbon/hydrogen problem. In bringing configurations A and B together, the assumption of an open system was introduced with fast diffusion relaxation rates. The hydrogen effect can be assessed by comparing the interaction energy W_H between configurations A and B to the interaction energy W in the absence of hydrogen as given by eq. (46).

In the following, the dislocation stress field is calculated as in HIRTH and LOTHE (1982) but use is made of the linear elastic moduli as affected by the corresponding local hydrogen composition. An elastic state $\left(\sigma, T, \varepsilon, \varepsilon_{elast}, \varepsilon^T, u\right)$ is defined over the region S loaded with tractions T along the boundary s by a transformation strain field ε^T, an elastic strain field ε_{elast}, a net strain field $\varepsilon = \varepsilon_{elast} + \varepsilon^T$, and a displacement field u such that

$$\left.\begin{aligned}
\sigma_{ij,j} &= 0 \\
\varepsilon_{ij} &= \frac{1}{2}\left(u_{i,j} + u_{j,i}\right) \\
\sigma_{ij} &= C_{ijkl}\left(\varepsilon_{kl} - \varepsilon_{kl}^{T}\right)
\end{aligned}\right\} \quad \text{in} \quad S$$

$$\sigma_{ij}n_j = T_i \qquad \text{on} \quad s. \tag{47}$$

When the configurations A and B interact, the final elastic state for configuration AB is found by linear superposition of states $\left(\sigma_D, T_D, \varepsilon = \varepsilon_D, \varepsilon_{elast} = \varepsilon_D, \varepsilon^T = 0, u_D\right)$ of the dislocation, $\left(\sigma_C, T_C = 0, \varepsilon = \varepsilon^{(C)}, \varepsilon_{elast} = \varepsilon_C, \varepsilon^T = \varepsilon^C, u^{(C)}\right)$ of the carbon atom furnished by the solution to the carbon/no-hydrogen problem and $\left(\sigma_H, T_H = 0, \varepsilon = \varepsilon^{(H)}, \varepsilon_{elast} = \varepsilon_H, \varepsilon^T = \varepsilon^H, u^{(H)}\right)$ of the hydrogen atmosphere as calculated in the carbon/hydrogen problem. The elastic state for the dislocation is found after the carbon/hydrogen problem is solved and the elastic moduli are determined by the corresponding hydrogen concentration. By linear superposition the potential energy $W(D,C,H)$ per unit length of configuration AB is given by

$$W(D,C,H) = \frac{1}{2}\int_{S}\left(\sigma_D + \sigma_C + \sigma_H\right)_{ij}\left(\varepsilon_D + \varepsilon_C + \varepsilon_H\right)_{ij} dS - \int_{s}\left(T_D\right)_i\left(u_D + u^{(C)} + u^{(H)}\right)_i ds \tag{48}$$

where D stands for dislocation, C for carbon and H for hydrogen. In Appendix B it is shown that eq. (48) may be cast into

$$W(D,C,H) = -\frac{1}{2}\int_{S-S_{core}}\left(\sigma_D\right)_{ij}\left(\varepsilon_D\right)_{ij} dS - \frac{1}{2}\int_{S}\left(\sigma_C\right)_{ij}\left(\varepsilon^C\right)_{ij} dS - \frac{1}{2}\int_{S}\left(\sigma_H\right)_{ij}\left(\varepsilon^H\right)_{ij} dS$$
$$-\int_{S}\left(\sigma_D\right)_{ij}\left(\varepsilon^C\right)_{ij} dS - \int_{S}\left(\sigma_D\right)_{ij}\left(\varepsilon^H\right)_{ij} dS - \int_{S}\left(\sigma_H\right)_{ij}\left(\varepsilon^C\right)_{ij} dS \tag{49}$$

where S_{core} is the excluded core region of the dislocation. The elastic state for configuration A is found by linear superposition of state $\left(\sigma_{DH}, T_{DH}, \varepsilon = \varepsilon_{DH}, \varepsilon_{elast} = \varepsilon_{DH}, \varepsilon^T = 0, u_{DH}\right)$ for the dislocation in an infinite medium and state $\left(\sigma_{HD}, T_{HD} = 0, \varepsilon = \varepsilon^{(HD)}, \varepsilon_{elast} = \varepsilon_{HD}, \varepsilon^T = \varepsilon^{HD}, u^{(HD)}\right)$ for its symmetric atmosphere in the absence of the carbon interstitial. Both states are calculated by solving the carbon/hydrogen problem with the carbon area S_C taken to be occupied by hydrogen

instead of the carbon atom. The stresses, strains and displacements in these two states of configuration A are different from the corresponding ones in configuration AB because the respective hydrogen atmospheres and consequently the elastic moduli are different. Similarly, by solving the carbon/hydrogen problem, one calculates the elastic state $\left(\sigma_{HC}, \mathbf{T}_{HC} = 0, \varepsilon = \varepsilon^{(HC)}, \varepsilon_{elast} = \varepsilon_{HC}, \varepsilon^{T} = \varepsilon^{HC}, \mathbf{u}^{(HC)}\right)$ for the hydrogen atmosphere around the carbon atom in the absence of the dislocation and its contribution to interaction energy W_{int} of eq. (7), and the elastic state $\left(\sigma_{CH}, \mathbf{T}_{CH} = 0, \varepsilon = \varepsilon^{(CH)}, \varepsilon_{elast} = \varepsilon_{CH}, \varepsilon^{T} = \varepsilon^{C}, \mathbf{u}^{(CH)}\right)$ for the carbon atom alone in an infinite medium whose moduli have been changed by the hydrogen atmosphere of configuration B. Superposing these two elastic states, one finds the elastic state for configuration B. The potential energy for configuration A is computed from eq. (48) by dropping the terms related to the carbon atom

$$W(D,H) = -\frac{1}{2}\int_{S-S_{core}}(\sigma_{DH})_{ij}(\varepsilon_{DH})_{ij}\,dS - \frac{1}{2}\int_{S}(\sigma_{HD})_{ij}(\varepsilon^{HD})_{ij}\,dS - \int_{S}(\sigma_{DH})_{ij}(\varepsilon^{HD})_{ij}\,dS \qquad (50)$$

and the potential energy for configuration B is computed by dropping the terms related to the dislocation

$$W(C,H) = -\frac{1}{2}\int_{S}(\sigma_{CH})_{ij}(\varepsilon^{C})_{ij}\,dS - \frac{1}{2}\int_{S}(\sigma_{HC})_{ij}(\varepsilon^{HC})_{ij}\,dS - \int_{S}(\sigma_{HC})_{ij}(\varepsilon^{C})_{ij}\,dS. \qquad (51)$$

The interaction energy between configurations A and B is defined as

$$W_{H} = W(D,C,H) - W(D,H) - W(C,H) \qquad (52)$$

and using eqs. (49), (50) and (51) one finds

$$W_H = \frac{1}{2} \int\limits_{S-S_{core}} (\sigma_{DH})_{ij} (\varepsilon_{DH})_{ij} dS - \frac{1}{2} \int\limits_{S-S_{core}} (\sigma_D)_{ij} (\varepsilon_D)_{ij} dS$$

$$+ \left(-\frac{1}{2} \int\limits_S (\sigma_C)_{ij} (\varepsilon^C)_{ij} dS \right) - \left(-\frac{1}{2} \int\limits_S (\sigma_{CH})_{ij} (\varepsilon^C)_{ij} dS \right)$$

$$+ \left(-\frac{1}{2} \int\limits_S (\sigma_H)_{ij} (\varepsilon^H)_{ij} dS \right) - \left(-\frac{1}{2} \int\limits_S (\sigma_{HD})_{ij} (\varepsilon^{HD})_{ij} dS \right) - \left(-\frac{1}{2} \int\limits_S (\sigma_{HC})_{ij} (\varepsilon^{HC})_{ij} dS \right)$$

$$- \int\limits_S (\sigma_D + \sigma_H - \sigma_{HC})_{ij} (\varepsilon^C)_{ij} dS$$

$$+ \left(-\int\limits_S (\sigma_D)_{ij} (\varepsilon^H)_{ij} dS \right) - \left(-\int\limits_S (\sigma_{DH})_{ij} (\varepsilon^{HD})_{ij} dS \right). \tag{53}$$

The first line in the right hand side of eq. (53) represents the difference in the strain energy of the edge dislocation between configurations A and AB. The second line represents the difference in the strain energy of solution of the carbon interstitial between configurations B and AB. The three terms in the third line represent the strain energy of solution of hydrogen in configurations AB, A and B respectively. The fourth line represents interaction energy between the dislocation in configuration AB, the hydrogen in configuration AB and the hydrogen in configuration B with the carbon atom. The last line represents the difference in the interaction energy of the edge dislocation with its hydrogen atmosphere between configurations AB and A. The formalism which led to eq. (53) is not restricted only to the case of hydrogen studied, but can be applied for interaction energy calculations involving stresses caused by any distribution of stress centers.

The issue of whether to include the elastic strain energy (the terms in the third line of eq. (53)) in the calculation of the interaction energy between the dislocation and the carbon atom in the presence of hydrogen solutes depends on whether the system is an "open" or "closed" system. An "open" system can exchange hydrogen with its thermodynamic reservoir, e.g. a gas phase, while a "closed" system is inhibited from doing so by kinetics, the presence of an

impermeable oxide film, etc. Processes in which the interactions between the dislocation and elastic centers, such as carbon solutes, are rapid compared to the time for equilibrium of the solid with the hydrogen reservoir can be considered "pseudo-closed." In this case the stress fields allow local rearrangements of the hydrogen solutes and concentrations without changing the overall hydrogen concentration in the solid by transfer of hydrogen across the external surfaces of the solid. In all of the previous calculations of the interaction stresses between the dislocations and the stress centers, the system was "closed" or "pseudo-closed" and local equilibration of the hydrogen concentration was allowed. An explicit choice must be made in the calculation of the elastic interaction energies as the terms in the third line must be included for an "open" system but not for a "closed" or "pseudo-closed" system. In these latter cases, the total amount of hydrogen in the system remains constant. It should be pointed out that the terms in the third line of eq. (53) account for only the strain energy portion of the energy of solution of hydrogen and that in general, the strain energy is only a small component of the total energy of solution.

In the present paper, the strain energy terms will not be considered in calculating the interaction energies between dislocations and elastic strain centers in the presence of hydrogen. This is appropriate for considerations of the effects of hydrogen on deformation and fracture as many systems have barriers to equilibrium with the ambient. In addition, the times appropriate to describe the interactions of dislocations with defects are very small compared to the equilibration times for solution of hydrogen from the gas phase. The stress effects on the total hydrogen concentration in the specimen (third line of eq. (53)) are appropriate in discussing the effects of dislocations in the solubility of hydrogen in equilibrium with a reference state (FLANNAGAN, MASON and BIRNBAUM, 1981; KIRCHHEIM, 1986)

Notice that in the absence of hydrogen only the first term in the third line survives and the result is identical to that of eq. (44). In the presence of hydrogen, but by neglecting the change in elastic moduli due to hydrogen and the strain energy of solution of hydrogen results in a modification of eq. (53) to yield for the interaction energy

$$W_H' = -\int_S (\sigma_D + \sigma_H - \sigma_{HC})_{ij} (\varepsilon^C)_{ij} dS + \left(-\int_S (\sigma_D)_{ij} (\varepsilon^H)_{ij} dS \right) - \left(-\int_S (\sigma_{DH})_{ij} (\varepsilon^{HD})_{ij} dS \right). \quad (54)$$

The calculation of the interaction energy W_H in eq. (53) is insensitive to the magnitude of the core area when the core cutoff radius is sufficiently small. For a small cutoff radius, stresses close to the core are sufficiently high to allow the tensile side of the dislocation to be saturated with hydrogen and the compressive side to be significantly depleted of hydrogen in configurations A and AB. In that case the region very close to the core exhibits the same elastic moduli in configurations A and AB and consequently the elastic strain energy associated with the dislocation singular stress field of that region is also the same for configurations A and AB. As a result, the corresponding contribution of the near core regions to the difference in the dislocation strain energy in eq. (53) is zero. Hydrogen concentrations at the core elements whose side was chosen equal to $0.02b$ were always at hydrogen saturation levels for elements on the tensile side of the core and zero for those on the compressive side.

In Figs. 26 through 28 the interaction energy per interatomic distance aW, between the dislocation and the carbon atom having the tetragonal axes in directions [100], [010] and [001], in the absence of hydrogen is plotted against the carbon atom position x_1/b, $x_2/b = -0.505$ relative to the dislocation which is fixed at the origin of the coordinate system. Energy aW is measured in eV per slab of thickness a and is calculated using eq. (46). The same figures show the results of

calculations in the presence of hydrogen for the interaction energy aW_H' calculated by eq. (54) with neglect of the modulus effect, and the interaction energy aW_H calculated using eq. (53) taking account of the modulus effect. Figures 26 to 28 demonstrate a negative interaction energy when the dislocation approaches the carbon interstitial as expected. The presence of hydrogen reduces the strength of the interaction with the effect being greater if the modulus effect is included in the calculation.

The dependence of the hydrogen effect on the distance x_2/b of the carbon atom from the slip plane was investigated by a series of calculations with $x_2/b = -3.046$. The results are shown in Fig. 29 where the interaction energies aW, aW_H' and aW_H are plotted against the carbon atom position x_1/b relative to the dislocation. The carbon atom occupied the interstitial position having a [010] tetragonal axis and the nominal H/M ratio was 0.1 As shown in Fig. 29, at large dislocation-carbon separations the presence of hydrogen increases the magnitude of the interaction energy slightly and alters the shape and position of the interaction relative to the solution in the absence of hydrogen. Figure 29 also shows that the modulus effect becomes relatively unimportant when the dislocation and the carbon atom are at distance greater than about 3 Burgers vectors. Since the force exerted by the C solute on the dislocation is given by the slope of the interaction curves, in Fig. 29 it is seen that at large values of x_2/b hydrogen significantly decreases the force on the dislocation for $x_1/b < 0$, in contrast to the small effect of hydrogen on the force at small values of x_2/b (Fig. 24).

(iv) *Discussion of the results*

The results shown in Figs. 23 to 28 are consistent with the well known phenomenon of the dislocation motion hindered by impurity atoms. The pinning of dislocations by interstitial solutes such as carbon results from a negative interaction energy when the defects are very close to each other. The addition of

hydrogen to the system decreases the magnitude of this negative interaction energy, thereby diminishing the ability of the solute atoms to pin the dislocations. As previously discussed, the present calculations take only the first order elastic interaction energy between the dislocation and the hydrogen solutes into account in calculating the H/M values near the dislocation. In general, the second order elastic interaction, due to hydrogen effects on the elastic moduli, is considerably less significant in determining the H/M values near the dislocation than the first order interaction, due to the elastic distortion field around the hydrogen, and is ignored in the present calculation. This second order elastic effect will be considered in a subsequent paper as it may make a significant contribution when the important interactions are close to the dislocation core, as in the present case of the dislocation - C - hydrogen interactions and when the shear modulus decreases as H/M increases leading to a negative value of $W_{int}^{(2)}$ and an increase in the H/M values close to the dislocation.

The calculated interactions between the edge dislocations and point defects and the influence of hydrogen on these interactions (Figs. 26 to 28) are in excellent agreement with the experimental measurements on the Ni-C-H system (SIROIS and BIRNBAUM, 1992). Hydrogen was shown to decrease the "activation enthalpy" for slip (corresponding to the decrease in the calculated interaction energy with hydrogen) and to decrease the "activation volume" (corresponding to the decrease in the width of the activation energy minimum). The magnitude and nature of the hydrogen effect depends strongly on the distance between the defects. Figures 26 to 29 show that the hydrogen effect is significant in weakening the interaction only when the dislocation slip plane-carbon distance is approximately less than $2b$. For defect distances greater than $2b$, the magnitude of the interaction energy is relatively unaffected by the presence of hydrogen. The force-displacement profile for the pinning interaction is markedly changed by hydrogen for dislocation slip plane-

carbon distances of $2b$ or greater and is unaffected by hydrogen for distances of less than $2b$. The same insensitivity of the interaction energy to the presence of hydrogen was observed when the edge dislocation slip plane was $3b$ below the carbon atom, i.e. when the carbon solute was in the compressive stress field.

Figures 26 to 29 indicate that at dislocation slip plane-defect distances less than $2b$ the hydrogen induced weakening of the interaction is predominantly due to the effect of hydrogen on the elastic moduli. Figure 29 shows that at distance greater than $3b$ the modulus effect causes almost no change to the interaction energy, compared to that caused by the dilatational effect. The local character of the modulus effect is in accordance with the same observation for the dislocation-dislocation interaction discussed in Section 3.3. It is worth noting, though, that at a nominal concentration of H/M = 0.1, the modulus effect on the dislocation-dislocation interaction was nearly independent of the defect distance (see Fig. 13) while in the case of the carbon-dislocation system the effect does exhibit a dependence on the defect separation particularly when it is less than $2b$. This can be attributed to the continuous modification of the shape and relative position of the hydrogen iso-concentration curves, and in turn of those of the elastic moduli, as the dislocation passes above the carbon atom whose distortion field is not symmetric.

Lastly, the minimal hydrogen effect on the shear stress exerted on the slip plane of the dislocation shown in Figs. 23 to 25 can be explained by the fact that the curves of Figs. 25 to 28 are almost parallel to one another and that stress $\left(\sigma_H + \sigma_C \right)_{12}$ equals the negative of the derivative of the interaction energy W_H with respect to distance.

4. 2. Screw dislocation

(i) *Interaction energy in the absence of hydrogen*

Consider Cartesian coordinates x_1, x_2, x_3 with axis x_3 parallel to the dislocation line along the [111] direction of the unit cell in a BCC lattice. Choose axis x_1 parallel to the direction [$2\bar{1}\bar{1}$] which is the projection of the 1-axis of the cell in the plane normal to the dislocation, (x_1, x_2 plane). The carbon atom position in the vicinity of the dislocation can be described by cylindrical polar coordinates (r, ϕ, x_3) with the angle ϕ measured from the positive x_1 axis. Using the rule of transformation of axes and eq. (40), one finds the components of the carbon transformation strain tensor in system x_1, x_2, x_3 as

$$\left[\varepsilon^{CT}\right]_{ij} = \begin{bmatrix} \frac{1}{6}(4\varepsilon_1 + \varepsilon_2 + \varepsilon_3) & \frac{1}{\sqrt{12}}(\varepsilon_3 - \varepsilon_2) & \frac{1}{\sqrt{18}}(2\varepsilon_1 - \varepsilon_2 - \varepsilon_3) \\ \frac{1}{\sqrt{12}}(\varepsilon_3 - \varepsilon_2) & \frac{1}{2}(\varepsilon_2 + \varepsilon_3) & \frac{1}{\sqrt{6}}(\varepsilon_2 - \varepsilon_3) \\ \frac{1}{\sqrt{18}}(2\varepsilon_1 - \varepsilon_2 - \varepsilon_3) & \frac{1}{\sqrt{6}}(\varepsilon_2 - \varepsilon_3) & \frac{1}{3}(\varepsilon_1 + \varepsilon_2 + \varepsilon_3) \end{bmatrix} \tag{55}$$

With respect to the same system, the stress components of the anti-plane dislocation strain field are given in HIRTH and LOTHE (1982) as

$$\left[\sigma_D\right]_{ij} = \frac{\mu b}{2\pi r} \begin{bmatrix} 0 & 0 & -\sin\phi \\ 0 & 0 & \cos\phi \\ -\sin\phi & \cos\phi & 0 \end{bmatrix} \tag{56}$$

Equations (55) and (56) can be used to calculate the interaction energy per slab of thickness a between the dislocation and the carbon interstitial atom

$$aW = -\int_{V_{cell}} (\sigma_D)_{ij} (\varepsilon^{TC})_{ij} dV$$

$$= -a^3 \frac{\mu b}{6\pi r} \left[\sqrt{6}(\varepsilon_2 - \varepsilon_3)\cos\phi - \sqrt{2}(2\varepsilon_1 - \varepsilon_2 - \varepsilon_3)\sin\phi\right] \tag{57}$$

where V_{cell} is the volume of the unit cell. It is worth noting that eq. (57) for the interaction energy differs from the corresponding relation

$$aW = \frac{\sqrt{2}b\mu a^3}{3\pi}(\varepsilon_1 - \varepsilon_2)\frac{\cos\theta}{r} \qquad (58)$$

given by COCHARDT et al. (1955) with θ defined as the fixed angle between their x_1 axis, labelled as x', and the $[2\bar{1}\bar{1}]$ direction. This relation, (58), appears to be in error as it suggests an interaction energy dependent on the choice of the x' coordinate axis, and does not account for the dependence of the interaction energy upon the relative angular position between the carbon atom and the screw dislocation.

(ii) Hydrogen effect

Equation (56) shows that the stress field of a screw dislocation is purely deviatoric. This implies, to first order, that there is no interaction between the dislocation and the hydrostatic distortion due to hydrogen atom. In the present calculation, the modulus effect on W_{int} for the evaluation of the hydrogen concentration field around the screw dislocation through eq. (7) was neglected. Therefore, the amount of hydrogen in configuration A is unaffected by the presence of the screw dislocation and the hydrogen concentration remains uniform in space and equal to the nominal concentration C_0. Moreover, as the the screw dislocation approaches configuration B and begins to interact with the carbon atom according to eq. (57), the hydrogen atmosphere in configuration B is not affected by the stress of the screw dislocation. Therefore, any changes to the interaction energy W given by eq. (57) are associated with configuration B, that is, the carbon interstitial and its hydrogen atmosphere. In view of this discussion, the interaction energy between configurations A and B was calculated using eq. (53)

$$W_H = W + \frac{1}{2}\int_{S-S_{core}}(\sigma_{DA})_{ij}(\varepsilon_{DA})_{ij}\,dS - \frac{1}{2}\int_{S-S_{core}}(\sigma_D)_{ij}(\varepsilon_D)_{ij}\,dS. \qquad (59)$$

The second term in the right hand side represents the strain energy of the screw dislocation in configuration A calculated as in HIRTH and LOTHE (1982) with the shear modulus evaluated by eq. (28) at nominal hydrogen concentration C_0, whereas the third term represents the strain energy of the dislocation accounting for the pointwise induced modulus change by the hydrogen atmosphere of the carbon atom. The hydrogen atmosphere in configuration B and the associated local constitutive moduli were calculated by solving the carbon/hydrogen problem, as in Section 4.1, with zero contribution from the dislocation stress field to the interaction energy W_{int} of eq. (7). This is a plane strain calculation where the carbon transformation strains ε_{ij}^C of eq. (41) were found by using eq. (55) with $\varepsilon_{13}^{CT} = \varepsilon_{23}^{CT} = 0$. This modification of the carbon transformation strain may be justified on the grounds that components ε_{13}^{CT} and ε_{23}^{CT} are out of plane shear strains and as such they do not interact with hydrogen.

(iii) *Results and discussion*

In Figs. 30, 31 and 32 the interaction energies aW and aW_H per slab of thickness a between the screw dislocation and carbon atoms having their tetragonal axes along directions [100], [010] and [001] respectively are plotted against its position x_1 / b, $x_2 / b = -0.505$ relative to the dislocation which is fixed at the origin of the coordinate system. The temperature was 300K and the nominal hydrogen concentration was H/M=0.1. As before with phenomena resulting from the second order modulus interaction, the hydrogen effect is significant only for dislocation-defect separations of approximately less than two Burgers vectors. Figure 30 shows that for [100] occupancy hydrogen increases the magnitude of the interaction of the screw dislocation with the carbon atom, thereby enhancing the latter's capability to hinder the dislocation motion. The equilibrium position is at $x_1 / b = 0$. Figure 31 shows that for [010] occupancy, hydrogen does not affect the dislocation motion from position

$x_1/b = 4$ towards the carbon atom at $x_1/b = 0$. However, the hydrogen reduces the energy barrier for the dislocation to move from the equilibrium position at $x_1/b \approx 0$ to negative values of x_1/b. Hydrogen thus facilitates the motion of the dislocation to negative x_1/b values introducing an asymmetry in the hydrogen softening. For [001] occupancy, Fig. 32 indicates a similar asymmetry in the hydrogen related decrease in the interaction energy, with the reduced interaction being in the region $x_1/b > -1$.

It is in the case of the screw dislocation - C - hydrogen interaction that the second order elastic interaction between the screw dislocation and the hydrogen solutes is expected to be the most significant. Since there is no first order elastic interaction which generates an increased H/M value in the vicinity of the dislocation, the hydrogen atmosphere is completely determined by the second order interaction energy, eq. (3). In the present calculations, the second order interaction energy is positive as the shear modulus increases with increasing H/M values and hence a hydrogen atmosphere will not occur around the screw dislocation, as is assumed. The case of a significant negative second order elastic interaction energy between solute hydrogen and the screw dislocation leading to a hydrogen atmosphere around the screw dislocation will be considered in a subsequent publication.

The interactions of screw dislocations with point defects having tetragonal symmetry are more complex than those which describe interactions with edge dislocations. One significant point is that the interaction can be asymmetric with respect to the direction of motion of the screw dislocation relative to the interstitial solute, e.g. for the system studied the interaction is asymmetric except for the C interstitial having the [100] tetragonal axis (Figs. 30, 31, and 32). The effects of hydrogen on the interactions of the C interstitials with screw dislocations are correspondingly complex. For interactions with defects having the [100] tetragonal

axis, the effect of hydrogen is to increase the interaction energy between the screw dislocation and the C solute (Fig. 30). For [010] and [001] tetragonal axis orientations, adding hydrogen to the system decreases the interaction energies in those regions where the C - screw dislocation interactions are repulsive and has little effect in the regions where there is an attractive interaction between the defects. The width of the repulsive interaction energy region is also significantly decreased by the addition of hydrogen.

All three C solute orientations are likely to be equally populated in the volume of a crystal far from dislocations. At the dislocation the C solute having a [100] orientation of the tetragonal axis is most probable due to the elastic interaction energy and since C reorientation can occur with only one defect jump, this orientation will be most highly populated. A moving screw dislocation is likely to experience interactions with all three C orientations with equal probability. The addition of hydrogen to the system will increase the probability of interactions of the screw dislocations with C solutes having [100] orientations when the interactions allow reorientation of the C solute. In these cases the H increases the magnitude of the attractive interaction between the screw dislocation and the [100] C solute. This should lead to a decrease in the mobility of the screw dislocations on adding H to the system containing C solutes at temperatures where they can reorient during the interactions. At lower temperatures where reorientation of the C solutes is not possible, the effects of H on the carbon-screw dislocation interactions are more complex. The increased magnitude of the attractive interaction energy for [100] C solutes (which should decrease the dislocation mobility) is balanced against the decreased magnitude of the repulsive interactions for the [010] and [001] C solutes (which should increase the mobility). Both attractive and repulsive interactions need to be overcome during the motion of the dislocations. In the Fe-H system (TABATA and BIRNBAUM, 1984) screw dislocation mobility was observed to

increase when hydrogen was added to the system. Detailed experimental measurements of these interactions have only been made in the Ni-C-H system (SIROIS and BIRNBAUM, 1992). Since this is an FCC system and hence the C interstitial solutes have a cubic distortion field, the calculations of the present paper are not directly applicable.

5. CLOSURE

A method for calculating the effects of a mobile solute species, such as hydrogen, on the interaction between elastic centers has been developed. This method allows modeling of the lattice distortion induced by a single or a continuous distribution of interstitial atoms coupled with the distortion field of lattice defects such as dislocations. The method was applied using analytical and finite element methods to study the effects of hydrogen on the interaction between dislocations and between dislocations and solutes such as C interstitials. Included in the calculational method is the minimization of elastic energy of the system thus allowing the hydrogen distribution to respond to the local stress field of the elastic centers. The mobile hydrogen solutes exhibit the phenomena of "elastic shielding" of the interactions between two elastic stress centers, i.e. the redistribution of the hydrogen solutes to decrease the elastic energy of the system. In most cases this "elastic shielding" results in a decrease of the interactions energy and forces between the elastic centers.

Model calculations were carried out for the case where hydrogen increased the shear modulus of the system and in which the second order elastic interaction between the dislocations and hydrogen could be neglected. These calculations, by both finite element and analytical methods, of the hydrogen induced "elastic shielding" of the interaction between two dislocations showed a decrease in the

elastic force between the two dislocations which varied with the distance between the dislocations and with the hydrogen concentration. The effect was largest when the dislocations were separated by small distances and resulted from the lattice dilatation of the hydrogen solutes and their effect on the local elastic modulus of the matrix. For a H/M value of 0.01 the decrease of the force between two edge dislocations separated by 3 Burgers vectors was about 8% and this increased to about 21% for H/M=0.1.

Calculations of the interactions between an edge dislocation and a C interstitial in a BCC solid were carried out using the method of COCHARDT et al. (1955) and the effect of hydrogen on these interactions was studied. The carbon-edge dislocation interaction results from the dilatational stress around the C as well as from the deviatoric components. Significant decreases in the interaction energies between the edge dislocation and the C interstitial due to "elastic shielding" by hydrogen was observed when the C was less than two Burgers vector below the slip plane. When the C was below the slip plane by greater than about 2 Burgers vectors, a small increase in the interaction energies was observed. The decrease in the elastic interaction energy between the edge dislocation and the C interstitial was observed for all three orientations of the tetragonal axis of the C solute. These effects on the interaction energies were shown to be due predominantly to the H induced local changes in the elastic moduli.

Hydrogen shielding effects were also studied for the interaction of C interstitials with screw dislocations in the BCC lattice. The carbon-screw dislocation interaction energy results from only the deviatoric components of the distortion field around the C. Hydrogen effects on the interaction energy in this case result from the local modulus changes due to the hydrogen atmosphere around the C interstitial. The effects of elastic shielding in this case are somewhat more complex

than in the case of the edge dislocation interaction. The interaction energy with one of the C orientations is increased while those with the other two are decreased.

APPENDIX A : HYDROGEN INDUCED SHEAR STRESS ON THE DISLOCATION SLIP PLANE - NUMERICAL INTEGRATION OF EQ. (21)

Consider the integrand of eq. (21) in the limit as $r \to 0$ along any radius such that $\pi < \phi < 2\pi$. This limit expresses the contribution to the shear stress τ_H of the hydrogen which resides at the core of the dislocation 2 (see Fig. 1). More specifically, it accounts for that part of the contribution that is found when the core is approached through the tensile region of the dislocation 2. On the tensile side of the core, the in-plane hydrostatic stress becomes infinite and the corresponding equilibrium hydrogen concentration is finite and equal to N_L. Therefore, the integrand of eq. (21) is singular for a value of r, namely for $r = 0$, which is close to the lower limit of integration, r_1. When the core of the dislocation 2 is approached along a radial direction in the compressive region it can be easily shown that the concentration tends to zero at a faster rate than the radius thus causing the integrand to be zero. At the core of the dislocation 1, that is at $r = l$, the hydrogen concentration is 0 on the side of the compressive region and N_L on the side of the tensile region. Since r is equal to l, that is, r is finite, the integrand of eq. (21) at the core of dislocation 1 is finite as well. Again, the circular area of the core of the dislocation 1 was excluded from the integration.

The singularity at $r = 0$ is treated by changing the variable of integration, i.e. by setting $r = 1/x$. In terms of the new variable, x, eq. (22) for the in-plane hydrostatic stress can be written as

$$\frac{\sigma_{11}^a + \sigma_{22}^a}{2} = -\frac{\mu}{2\pi(1-\nu)} x \left(b_2 \sin\phi + b_1 \frac{\sin\phi - xl\sin\omega}{1 + x^2 l^2 - 2xl\cos(\phi - \omega)} \right) \tag{A1}$$

whereas eq. (21)

$$\tau_H = -\frac{\mu}{2\pi(1-\nu)}\frac{V_H}{N_A}\int_0^{2\pi}\int_{\frac{1}{R}}^{\frac{1}{2}}C(x,\phi)\frac{\sin 2\phi}{x}\,dx\,d\phi \tag{A2}$$

In the limit as $x \to 0$ eq. (A1) gives zero in-plane hydrostatic stress which forces a finite equilibrium concentration equal to C_0, and thereby causing the integrand of eq. (A2) to be singular at $x = 0$. Expanding the concentration $C(x,\phi)$ in a Taylor series about $x = 0$ at constant ϕ one finds that

$$C(x,\phi) = C_0 + \frac{\partial C(x,\phi)}{\partial x}\bigg|_{x=0} x + O(x^2) \tag{A3}$$

where it can be shown that the second term in the right hand side of eq. (A3) is different from zero and finite. Therefore eq. (A2) may be recast into

$$\tau_H = -\frac{\mu}{2\pi(1-\nu)}\frac{V_H}{N_A}\int_0^{2\pi}\int_{\frac{1}{R}}^{\frac{1}{R}}\frac{C(x,\phi)-C_0}{x}\sin 2\phi\,dx\,d\phi \tag{A4}$$

with the integrand now being finite at $x = 0$.

For a given outer cutoff radius, R, of the hydrogen atmosphere the shear stress τ_H was evaluated numerically through eq. (A4) by slicing the domain of integration in the ϕ direction into sectors of equal angle. In each sector the double integral of eq. (A4) was calculated by using a 40 by 40 Gauss rule. The calculation was repeated by increasing the number of sectors until the values of the calculated shear stress τ_H was found independent of the number of sectors used.

APPENDIX B: INTERACTION ENERGY BETWEEN CONFIGURATION A (DISLOCATION AND ITS HYDROGEN ATMOSPHERE) AND CONFIGURATION B (CARBON ATOM AND ITS HYDROGEN ATMOSPHERE)

Excluding the area of the dislocation core region, S_{core}, one may write eq. (48) as follows

$$
\begin{aligned}
W(D,C,H) = & \frac{1}{2} \int_{S-S_{core}} (\sigma_D)_{ij} (\varepsilon_D)_{ij} dS + \frac{1}{2} \int_{S-S_{core}} (\sigma_D)_{ij} (\varepsilon_C)_{ij} dS + \frac{1}{2} \int_{S-S_{core}} (\sigma_D)_{ij} (\varepsilon_H)_{ij} dS \\
& + \frac{1}{2} \int_{S-S_{core}} (\sigma_C)_{ij} (\varepsilon_D)_{ij} dS + \frac{1}{2} \int_{S-S_{core}} (\sigma_C)_{ij} (\varepsilon_C)_{ij} dS + \frac{1}{2} \int_{S-S_{core}} (\sigma_C)_{ij} (\varepsilon_H)_{ij} dS \\
& + \frac{1}{2} \int_{S-S_{core}} (\sigma_H)_{ij} (\varepsilon_D)_{ij} dS + \frac{1}{2} \int_{S-S_{core}} (\sigma_H)_{ij} (\varepsilon_C)_{ij} dS + \frac{1}{2} \int_{S-S_{core}} (\sigma_H)_{ij} (\varepsilon_H)_{ij} dS \\
& - \int_{s+s_{core}} (T_D)_i \left(u_D + u^{(C)} + u^{(H)} \right)_i ds
\end{aligned}
$$

(B1)

where s_{core} is the circular boundary of S_{core}. Symmetry $C_{ijkl} = C_{klij}$ of the elasticity tensor implies that

$$
\begin{aligned}
(\sigma_C)_{ij} (\varepsilon_D)_{ij} &= (\sigma_D)_{ij} (\varepsilon_C)_{ij} \\
(\sigma_H)_{ij} (\varepsilon_D)_{ij} &= (\sigma_D)_{ij} (\varepsilon_H)_{ij} \\
(\sigma_C)_{ij} (\varepsilon_H)_{ij} &= (\sigma_H)_{ij} (\varepsilon_C)_{ij}
\end{aligned}
$$

(B2)

and by the principle of virtual work

$$
\int_{S-S_{core}} (\sigma_D)_{ij} (\varepsilon_D)_{ij} dS = \int_{s+s_{core}} (T_D)_i (u_D)_i ds
$$

(B3)

Use of eqs. (B2), (B3) and

$$
\begin{aligned}
(\varepsilon_C)_{ij} &= \left(\varepsilon^{(C)} \right)_{ij} - \left(\varepsilon^C \right)_{ij}, \\
(\varepsilon_H)_{ij} &= \left(\varepsilon^{(H)} \right)_{ij} - \left(\varepsilon^H \right)_{ij}
\end{aligned}
$$

(B4)

in eq. (B1) yields

$$W(D,C,H) = -\frac{1}{2}\int\limits_{S-S_{core}}(\sigma_D)_{ij}(\varepsilon_D)_{ij}\,dS + \int\limits_{S-S_{core}}(\sigma_D)_{ij}\left(\varepsilon^{(C)}-\varepsilon^C\right)_{ij}\,dS + \int\limits_{S-S_{core}}(\sigma_D)_{ij}\left(\varepsilon^{(H)}-\varepsilon^H\right)_{ij}\,dS$$

$$+ \int\limits_{S-S_{core}}(\sigma_H)_{ij}\left(\varepsilon^{(C)}-\varepsilon^C\right)_{ij}\,dS + \frac{1}{2}\int\limits_{S-S_{core}}(\sigma_C)_{ij}\left(\varepsilon^{(C)}-\varepsilon^C\right)_{ij}\,dS + \frac{1}{2}\int\limits_{S-S_{core}}(\sigma_H)_{ij}\left(\varepsilon^{(H)}-\varepsilon^H\right)_{ij}\,dS$$

$$- \int\limits_{s+s_{core}}(T_D)_i\left(u^{(C)}+u^{(H)}\right)_i\,ds \qquad (B5)$$

By the principle of virtual work

$$\int\limits_{S-S_{core}}(\sigma_D)_{ij}\left(\varepsilon^{(C)}\right)_{ij}\,dS = \int\limits_{s+s_{core}}(T_D)_i\left(u^{(C)}\right)_i\,ds$$

$$\int\limits_{S-S_{core}}(\sigma_D)_{ij}\left(\varepsilon^{(H)}\right)_{ij}\,dS = \int\limits_{s+s_{core}}(T_D)_i\left(u^{(H)}\right)_i\,ds \qquad (B6)$$

and substituting into eq. (B5) one finds

$$W(D,C,H) = -\frac{1}{2}\int\limits_{S-S_{core}}(\sigma_D)_{ij}(\varepsilon_D)_{ij}\,dS - \int\limits_{S-S_{core}}(\sigma_D)_{ij}\left(\varepsilon^C\right)_{ij}\,dS - \int\limits_{S-S_{core}}(\sigma_D)_{ij}\left(\varepsilon^H\right)_{ij}\,dS$$

$$+ \int\limits_{S-S_{core}}(\sigma_H)_{ij}\left(\varepsilon^{(C)}\right)_{ij}\,dS - \int\limits_{S-S_{core}}(\sigma_H)_{ij}\left(\varepsilon^C\right)_{ij}\,dS$$

$$+ \frac{1}{2}\int\limits_{S-S_{core}}(\sigma_C)_{ij}\left(\varepsilon^{(C)}\right)_{ij}\,dS - \frac{1}{2}\int\limits_{S-S_{core}}(\sigma_C)_{ij}\left(\varepsilon^C\right)_{ij}\,dS$$

$$+ \frac{1}{2}\int\limits_{S-S_{core}}(\sigma_H)_{ij}\left(\varepsilon^{(H)}\right)_{ij}\,dS - \frac{1}{2}\int\limits_{S-S_{core}}(\sigma_H)_{ij}\left(\varepsilon^H\right)_{ij}\,dS \qquad (B7)$$

As it is explained in the formulation of the boundary value problem for the hydrogen stress field in Section 3.2, exclusion of the dislocation core area may be disregarded in the solution process of the carbon/hydrogen and carbon/no-hydrogen problems. Therefore the domain of integration in all integrals of eq. (B7), but the first, can be extended to include the core region S_{core} and thus its boundary s_{core} is eliminated. Then application of the principle of virtual work yields

$$\int\limits_S(\sigma_H)_{ij}\left(\varepsilon^{(C)}\right)_{ij}\,dS = 0$$

$$\int\limits_S(\sigma_C)_{ij}\left(\varepsilon^{(C)}\right)_{ij}\,dS = 0$$

$$\int\limits_S(\sigma_H)_{ij}\left(\varepsilon^{(H)}\right)_{ij}\,dS = 0 \qquad (B8)$$

By substitution of eqs. (B8) into eq. (B7) one finds

$$W(D,C,H) = -\frac{1}{2}\int\limits_{S-S_{core}}(\sigma_D)_{ij}(\varepsilon_D)_{ij}\,dS - \frac{1}{2}\int\limits_{S}(\sigma_C)_{ij}(\varepsilon^C)_{ij}\,dS - \frac{1}{2}\int\limits_{S}(\sigma_H)_{ij}(\varepsilon^H)_{ij}\,dS$$

$$-\int\limits_{S}(\sigma_D)_{ij}(\varepsilon^C)_{ij}\,dS - \int\limits_{S}(\sigma_D)_{ij}(\varepsilon^H)_{ij}\,dS - \int\limits_{S}(\sigma_H)_{ij}(\varepsilon^C)_{ij}\,dS \qquad \text{(B9)}$$

ACKNOWLEDGMENTS

REFERENCES

BILBY, B. A. (1950) *Pr. Phys. Soc. Lond.* A **63**, 191.

BIRNBAUM, H. K. and SOFRONIS, P. (1993) *J. Mat. Res.* To be published.

BOND, G., ROBERTSON, I. M. and BIRNBAUM, H. K. (1988a) *Acta Metall.* **36**, 2193.

BOND, G., ROBERTSON, I. M. and BIRNBAUM, H. K. (1988b) *Acta Metall.* **35**, 2289.

COCHARDT, A. W., SCHOEK, G., and WIEDERSICH, H. (1955) *Acta Metall.* **3**, 533.

COTTRELL, A. H. (1948) *Strength of Solids* (Report of a conference, H. H. Wills Physical Laboratory, University of Bristol, 7-9 July 1947), p. 30 (Published by the Physical Society) 1 Lowther Gardens, Prince Consort Road, London S. W. 7.

COTTRELL, A. H. and BILBY, B. A. (1949) *Pr. Phys. Soc. Lond.* A **62**, 49.

COTTRELL, A. H. and JAWSON, M. A. (1949) *Pr. Roy. Soc. Lond.* A **199**, 104.

ESHELBY, J. D. (1951) *Phil. Trans. Roy. Soc.* A **244**, 87.

ESHELBY, J. D. (1954) *J. Appl. Phys.* **25**, 255.

ESHELBY, J. D. (1955) *Acta Metall.* **3**, 487.

ESHELBY, J. D. (1956) *Solid State Phys.* **3**, 79.

ESHELBY, J. D. (1957) *Pr. Roy. Soc. Lond.* A **241**, 376.

FLANNAGAN, T. B., MASON, N. B. and BIRNBAUM, H. K. (1981) *Scripta Metall.* **15**, 109.

FUENTES-SAMANIEGO, R., GASCA-NERI, R., HIRTH, J. P. (1984) *Phil. Mag.* A **49**, 31.

HIRTH, J. P. and CARNAHAN, B. (1978) *Acta Metall.* **26**, 1795.

HIRTH, J. P. and LOTHE, J. (1982) *Theory of Dislocations*, John Wiley & Sons, Inc.

KIRCHHEIM, R. (1986) *Acta Metall.* **34**, 37.

MAZZOLAI, F. M. and BIRNBAUM, H. K. (1985a) *J. Phys. F: Met. Phys.* **15**, 507.

MAZZOLAI, F. M. and BIRNBAUM, H. K. (1985b) *J. Phys. F: Met. Phys.* **15**, 525.

PEISL, H. (1978) *Hydrogen in Metals, Topics in Applied Physics.* Vol. **28**, p. 53 (edited by G. Alefeld and J. Volkl), Springer, Berlin, Heidelberg.

ROBERTSON, I. M. and BIRNBAUM, H. K. (1986) *Acta Metall.* **34**, 353.

ROZENAK, P., ROBERTSON, I. M. and BIRNBAUM, H. K. (1990) *Acta Metall.* **38**, 2031.

SHIH, D., ROBERTSON, I. M. and BIRNBAUM, H. K. (1988) *Acta Metall.* **36**, 111.

SIROIS, E. and BIRNBAUM, H. K. (1992) *Acta Metall.* **40**, 1377.

SIROIS, E., SOFRONIS, P. and BIRNBAUM, H. K. (1992) *Fundamental Aspects of Stress Corrosion Cracking* (Proc. of Parkins Symposium), p. 173 (edited by S. M. Bruemmer, E. I. Meletis, R. H. Jones, W. W. Gerberich, F. P. Ford, and R. W. Staehle), The Minerals, Metals and Materials Society.

STROH, A. N. (1957) *Adv. Phys.* **6**, 418.

TABATA, T. and BIRNBAUM, H. K. (1984) *Scripta Metall.* **18**, 231.

ZENER, C. (1948) *Fracturing of Metals,* American Society of Metals, Metals Park, Ohio.

FIGURE CAPTIONS

1. Schematic model indicating the shear stress $d\tau_H$ induced at the core of the dislocation 2 by the hydrogen dilatation lines of an infinitesimal area dS at position (r, ϕ). The radius R of the hydrogen atmosphere stretches as far as the infinity.

2. Contours of normalized hydrogen concentration c / c_0 around a single edge dislocation at a nominal hydrogen concentration $c_0 = 0.1$ and temperature 300K.

3. Contours of normalized hydrogen concentration c / c_0 around two parallel edge dislocations of equal Burgers vectors with magnitude b and on the same slip system at a nominal hydrogen concentration $c_0 = 0.1$, temperature 300K, and dislocation distances; a) $10b$; b) $8b$; c) $6b$.

4. Contours of normalized hydrogen concentration c / c_0 around two parallel edge dislocations of opposite and equal Burgers vectors with magnitude b and on the same slip system at a nominal hydrogen concentration $c_0 = 0.1$, temperature 300K, and dislocation distance; a) $10b$; b) $8b$; c) $6b$.

5. Plot of the normalized shear stress, τ_H / μ, due to hydrogen, τ_D / μ, due to dislocation 1, and net shear stress, $(\tau_D + \tau_H) / \mu$, at the core of dislocation 2 along the slip plane versus normalized distance, l / b, at temperature 300K and nominal hydrogen concentrations of H/M = 0.1, 0.01 and 0.001. The dislocation Burgers vectors were of the same sign.

6. Plot of the normalized shear stress, τ_H/μ, due to hydrogen, τ_D/μ, due to dislocation 1, and net shear stress, $(\tau_D+\tau_H)/\mu$, at the core of dislocation 2 along the slip plane versus normalized distance, l/b, at temperature 300K and nominal hydrogen concentrations of H/M = 0.1, 0.01 and 0.001. The Burgers vector of dislocation 2 was negative.

7. Summary of the boundary value problem for the calculation of the hydrogen stress field. The superposed stress fields of dislocations 1 and 2 are used in the calculation of the hydrogen concentration which determines the transformation strain due to hydrogen and the elastic moduli throughout the modeled region.

8. Contours of the normalized hydrogen concentration c/c_0 around two parallel edge dislocations of equal Burgers vectors magnitude b and on the same slip system at a nominal hydrogen concentration $c_0 = 0.1$, temperature 300K, and distance $6b$. Hydrogen induced relaxation of the hydrostatic stress and modulus change were not accounted for.

9. Effect of the hydrogen induced relaxation of the hydrostatic stress on the normalized hydrogen concentration c/c_0 around two parallel edge dislocations of equal Burgers vectors magnitude b and on the same slip system at a nominal hydrogen concentration $c_0 = 0.1$, temperature 300K, and distance $6b$. The hydrogen effect on the elastic moduli was not accounted for.

10. Effect of the hydrogen induced relaxation of the hydrostatic stress on the normalized shear stress, τ_H/μ, due to hydrogen plotted versus dislocation distance, l/b, at temperature 300K and a nominal hydrogen concentrations of

H/M = 0.1, 0.01 and 0.001. Stress τ_D/μ due to dislocation 1 and the net shear stress $(\tau_D + \tau_H)/\mu$ are also shown. The hydrogen effect on the elastic moduli was not accounted for.

11. Effect of the hydrogen induced modulus change and relaxation of the hydrostatic stress on the normalized hydrogen concentration c/c_0 around two parallel edge dislocations of equal Burgers vectors magnitude b and on the same slip system at a nominal hydrogen concentration $c_0 = 0.1$, temperature 300K, and distance $6b$.

12. Effect of the hydrogen induced modulus change and relaxation of the hydrostatic stress on the normalized shear stress, τ_H/μ, due to hydrogen plotted versus dislocation distance, l/b, at temperature 300K and nominal hydrogen concentrations of H/M = 0.1, 0.01 and 0.001. Stress, τ_D/μ, due to dislocation 1 and the net shear stress, $(\tau_D + \tau_H)/\mu$, are also shown.

13. Comparison of the volumetric effect with the combined modulus and volumetric effect on the percent reduction of the shear stress, τ_D, due to dislocation 1 in the absence of hydrogen at temperature 300K.

14. Contours of normalized shear modulus, μ/μ_0, at nominal hydrogen concentration $c_0 = 0.1$, temperature 300K, and dislocation distance $6b$. The parameter μ_0 is the shear modulus for the hydrogen free material and is equal to 30.8 GPa.

15. Contours of Poisson's ratio v in niobium at nominal hydrogen concentration $c_0 = 0.1$, temperature 300K, and dislocation distance $6b$. The Poisson's ratio for the hydrogen free material equals 0.415.

16. Comparison of the volumetric effect with the combined modulus and volumetric effect on the percent reduction of the shear stress τ_D due to dislocation 1 with the moduli calculated at a nominal hydrogen concentration of H/M = 0.1 at temperature 300K.

17. Comparison of the shear stress exerted at the core of the dislocation by the carbon atom predicted by the finite element method with the exact analytical interaction stress in the absence of hydrogen. The carbon interstitial solute tetragonal axes lie along [100], [010], and [001]. The lines are the results of the analytic calculation and the points are from the finite element calculations. The calculations labelled "all directions" is for a defect with a cubic distortion field and volume of solution 3 times that of a carbon interstitial.

18. Comparison of the dislocation-carbon interaction energy measured in eV per slab of thickness a predicted by the numerical integration of eq. (44) with the exact analytical interaction energy in the absence of hydrogen. The carbon interstitial solute tetragonal axes lie along [100], [010], and [001]. The lines are the results of the analytic calculation and the points are from the numerical integrations. The calculations labelled "all directions" is for a defect with a cubic distortion field and volume of solution 3 times that of a carbon interstitial.

19.   Comparison of the shear stress exerted at the core of the dislocation by the carbon atom at various angular positions at $r/b = 1.2$ around the dislocation as predicted by the finite element method (points) with the exact analytical interaction stress in the absence of hydrogen (lines).

20   Comparison of the dislocation-carbon interaction energy measured in eV per slab of thickness a at various carbon angular positions at $r/b = 1.2$ around the dislocation predicted by the numerical integration of eq. (44) (points) with the exact analytical interaction energy in the absence of hydrogen (lines).

21.   Contours of normalized hydrogen concentration c/c_0 around an edge dislocation and a carbon atom with a tetragonal axis [001] at $r/b = 1.2$, $\phi = -37.5^0$ relative to the dislocation, at a nominal hydrogen concentration $c_0 = 0.1$ and temperature 300K. The hydrogen effect on the elastic moduli was not accounted for.

22.   Contours of normalized hydrogen concentration c/c_0 around an edge dislocation and a carbon atom with a tetragonal axis [001] at $r/b = 1.2$, $\phi = -37.5^0$ relative to the dislocation in niobium at nominal hydrogen concentration $c_0 = 0.1$ and temperature 300K. Both hydrogen effects modulus and volumetric were accounted for.

23.   Plot of the normalized shear stress exerted on the dislocation by the carbon atom and the hydrogen atmosphere versus carbon atom position x_1/b, $x_2/b = -0.505$ relative to the dislocation for a carbon atom with a tetragonal axis [100] at temperature 300K and nominal hydrogen concentration of H/M = 0.1.

24. Plot of the normalized shear stress exerted on the dislocation by the carbon atom and the hydrogen atmosphere versus carbon atom position x_1 / b, $x_2 / b = -0.505$ relative to the dislocation for a carbon atom with a tetragonal axis [010] at temperature 300K and nominal hydrogen concentration of H/M = 0.1.

25. Plot of the normalized shear stress exerted on the dislocation by the carbon atom and the hydrogen atmosphere versus carbon ˙atom position x_1 / b, $x_2 / b = -0.505$ relative to the dislocation for a carbon atom with a tetragonal axis [001] at temperature 300K and nominal hydrogen concentration of H/M = 0.1.

26. Plot of the edge dislocation-carbon atom interaction energy measured in eV per slab of thickness a versus carbon atom position x_1 / b, $x_2 / b = -0.505$ relative to the dislocation for a carbon atom with a tetragonal axis [100]. The hydrogen effect was calculated at temperature 300K and nominal hydrogen concentration of H/M = 0.1.

27. Plot of the edge dislocation-carbon atom interaction energy measured in eV per slab of thickness a versus carbon atom position x_1 / b, $x_2 / b = -0.505$ relative to the dislocation for a carbon atom with a tetragonal axis [010]. The hydrogen effect was calculated at temperature 300K and nominal hydrogen concentration of H/M = 0.1.

28. Plot of the edge dislocation-carbon atom interaction energy measured in eV per slab of thickness a versus carbon atom position x_1 / b, $x_2 / b = -0.505$

relative to the dislocation for a carbon atom with a tetragonal axis [001]. The hydrogen effect was calculated at temperature 300K and nominal hydrogen concentration of H/M = 0.1.

29.   Plot of the edge dislocation-carbon atom interaction energy measured in eV per slab of thickness a versus carbon atom position x_1/b, $x_2/b = -3.046$ relative to the dislocation for a carbon atom with a tetragonal axis [010]. The hydrogen effect was calculated at temperature 300K and nominal hydrogen concentration of H/M = 0.1.

30   Plot of the screw dislocation-carbon atom interaction energy measured in eV per slab of thickness a versus carbon atom position x_1/b, $x_2/b = -0.505$ relative to the dislocation for a carbon atom with a tetragonal axis [100]. The hydrogen effect was calculated at temperature 300K and nominal hydrogen concentration of H/M = 0.1.

31.   Plot of the screw dislocation-carbon atom interaction energy measured in eV per slab of thickness a versus carbon atom position x_1/b, $x_2/b = -0.505$ relative to the dislocation for a carbon atom with a tetragonal axis [010]. The hydrogen effect was calculated at temperature 300K and nominal hydrogen concentration of H/M = 0.1.

32   Plot of the screw dislocation-carbon atom interaction energy measured in eV per slab of thickness a versus carbon atom position x_1/b, $x_2/b = -0.505$ relative to the dislocation for a carbon atom with a tetragonal axis [001]. The hydrogen effect was calculated at temperature 300K and nominal hydrogen concentration of H/M = 0.1.
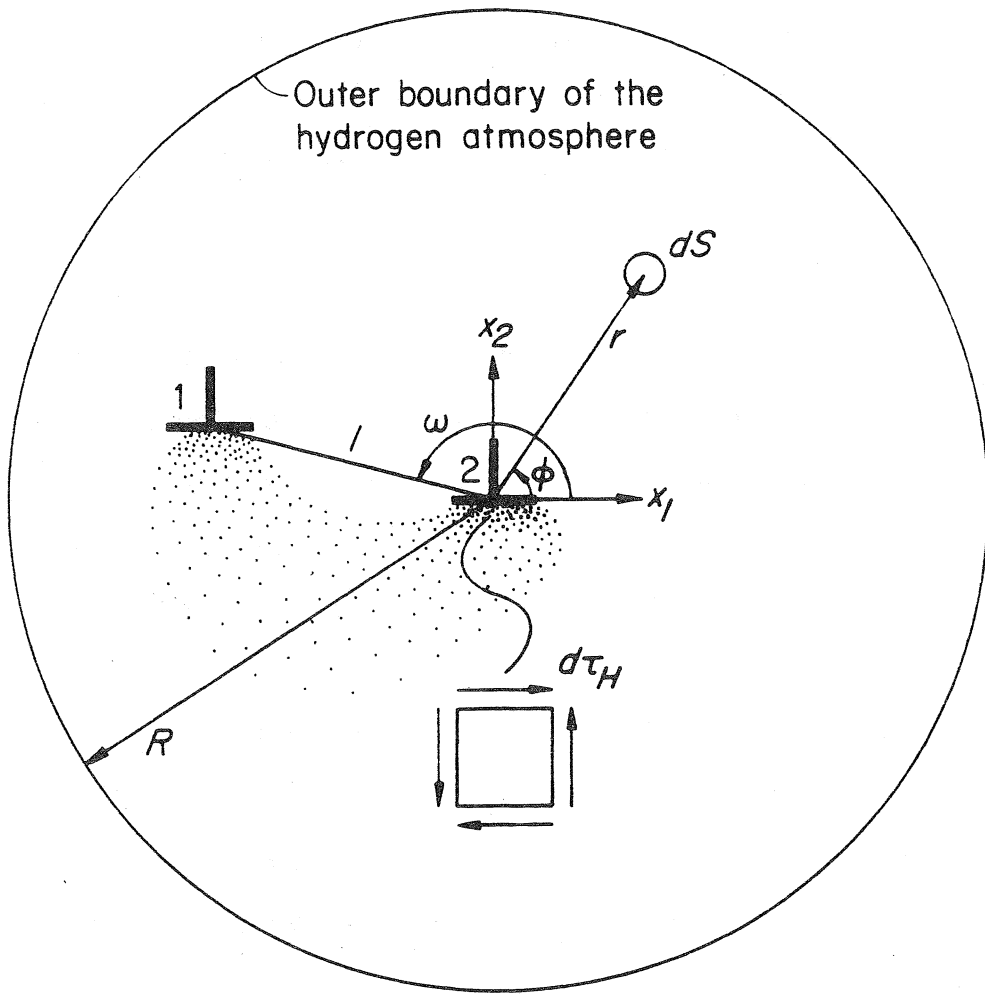
Fig. 1
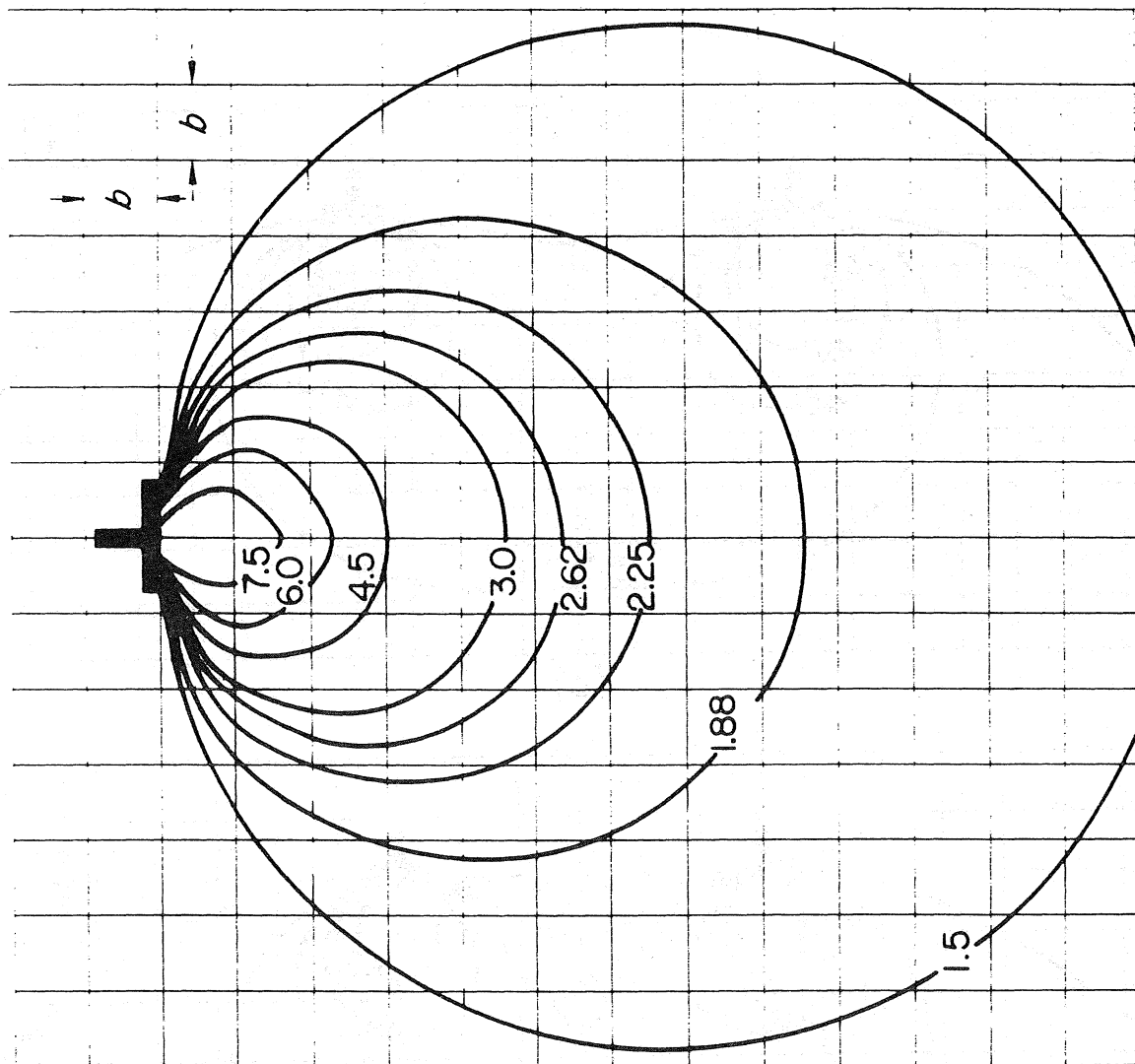
Fig. 2
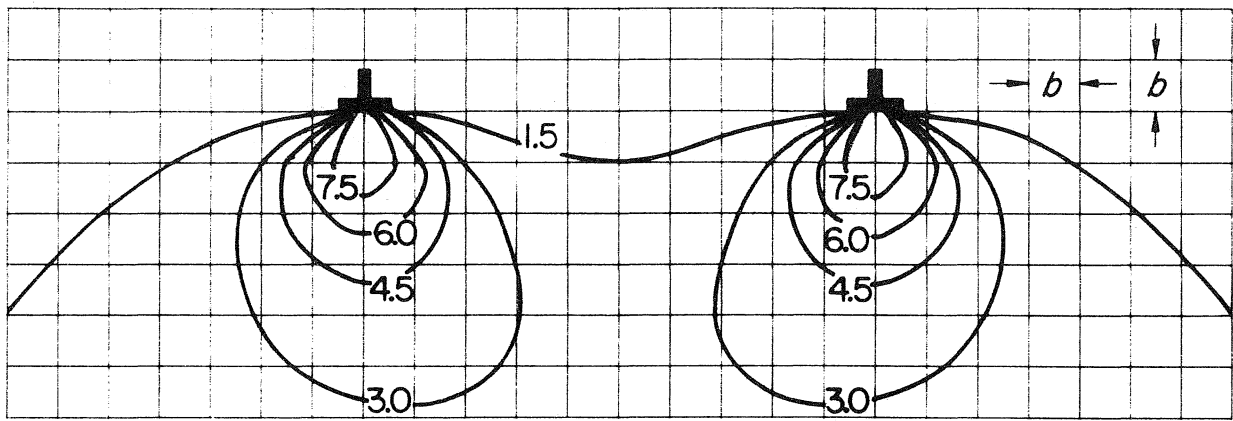
(a)
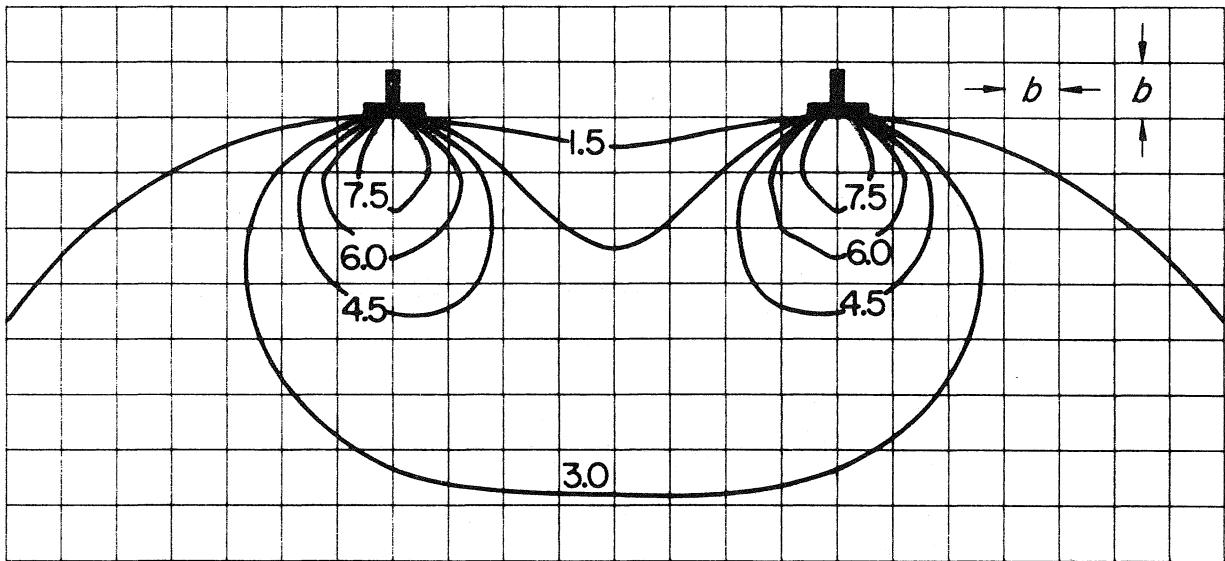
(b)
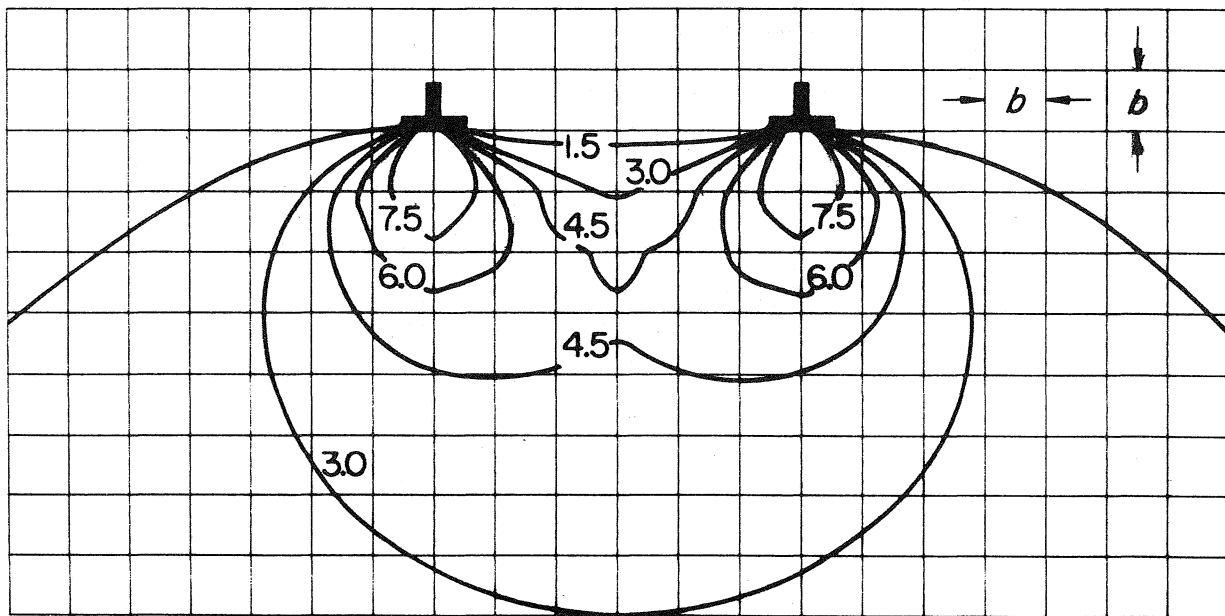
(c)

Fig. 3
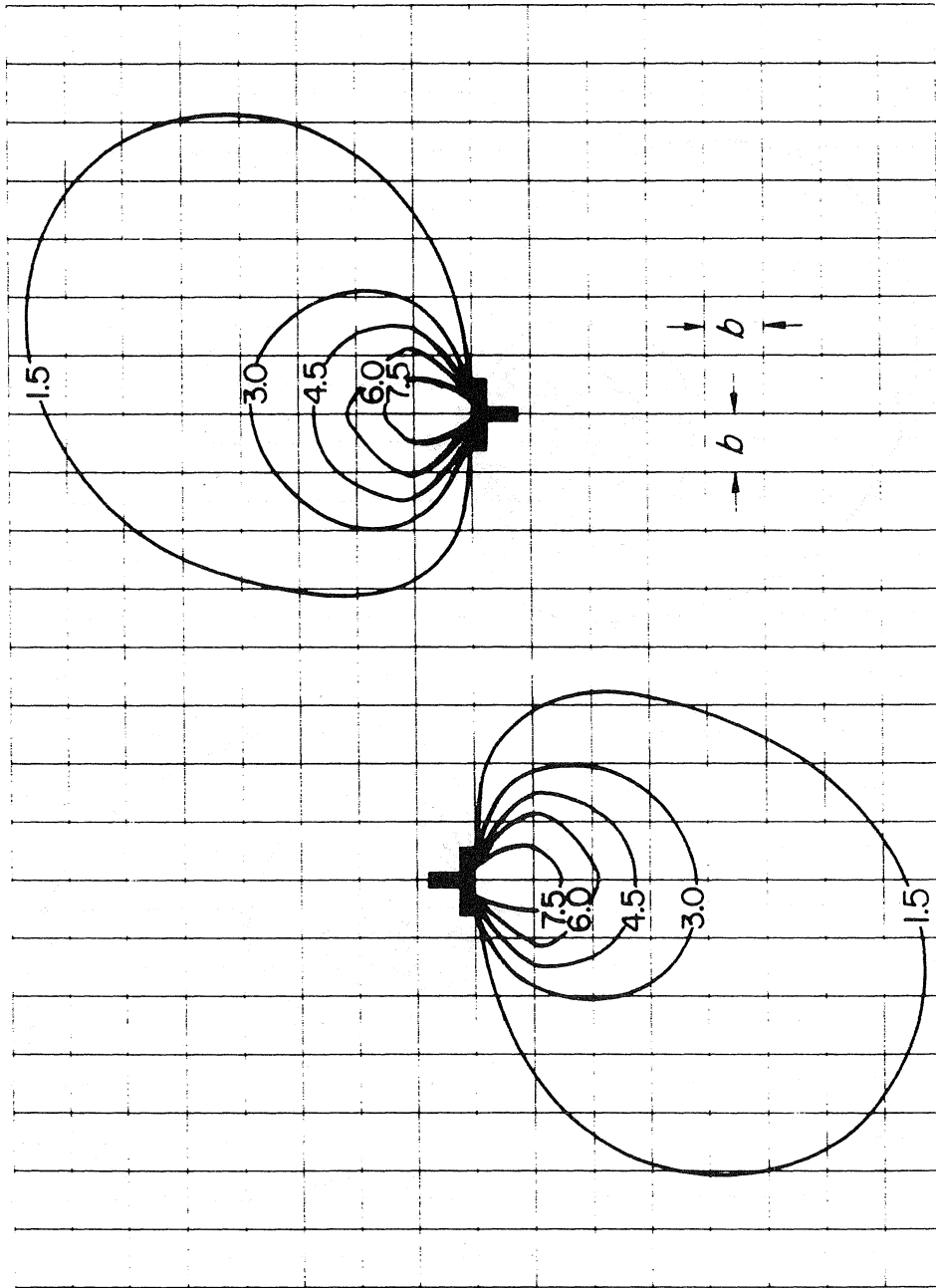
Fig. 4a

Fig. 4b

Fig. 4c

Fig. 5

Fig. 6

Modeled region

T = 0

0.12 x 10⁶b

$T_2 = 0$

$u_1 = 0$

x_2

1   2

x_1

T = 0

discretized region
into finite element mesh

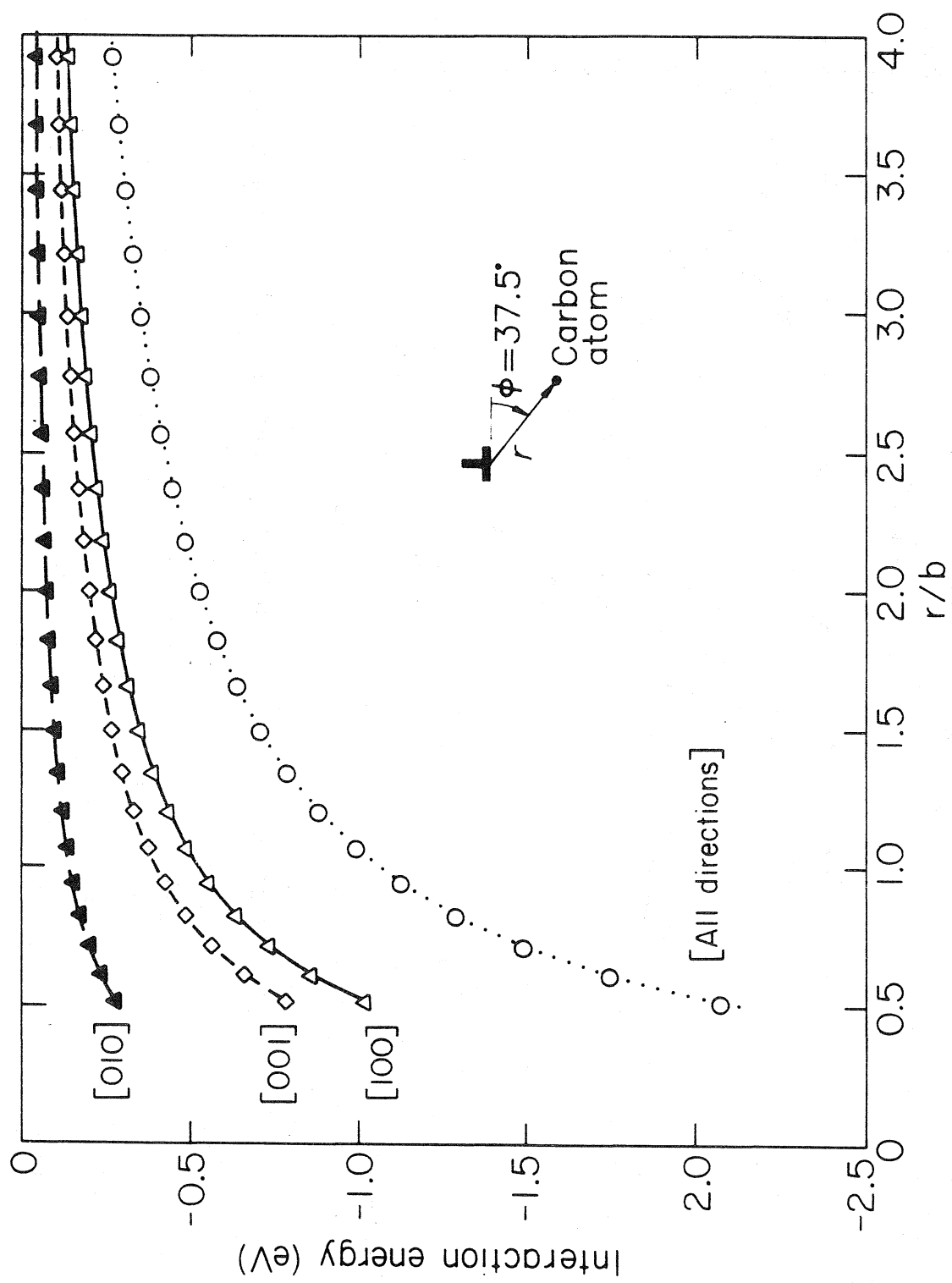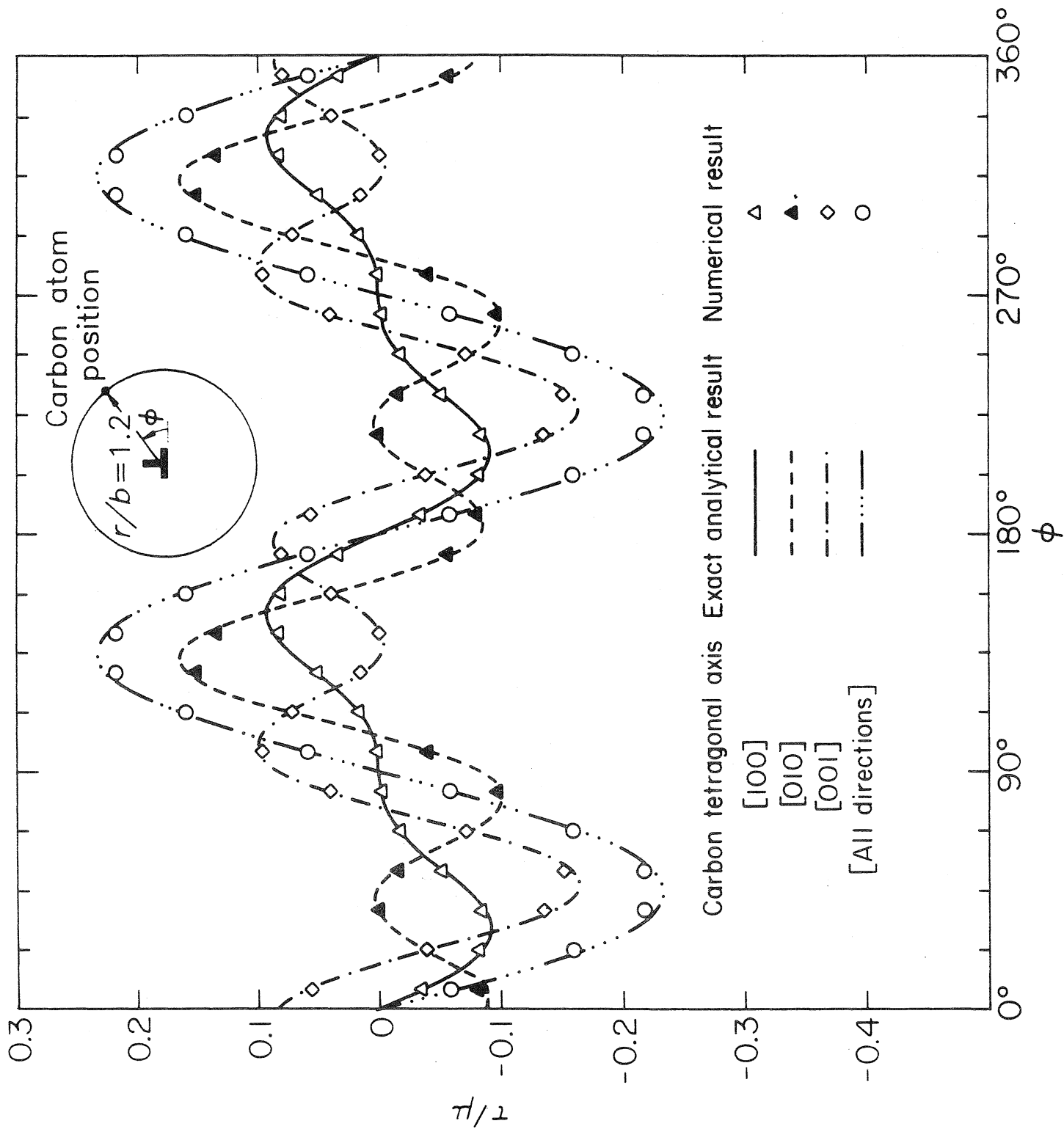0.1 x 10⁶b

T = 0

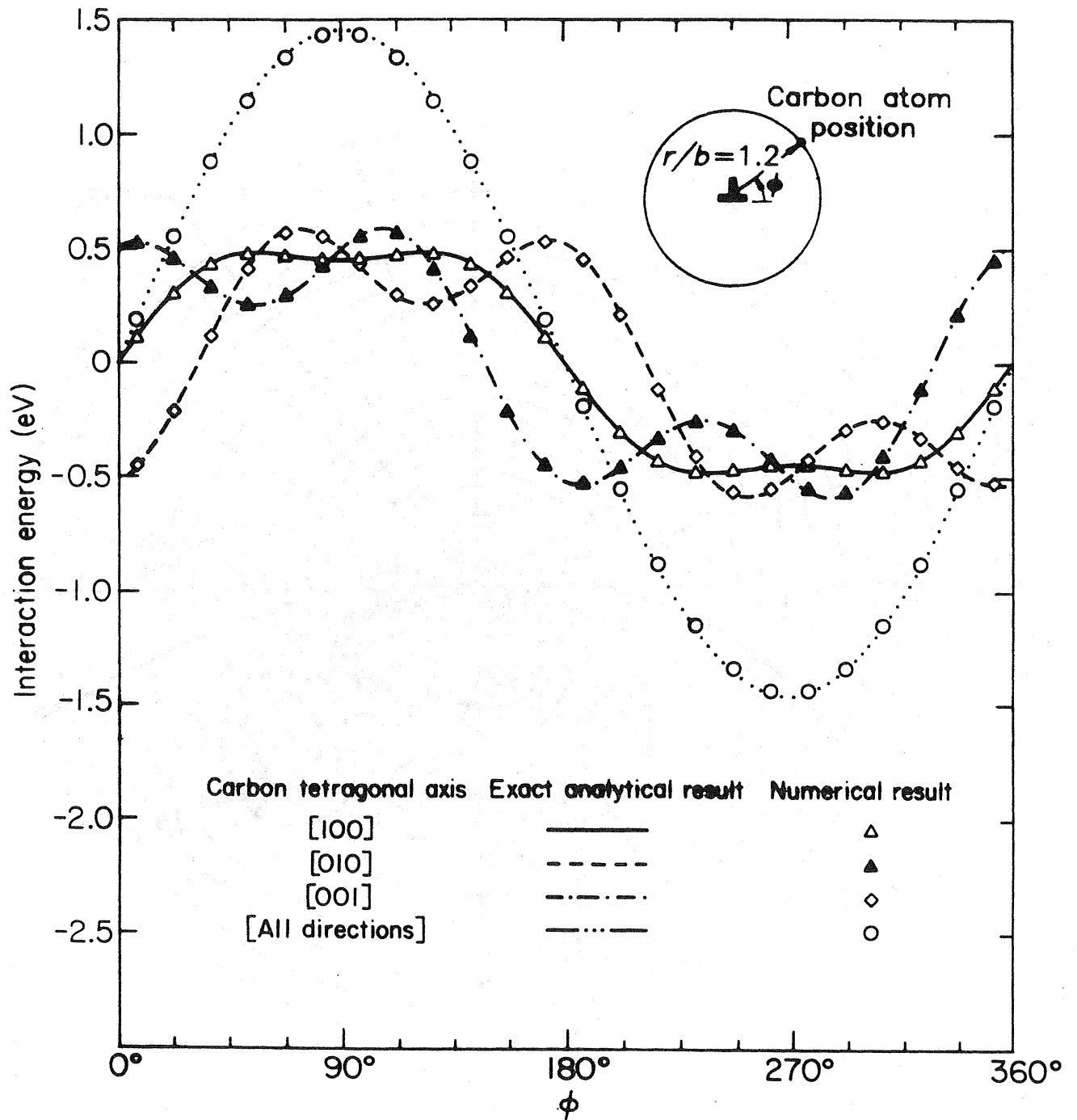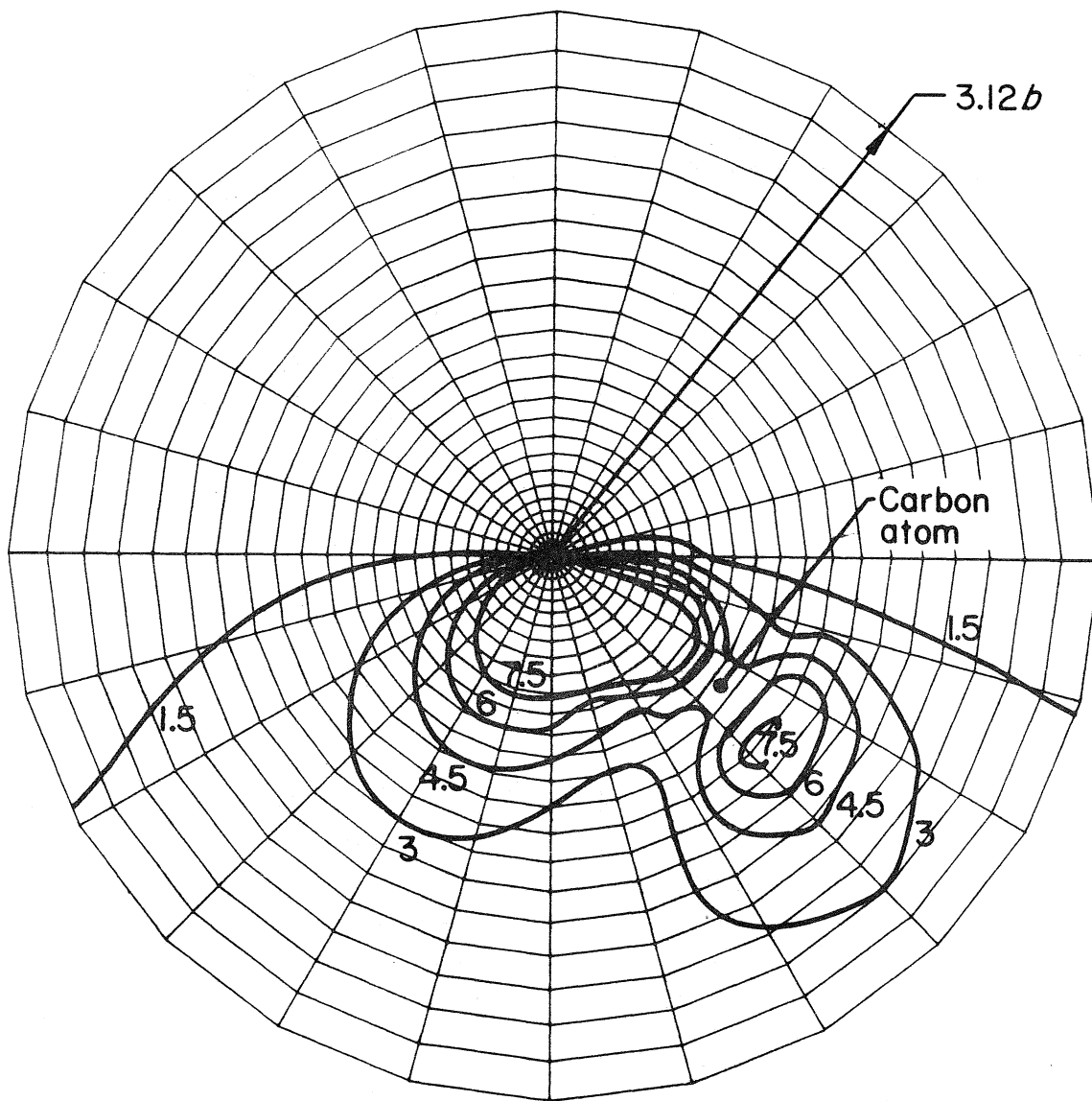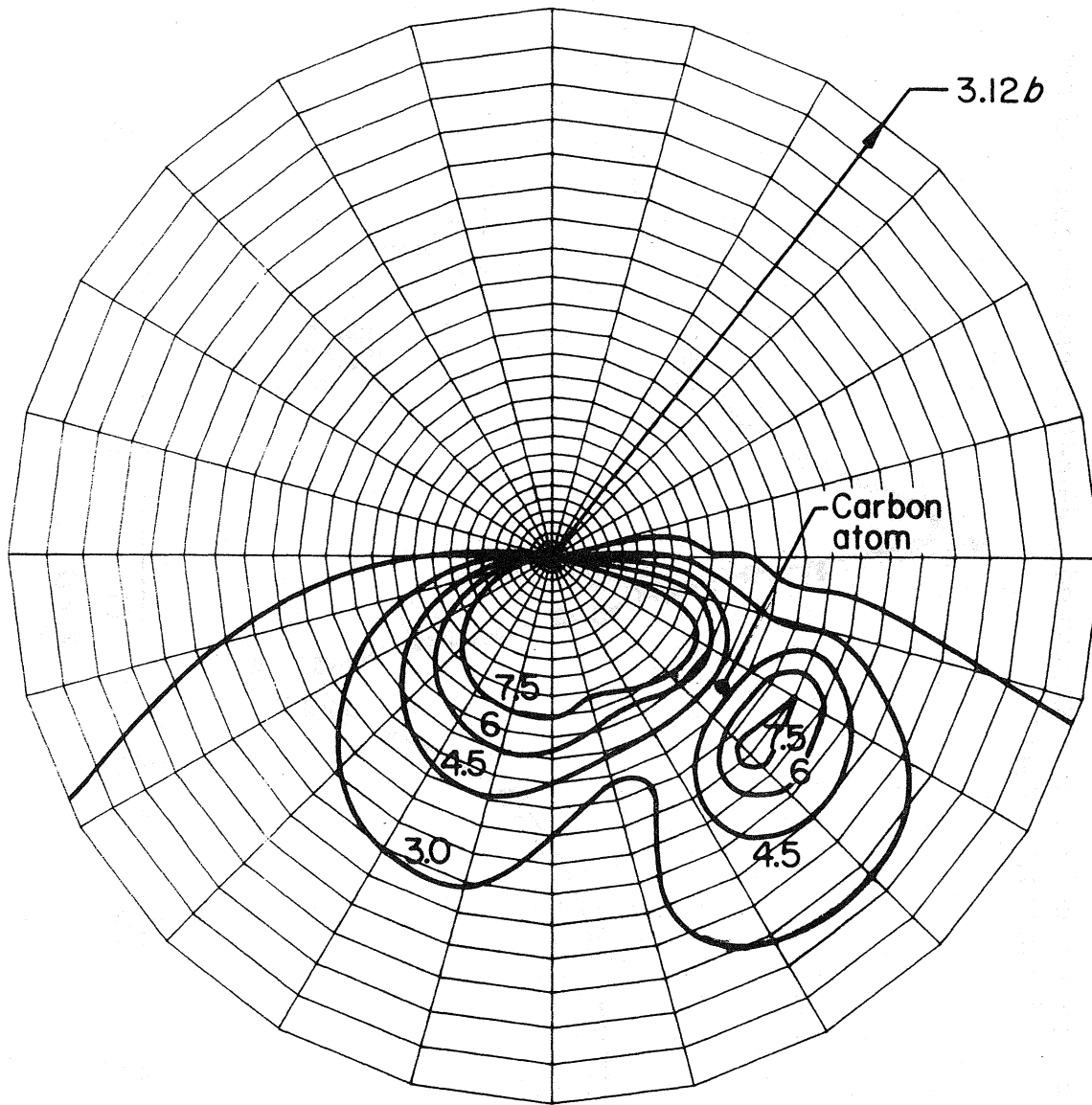Fig. 7

Fig. 8

4.5　　　　4.5

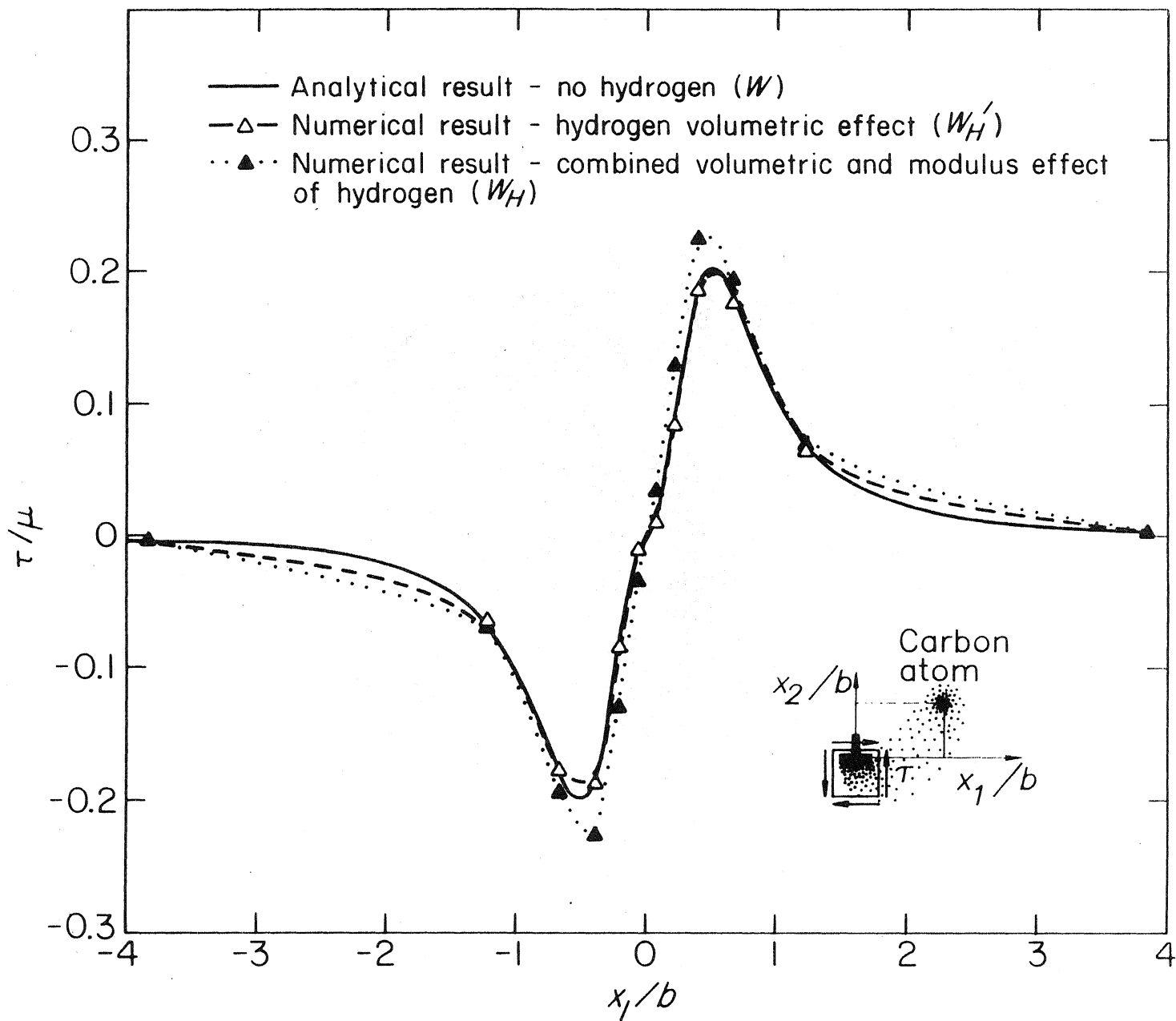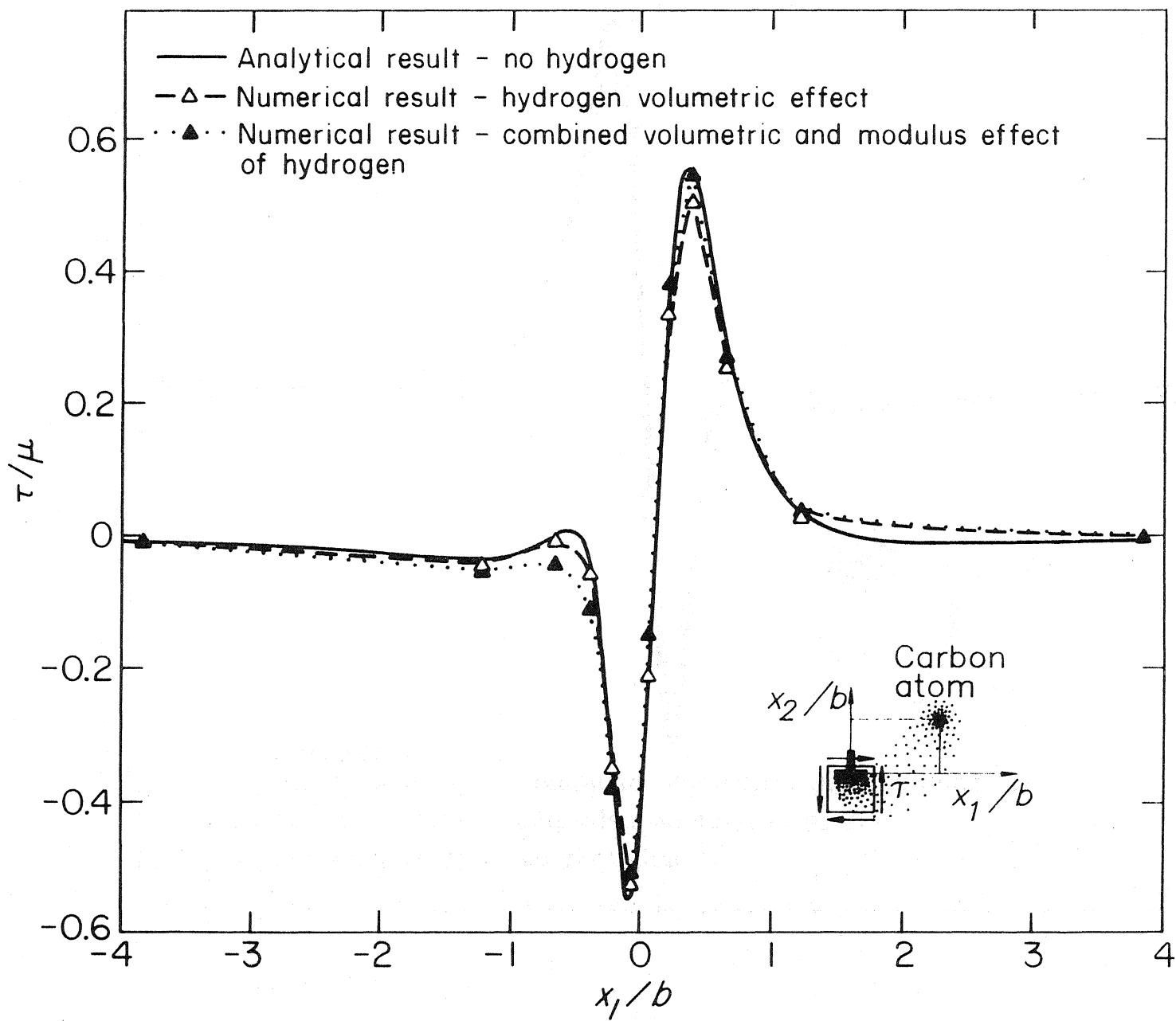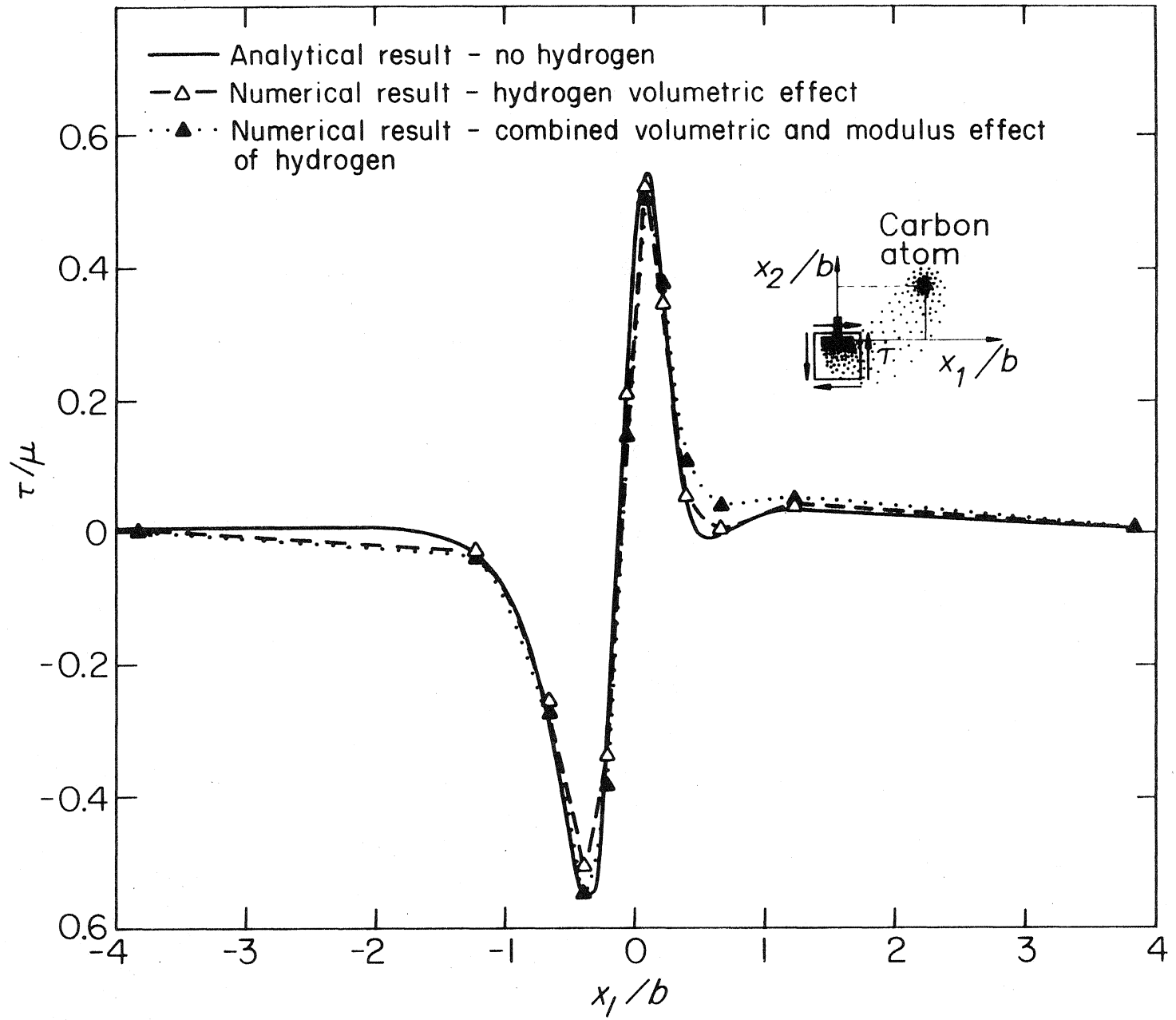3.0　　　　3.0
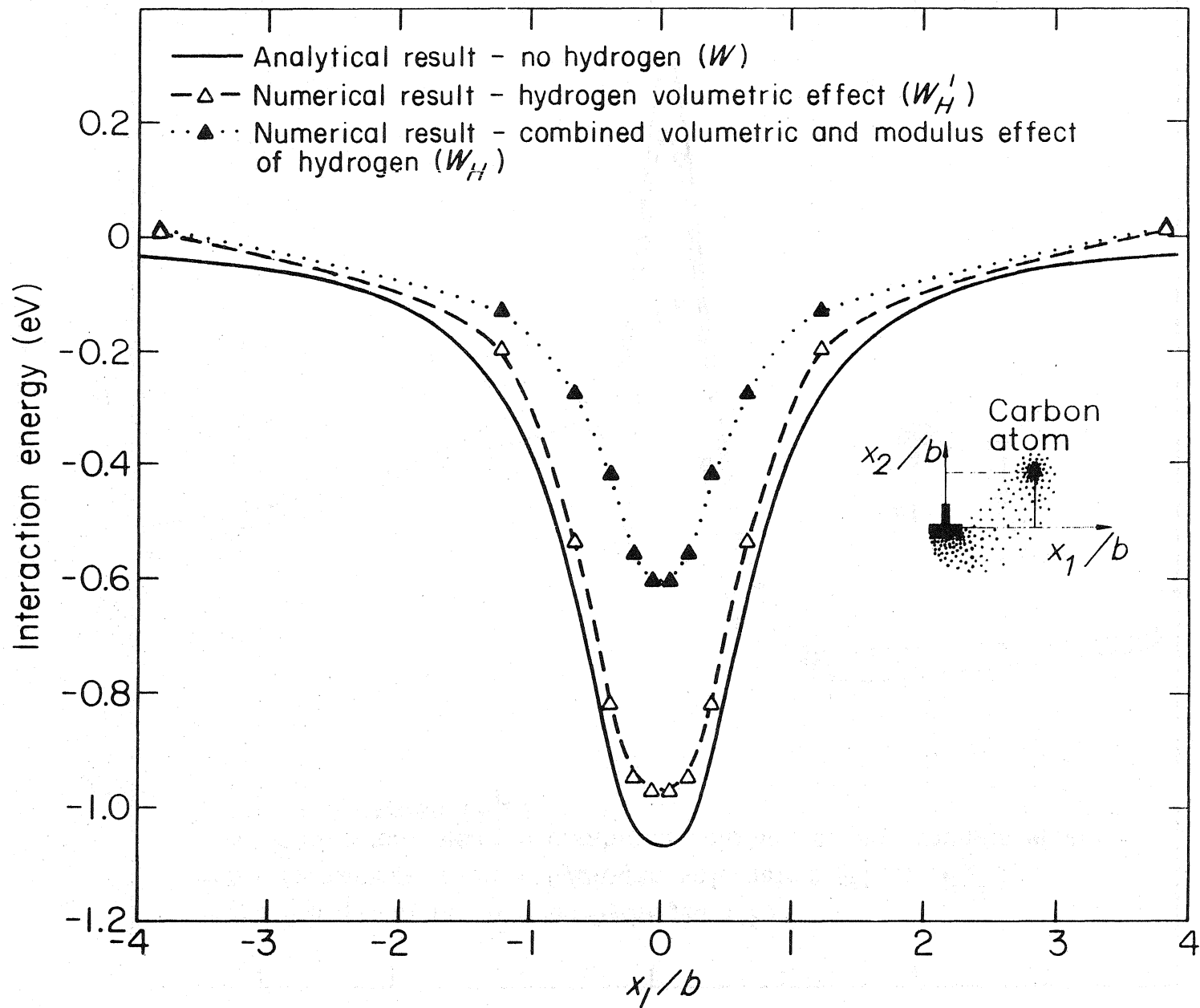
2.62　　　2.62
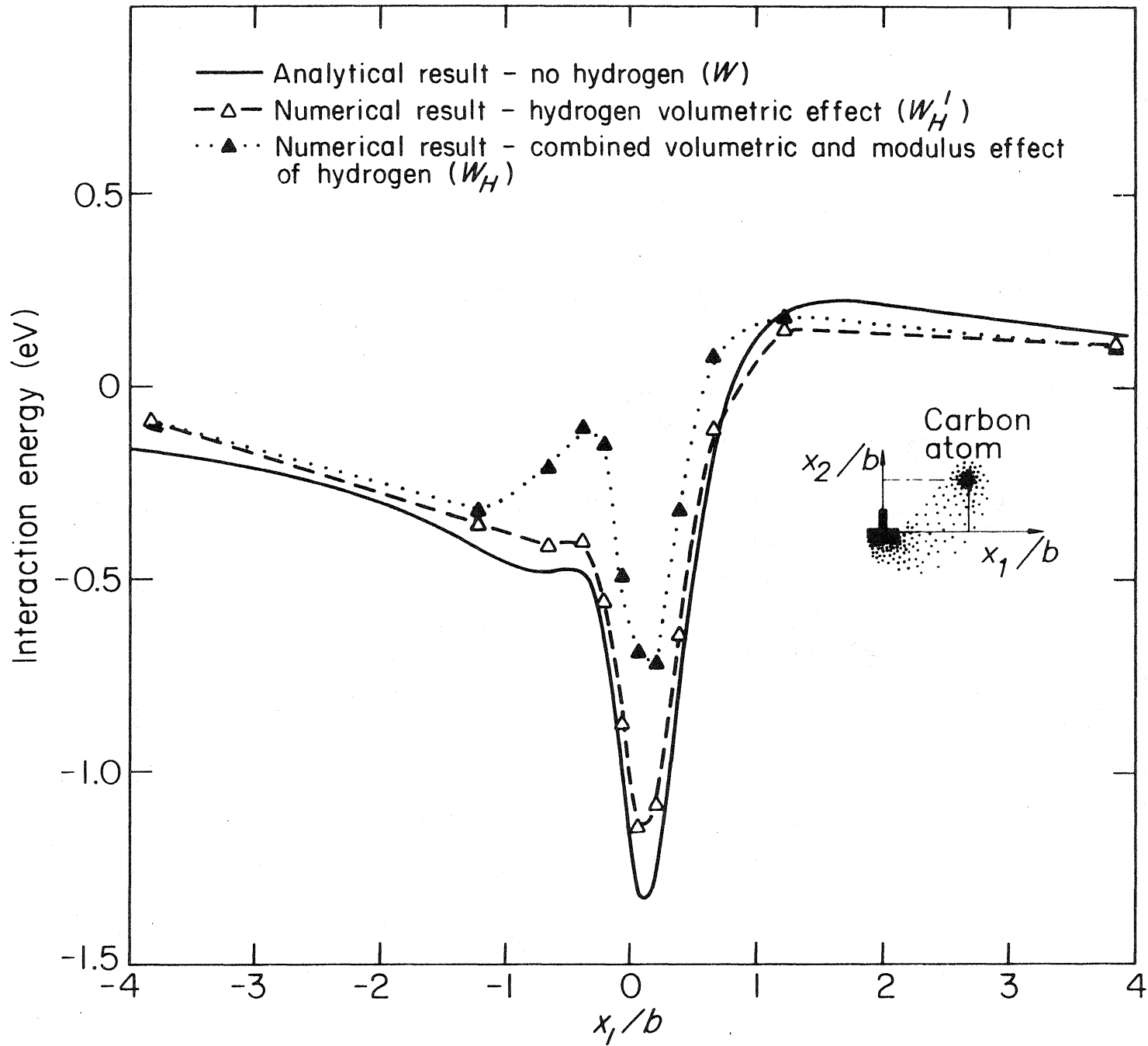
2.25

1.88

1.5
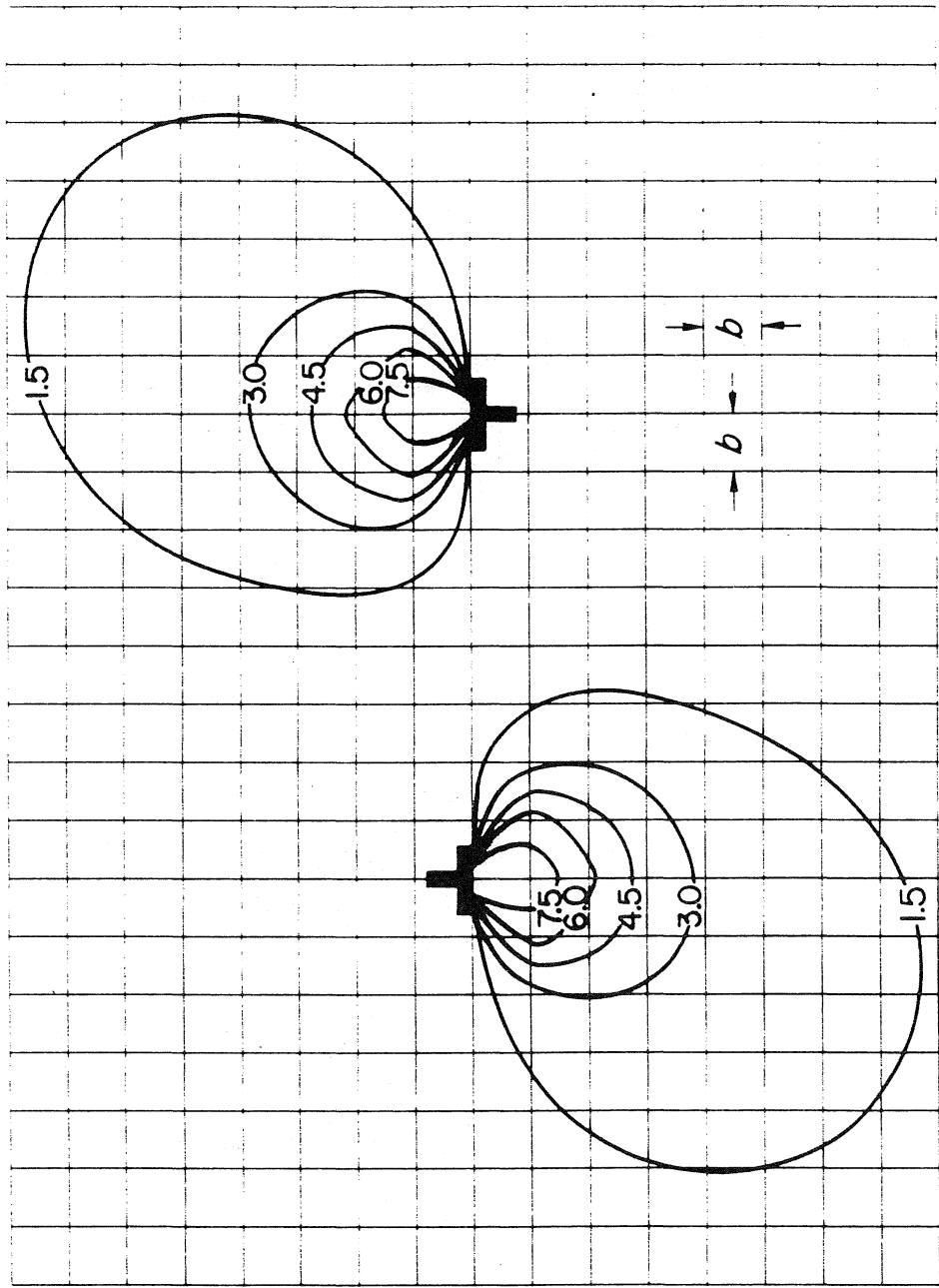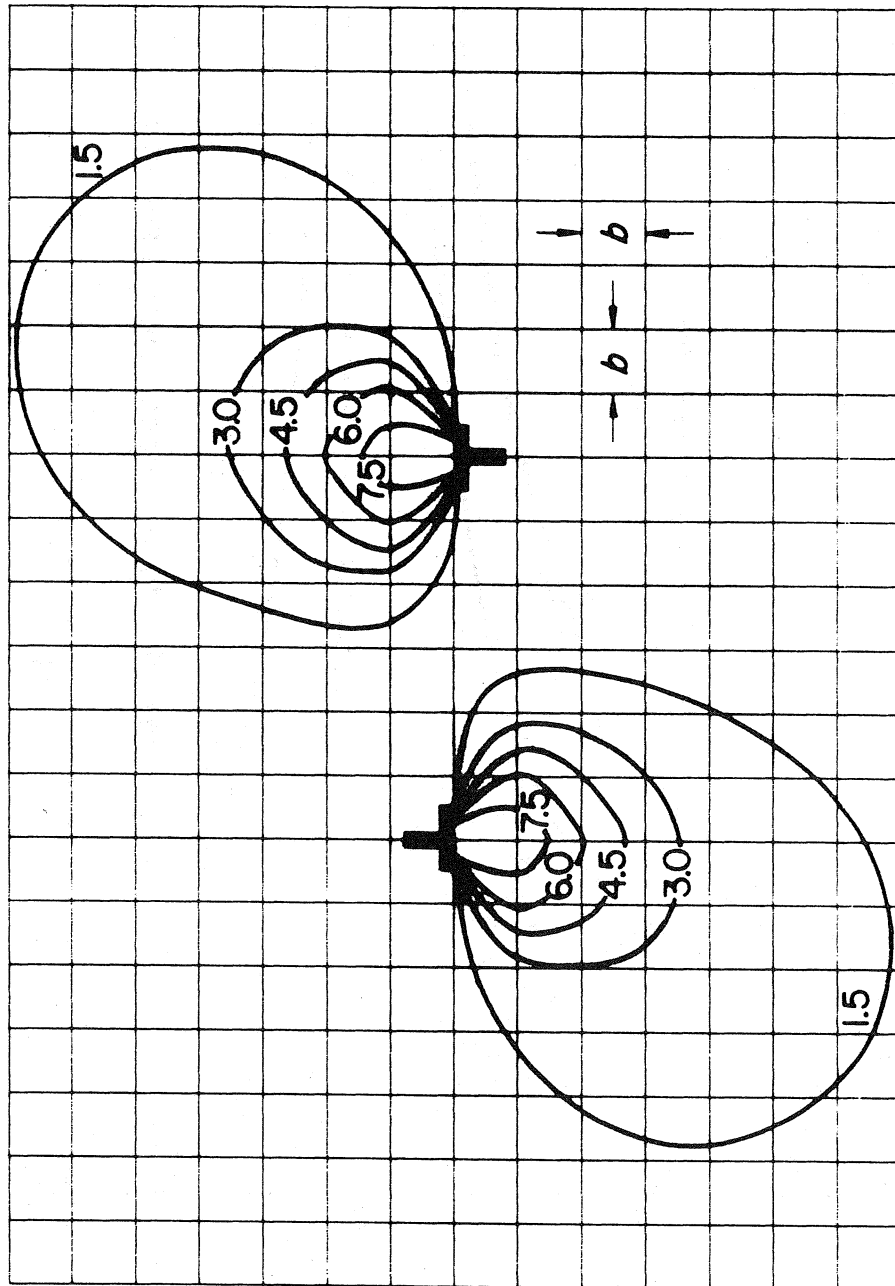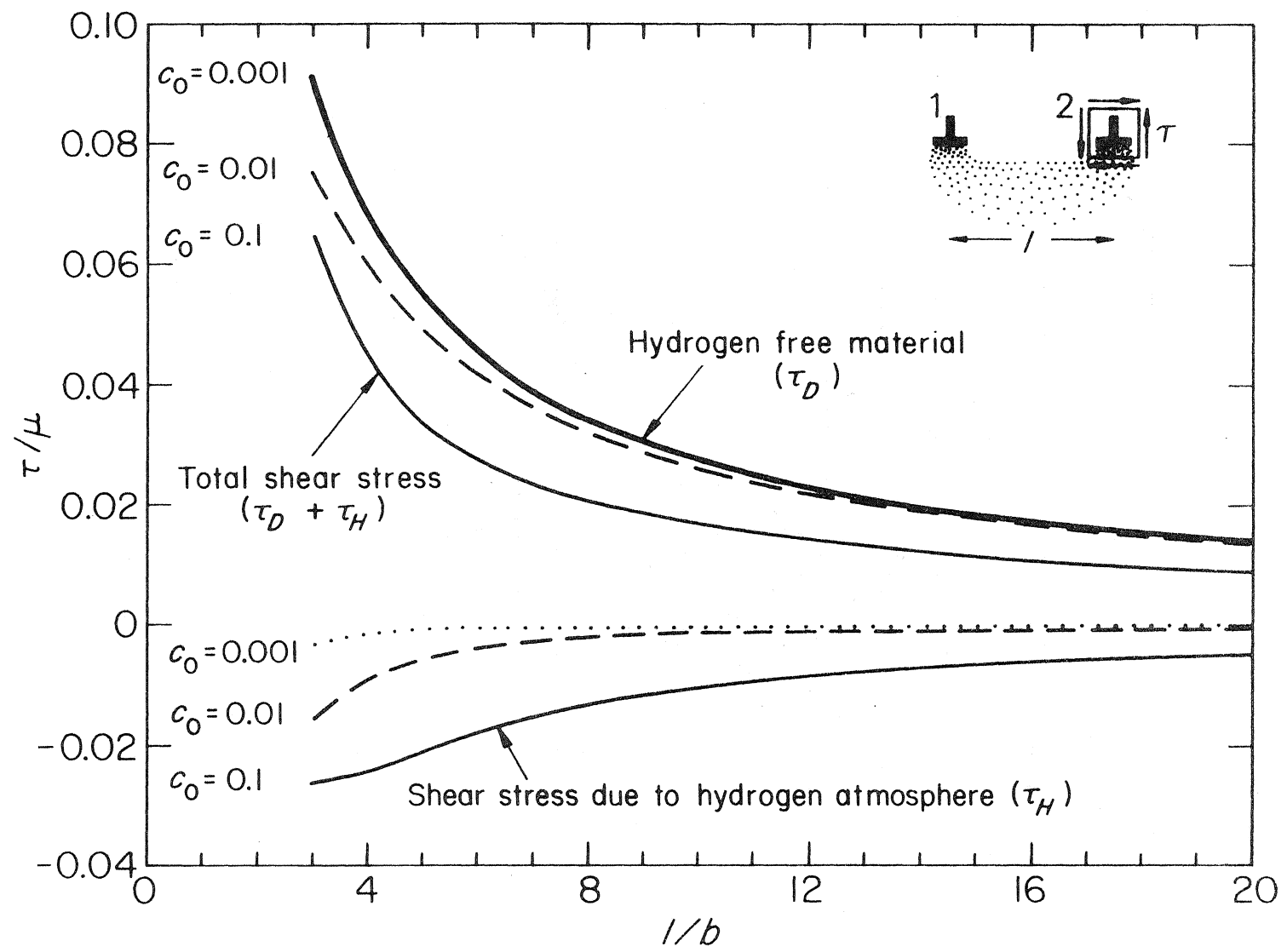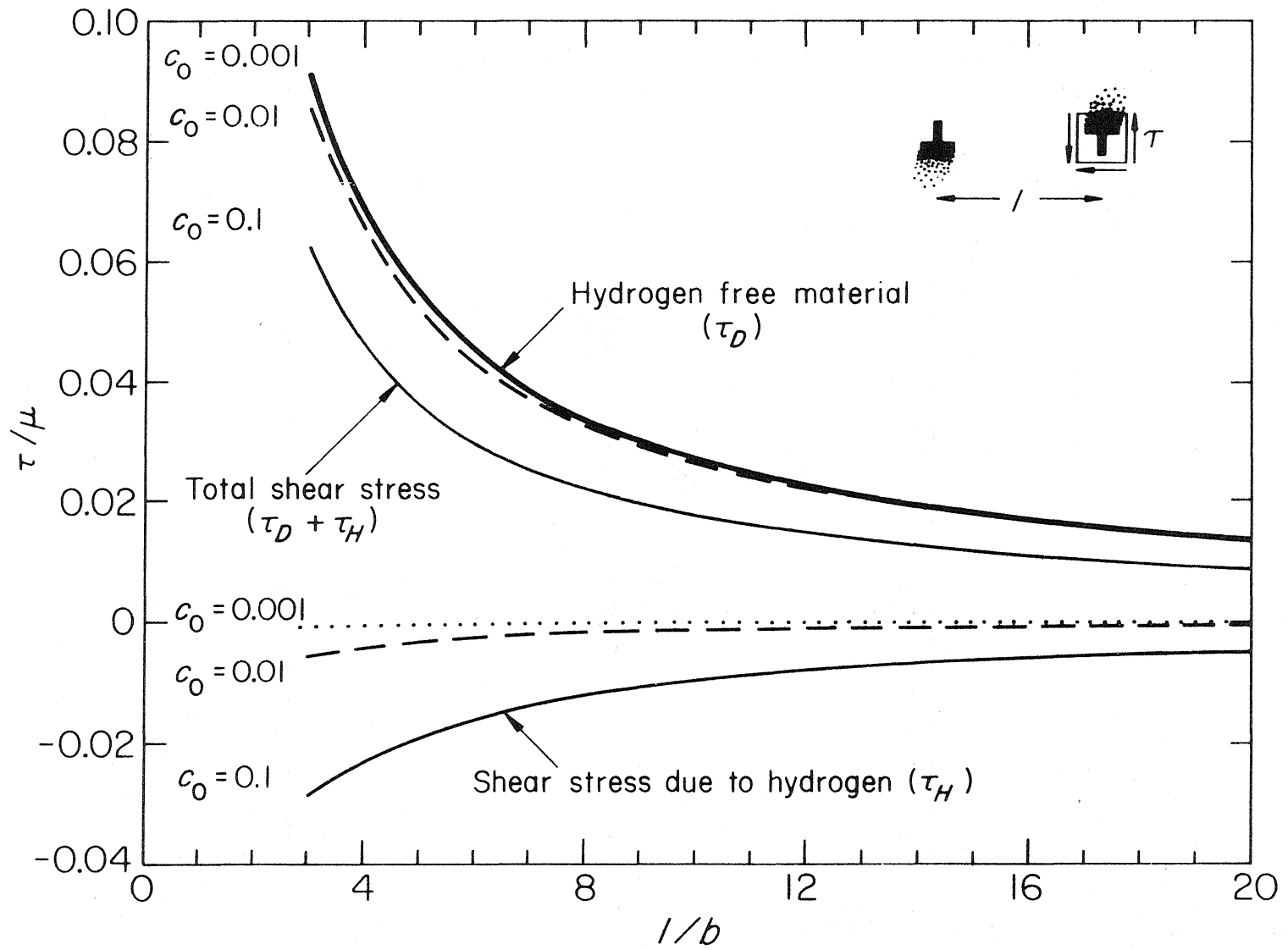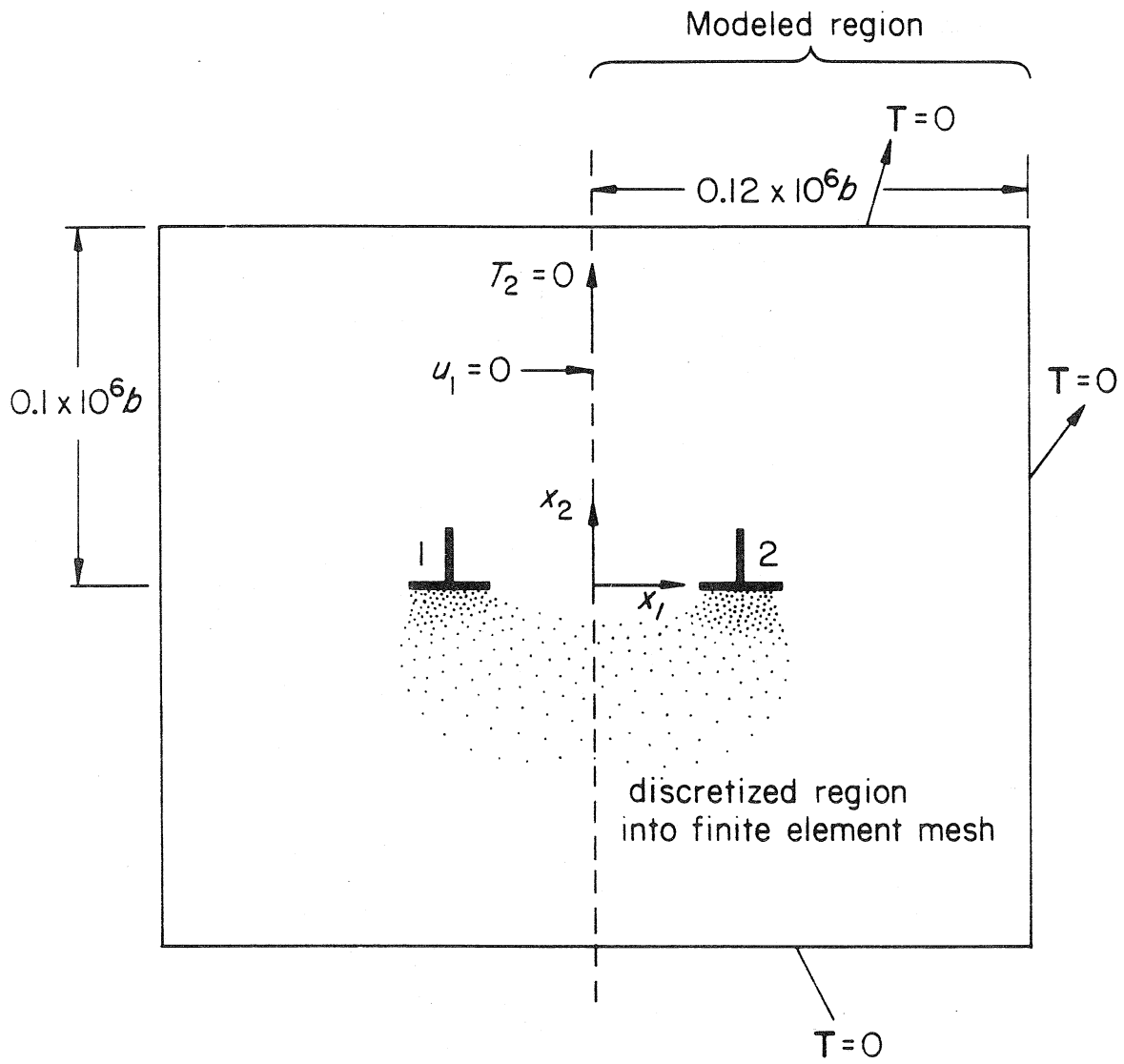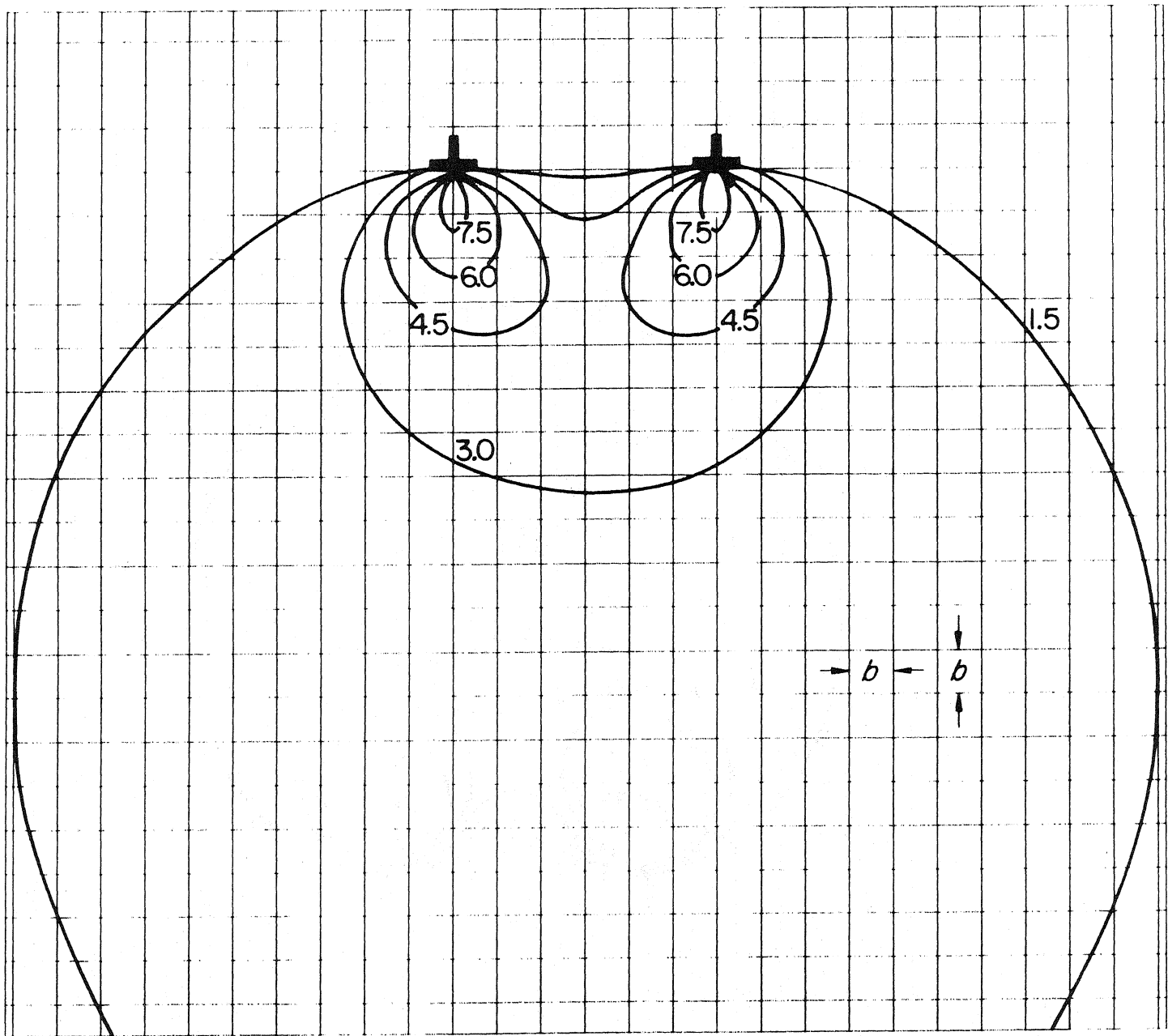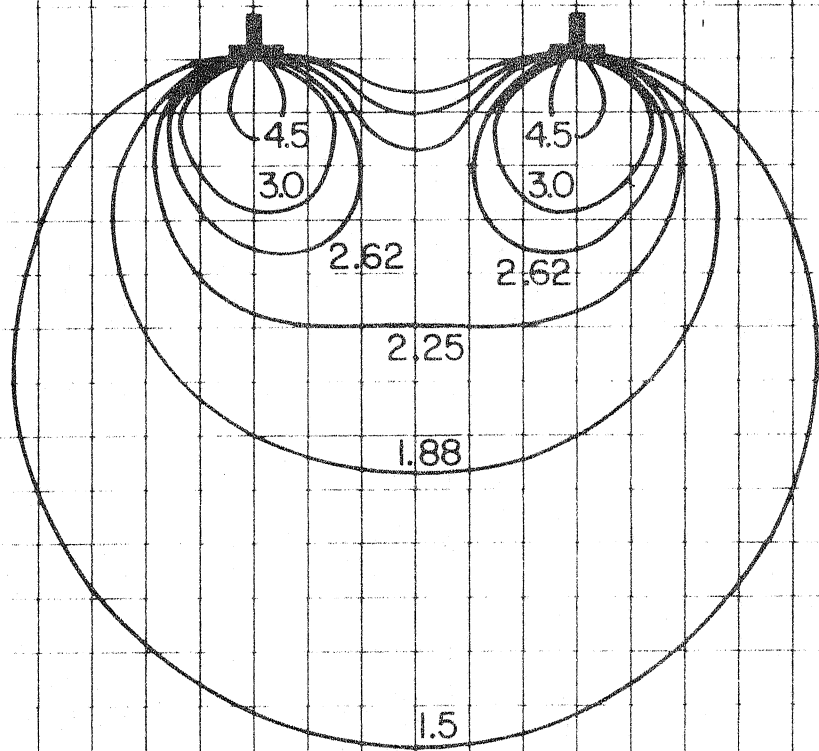
Fig. 9

Fig. 10
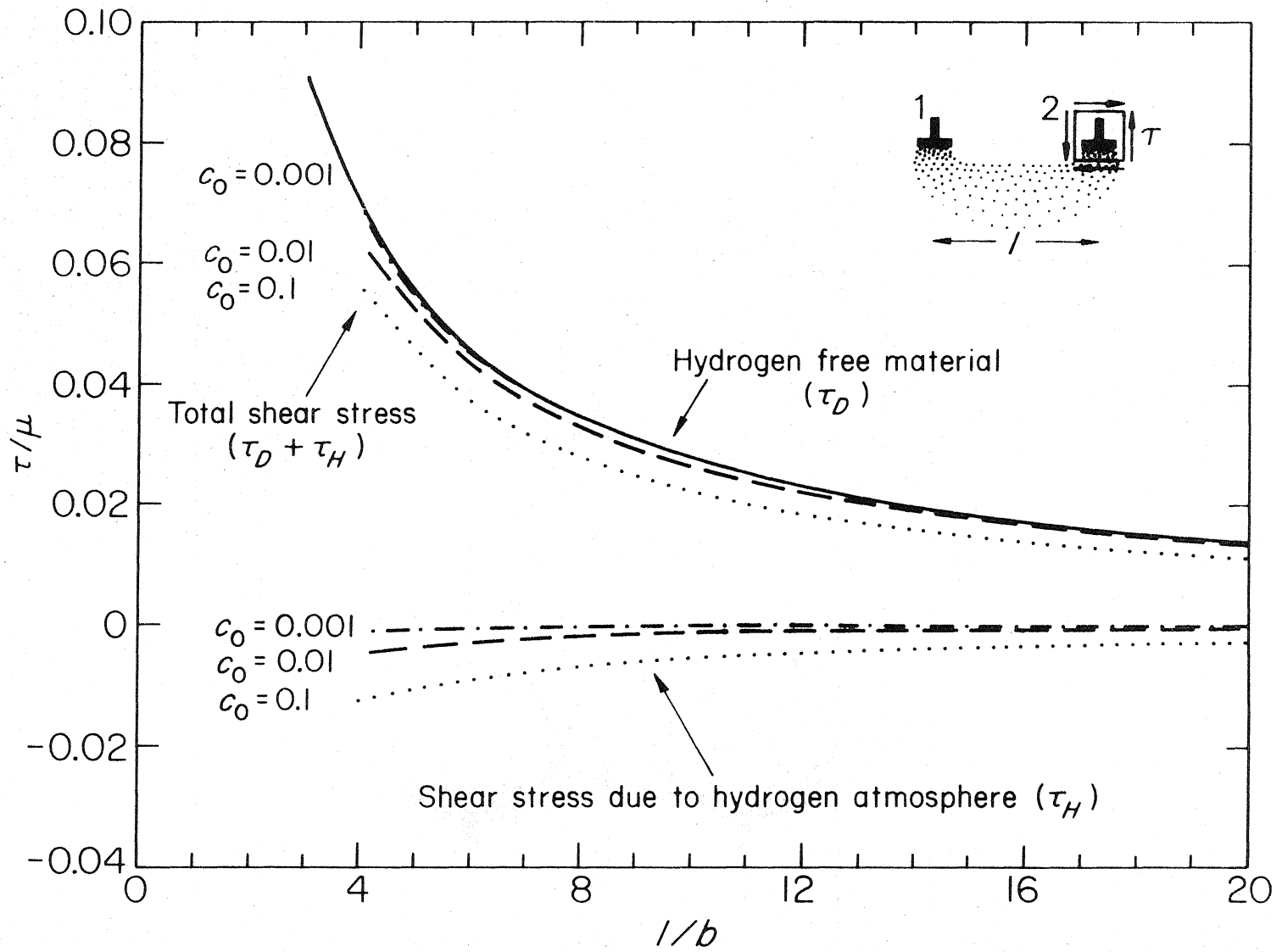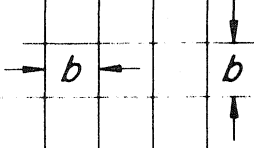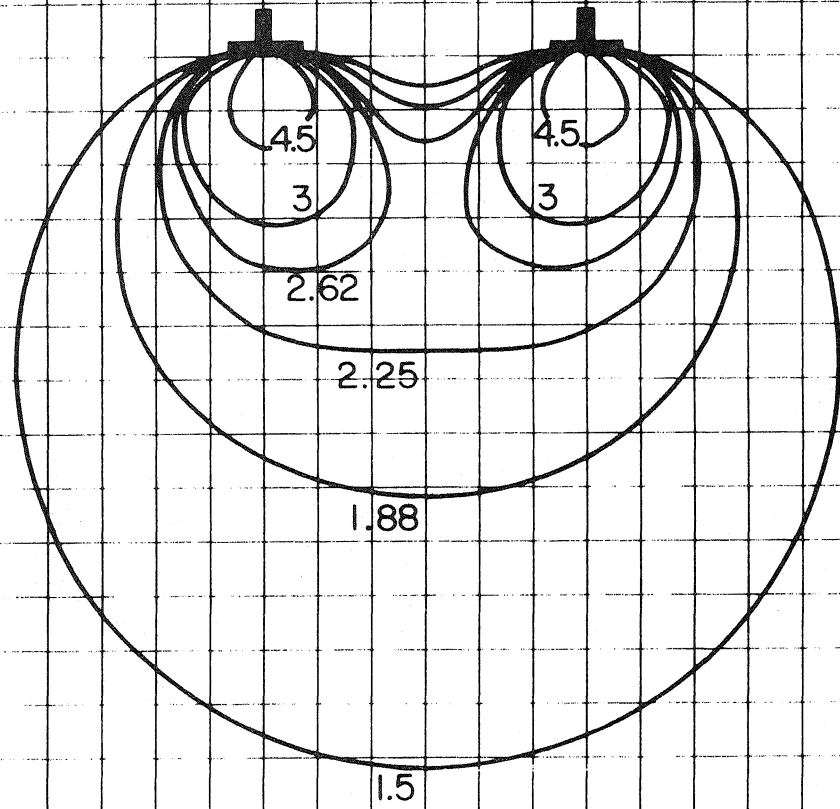
Fig. 11

Fig. 12
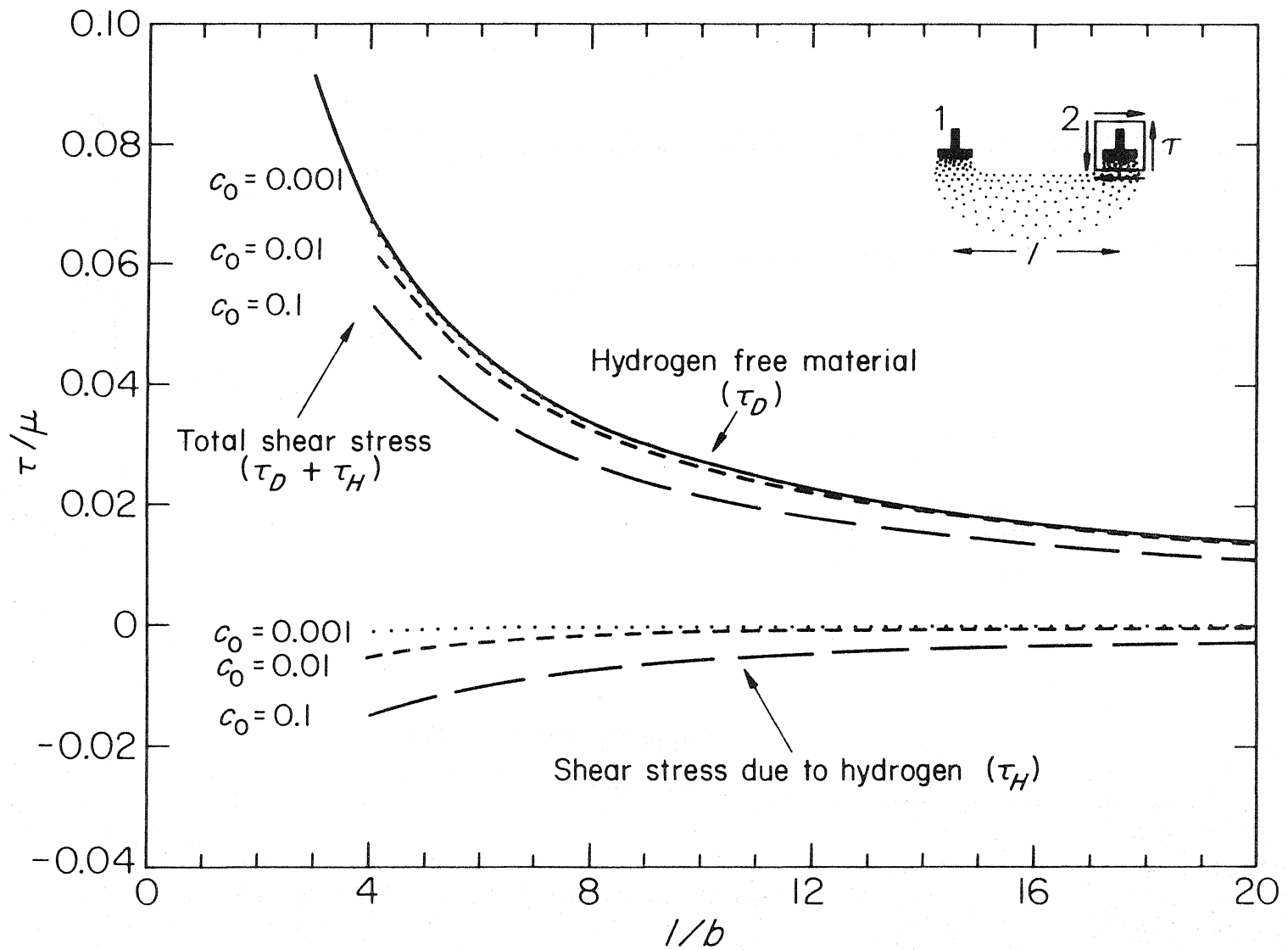
Fig. 13
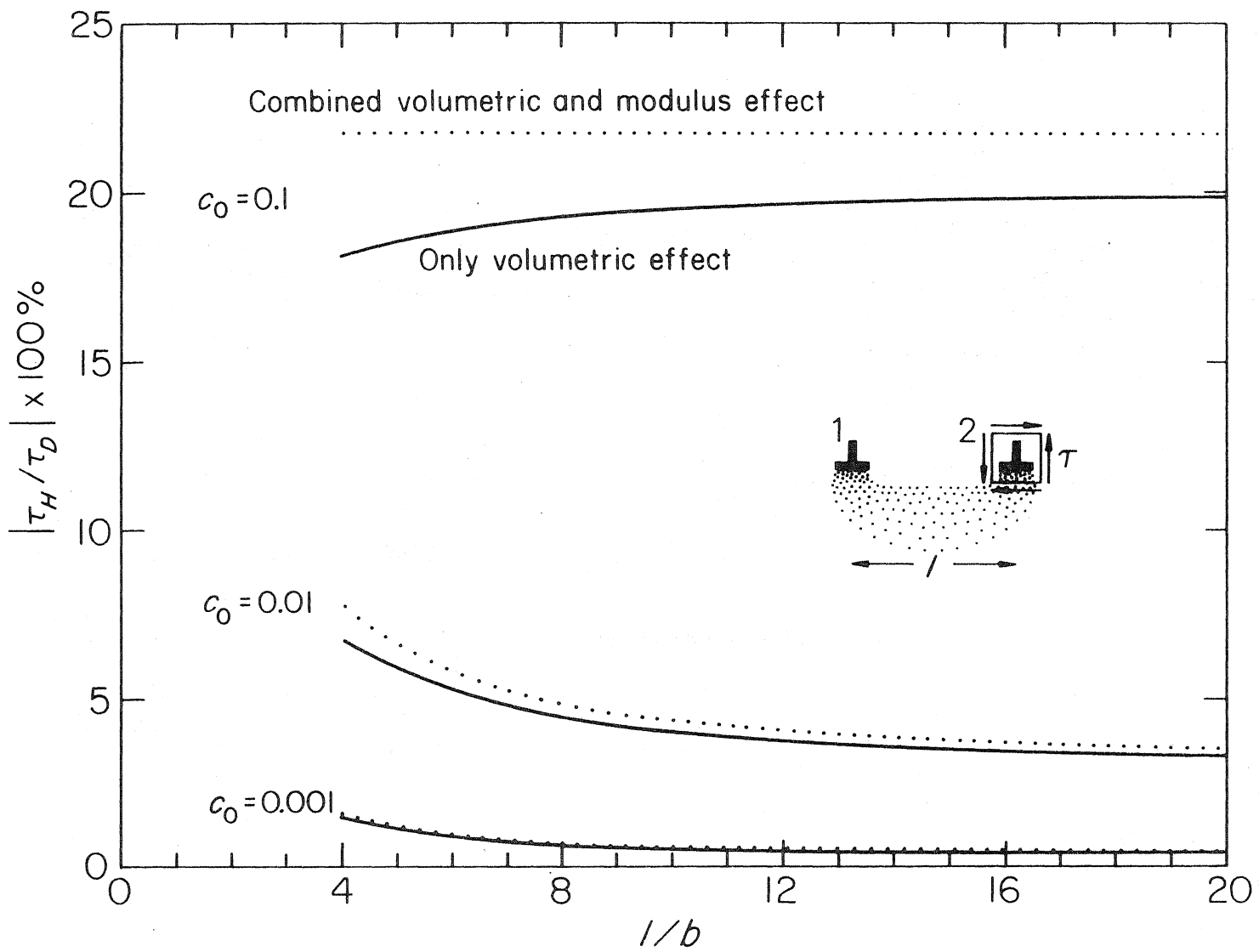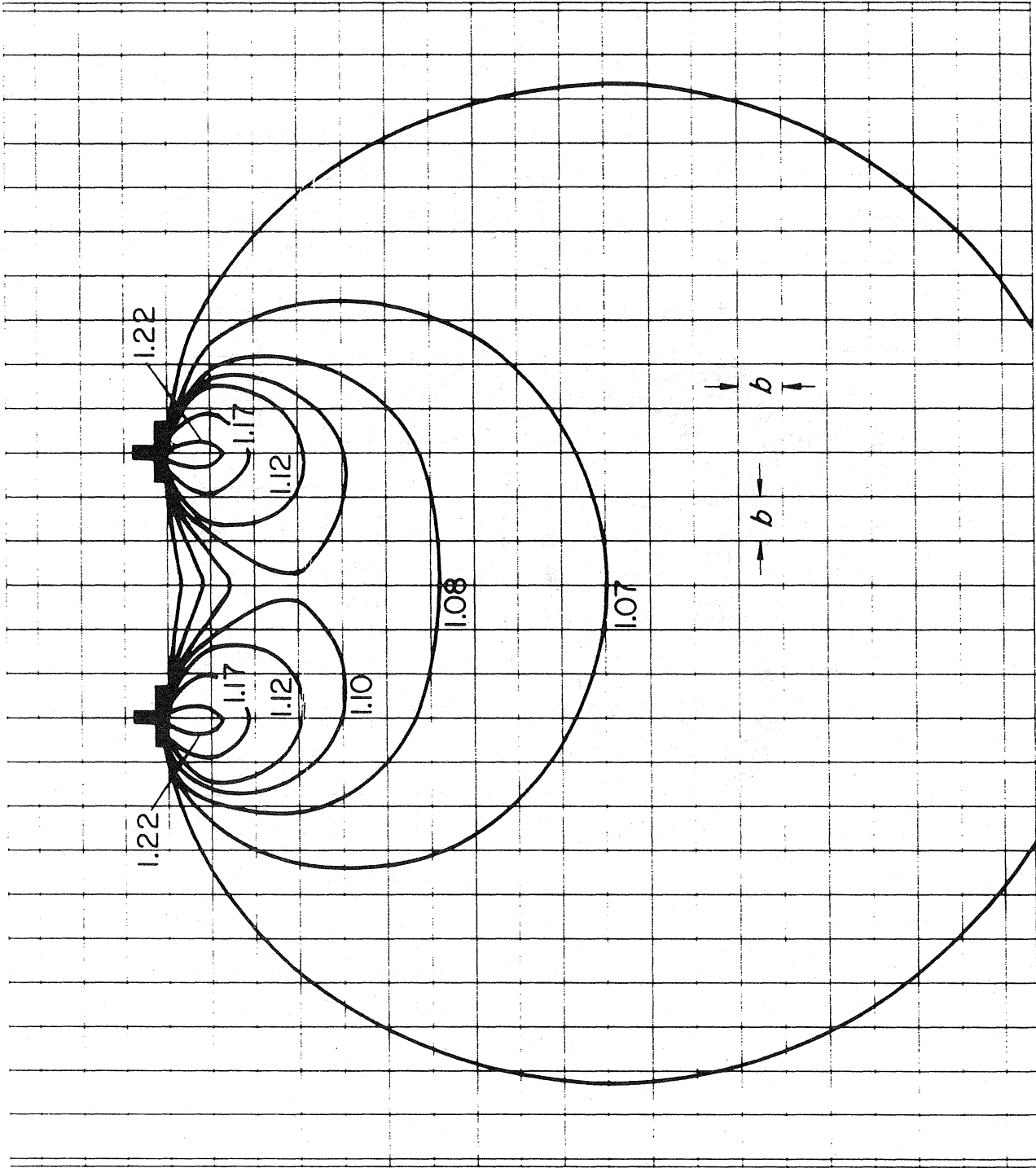
Fig. 14
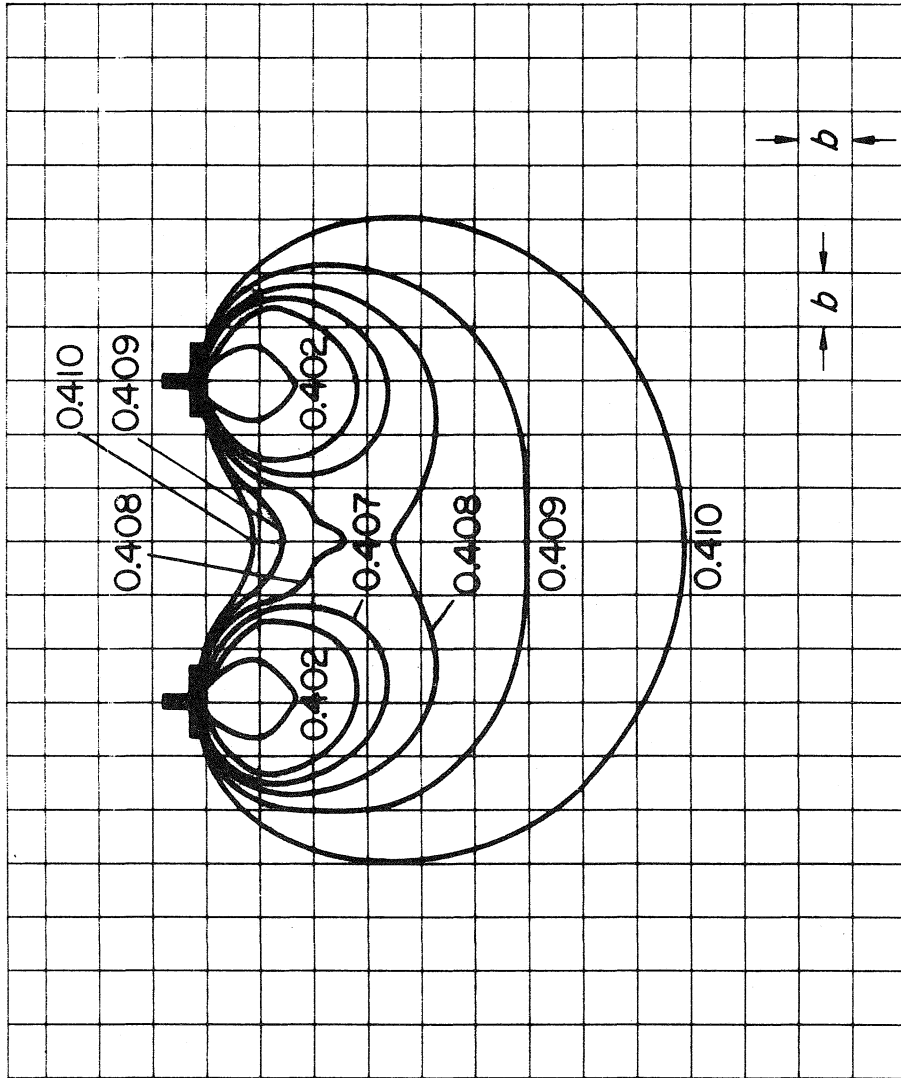
Fig. 15

Fig. 16
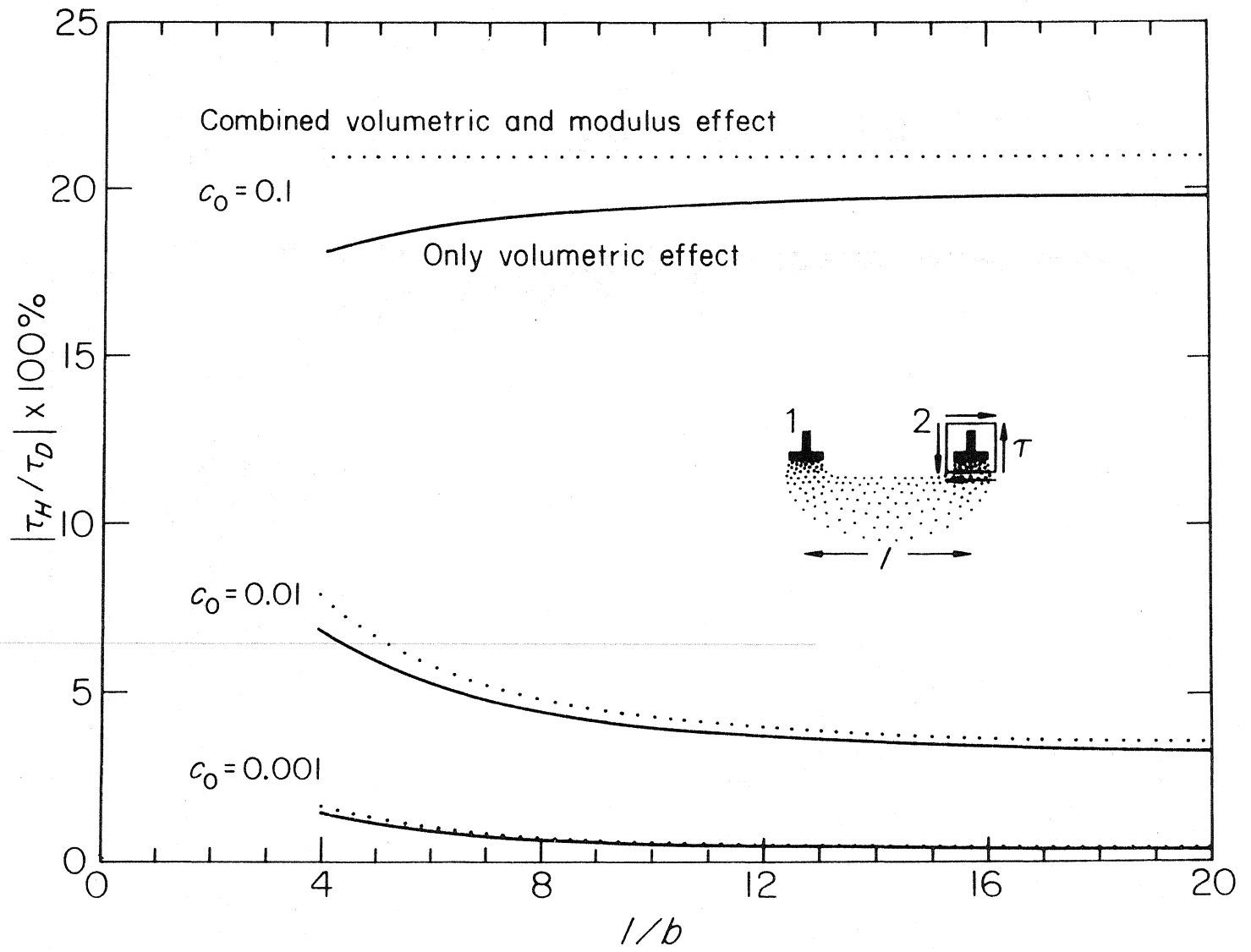
Fig. 17
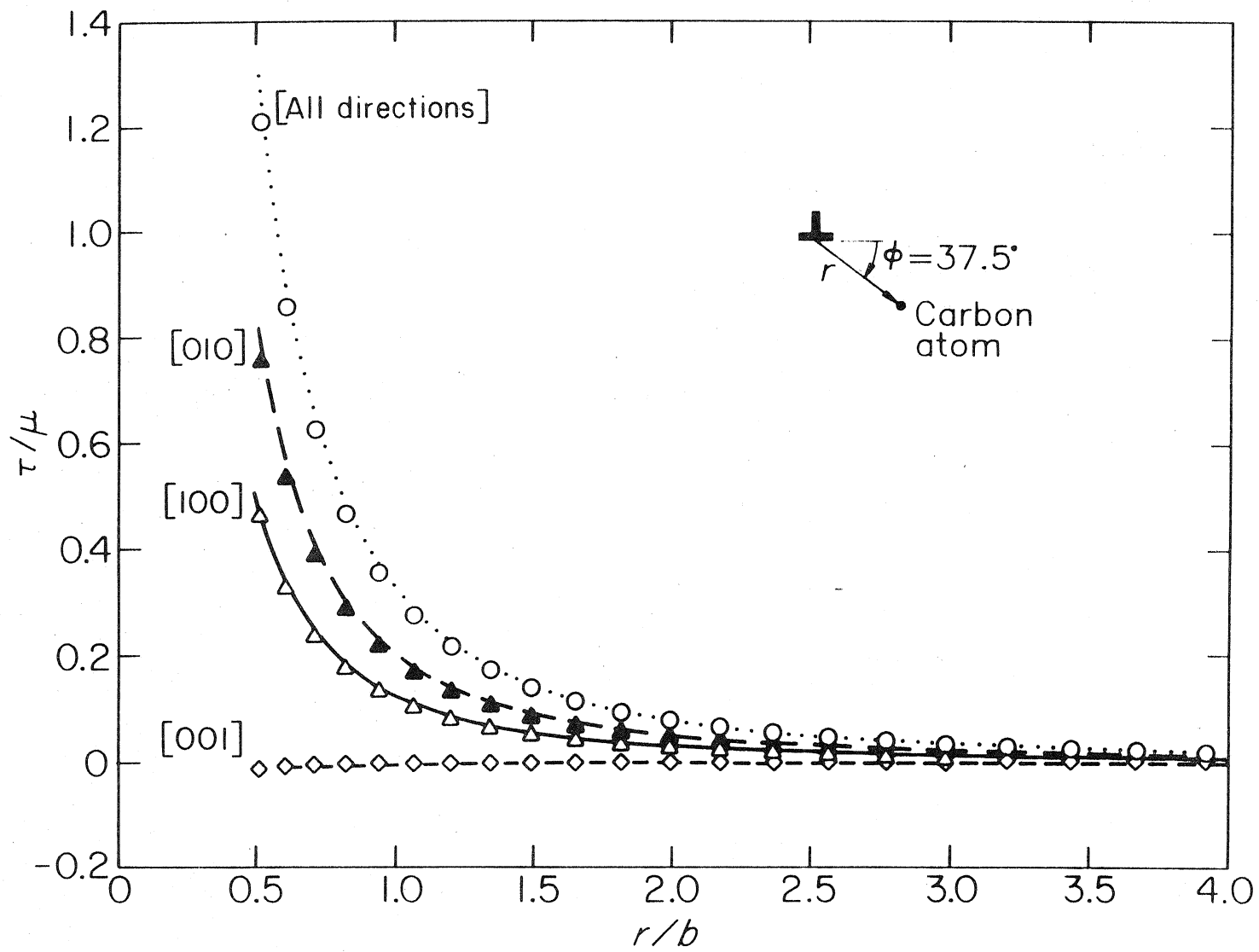
Fig. 18

Fig. 19

Fig. 20

Fig. 21

Fig. 22

Fig. 23

Fig. 24

Fig. 25

Fig. 26

Fig. 27

Fig. 28

Fig. 29

Fig. 30

Legend:
— Analytical result – no hydrogen (W)
--△-- Numerical result – hydrogen effect (W_H)

Y-axis: Interaction energy (eV)
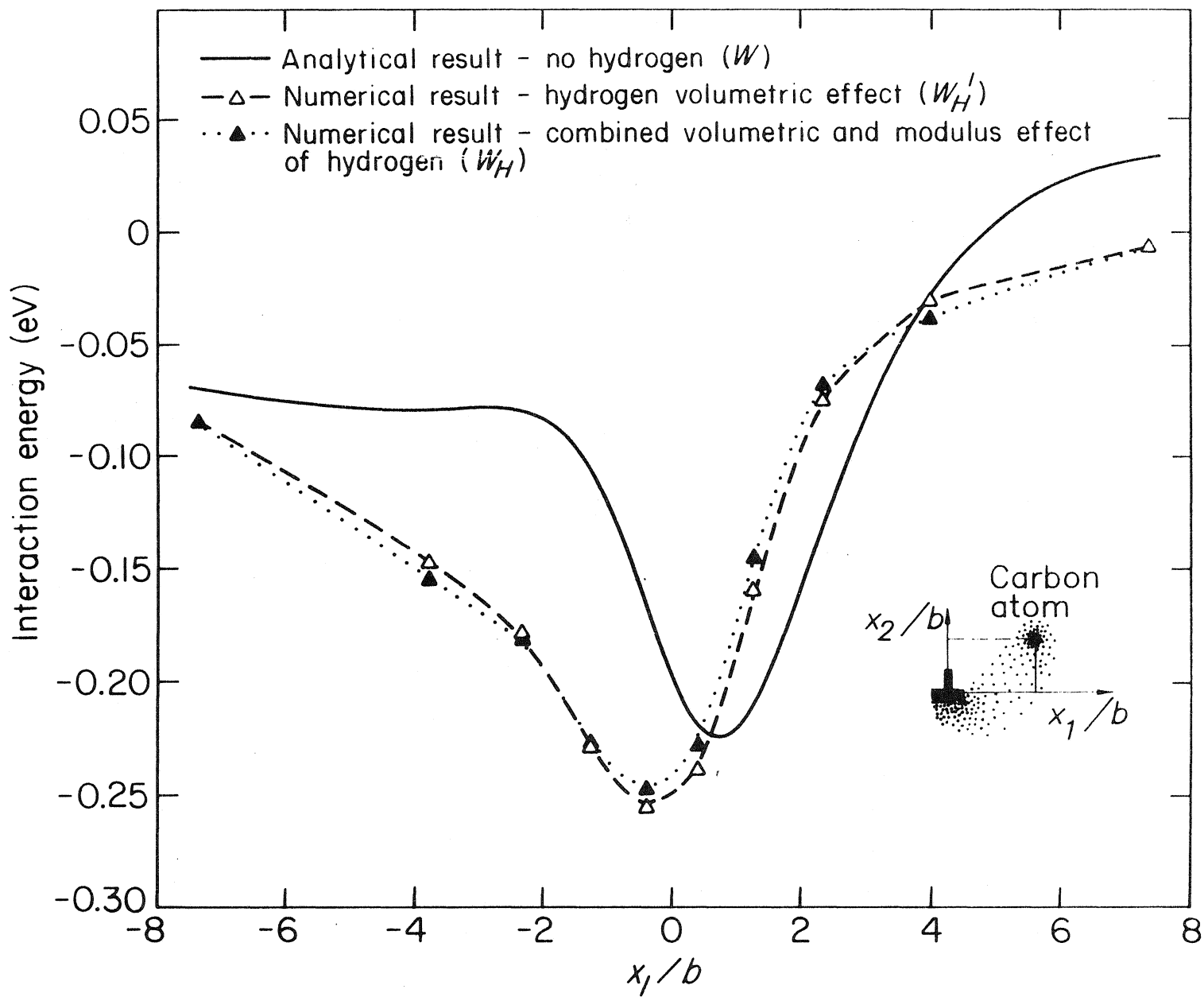X-axis: x_1/b

Inset labels: Carbon atom, x_2/b, S, x_1/b
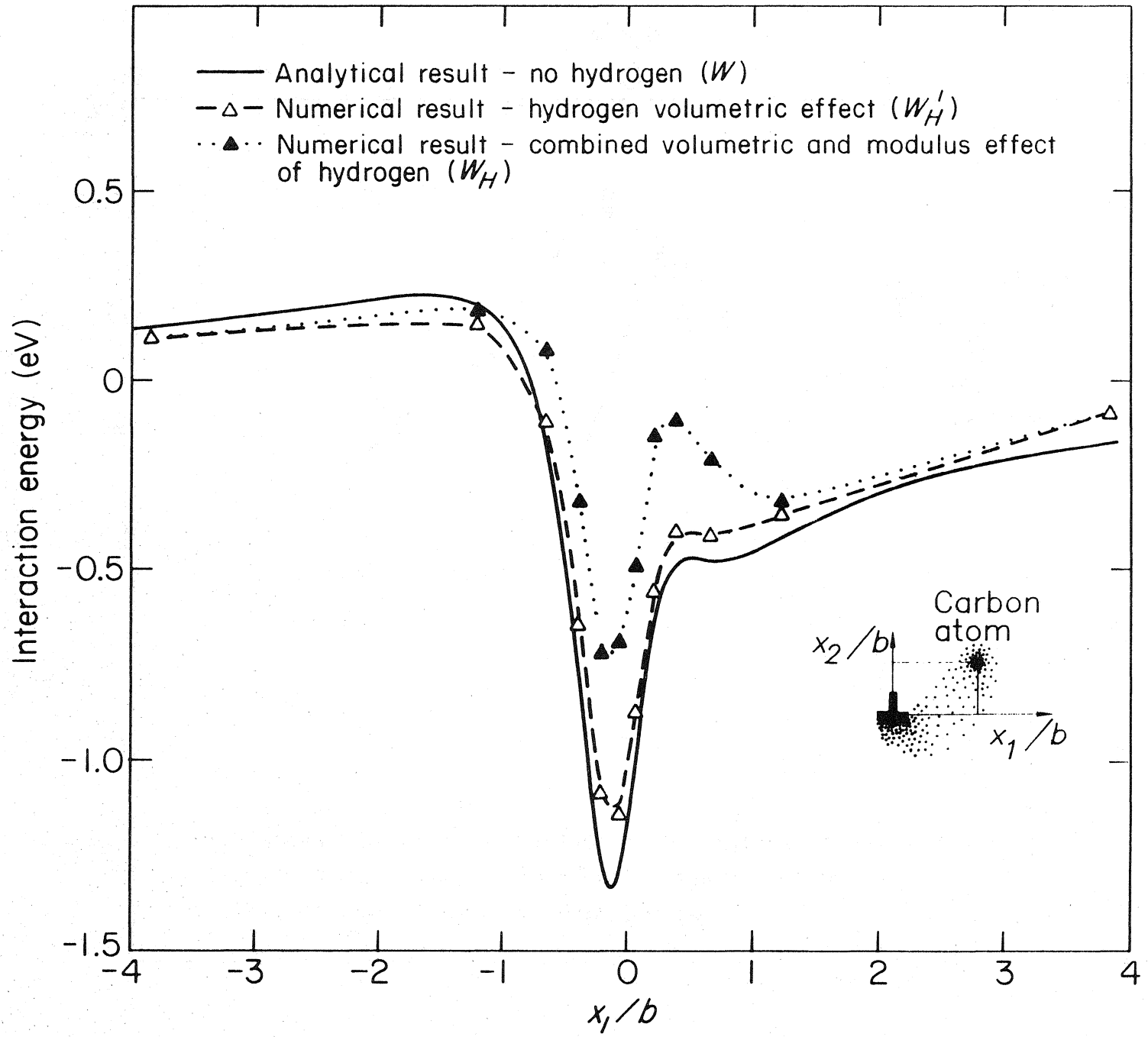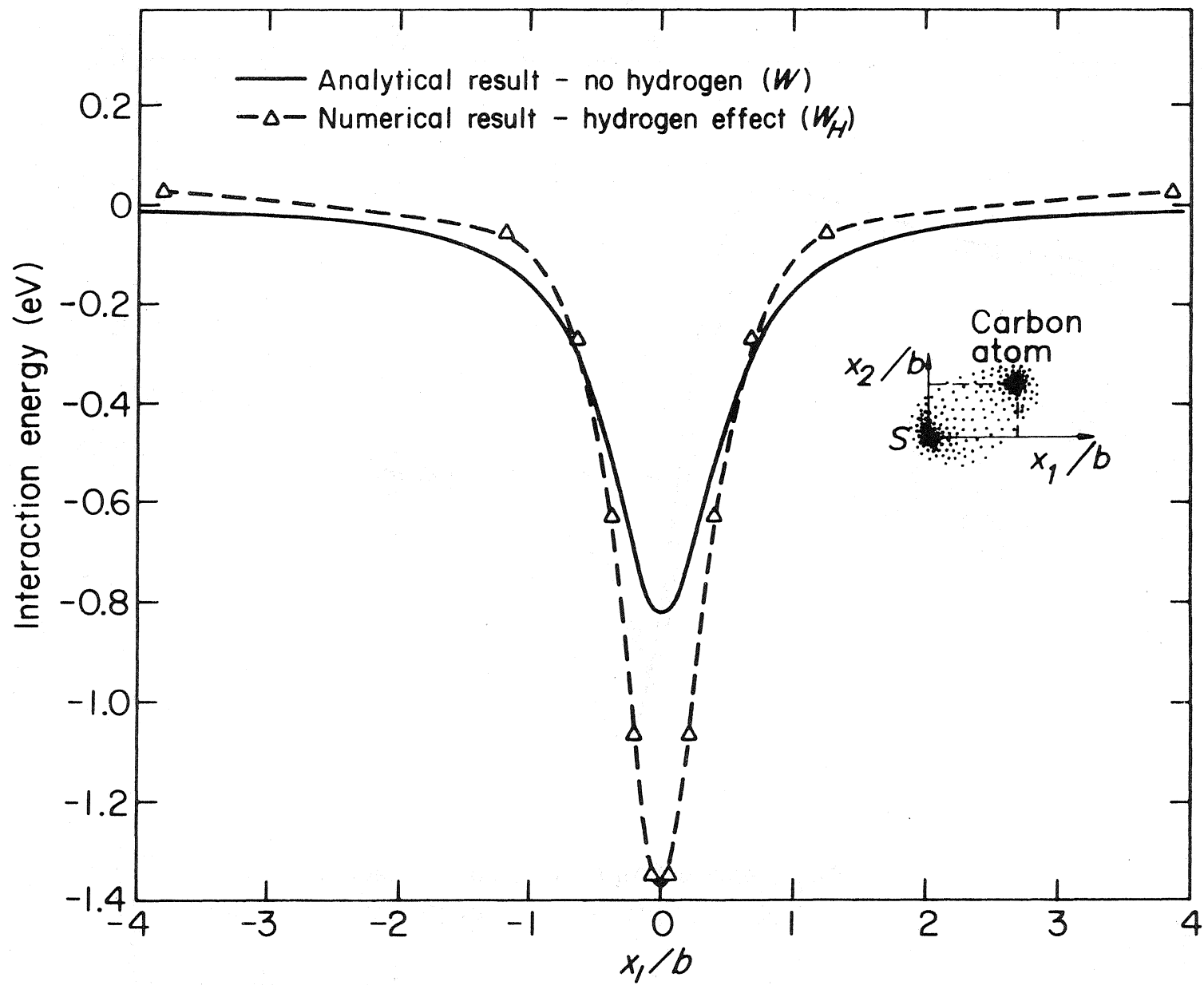
Fig. 31
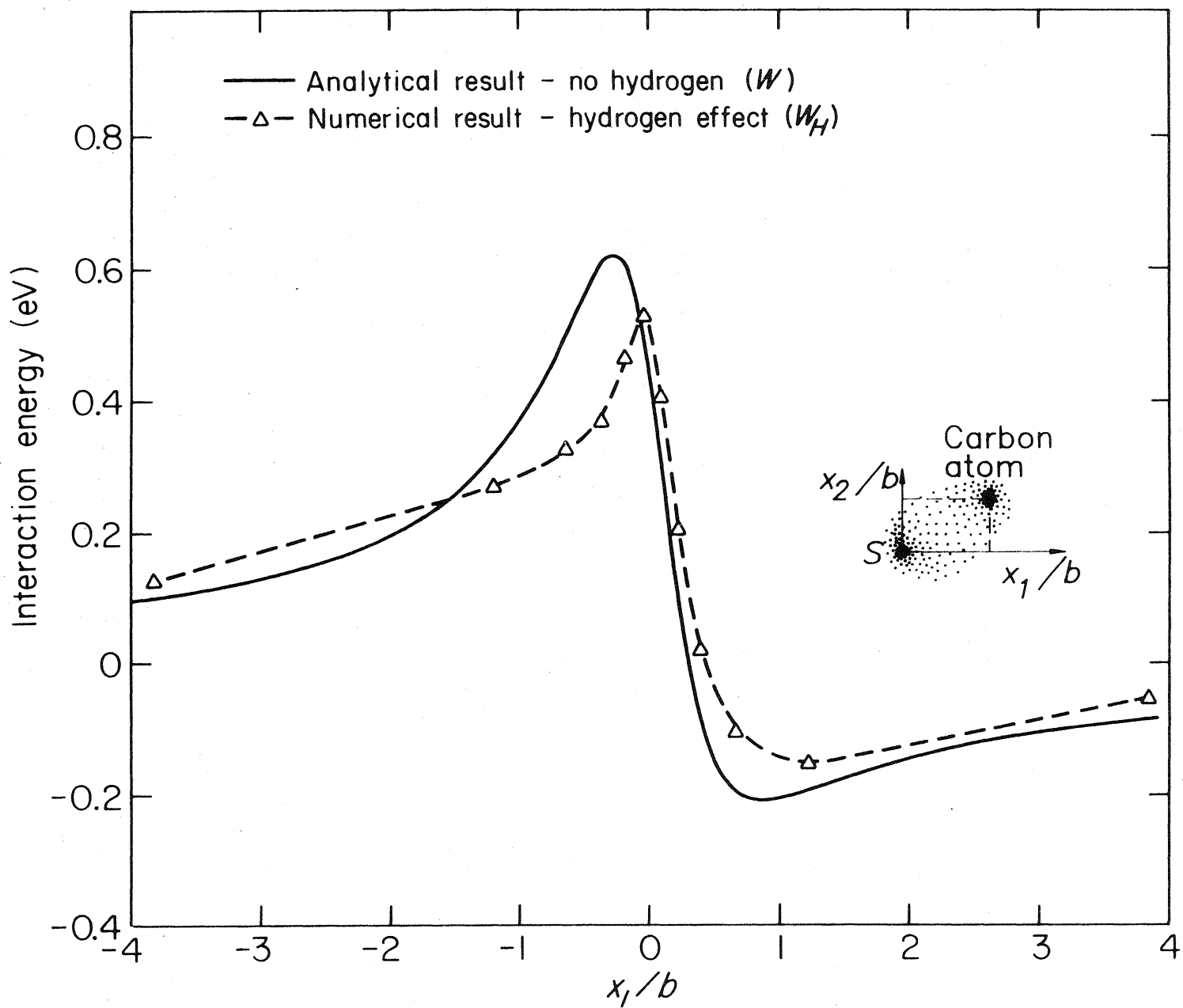
Fig. 32
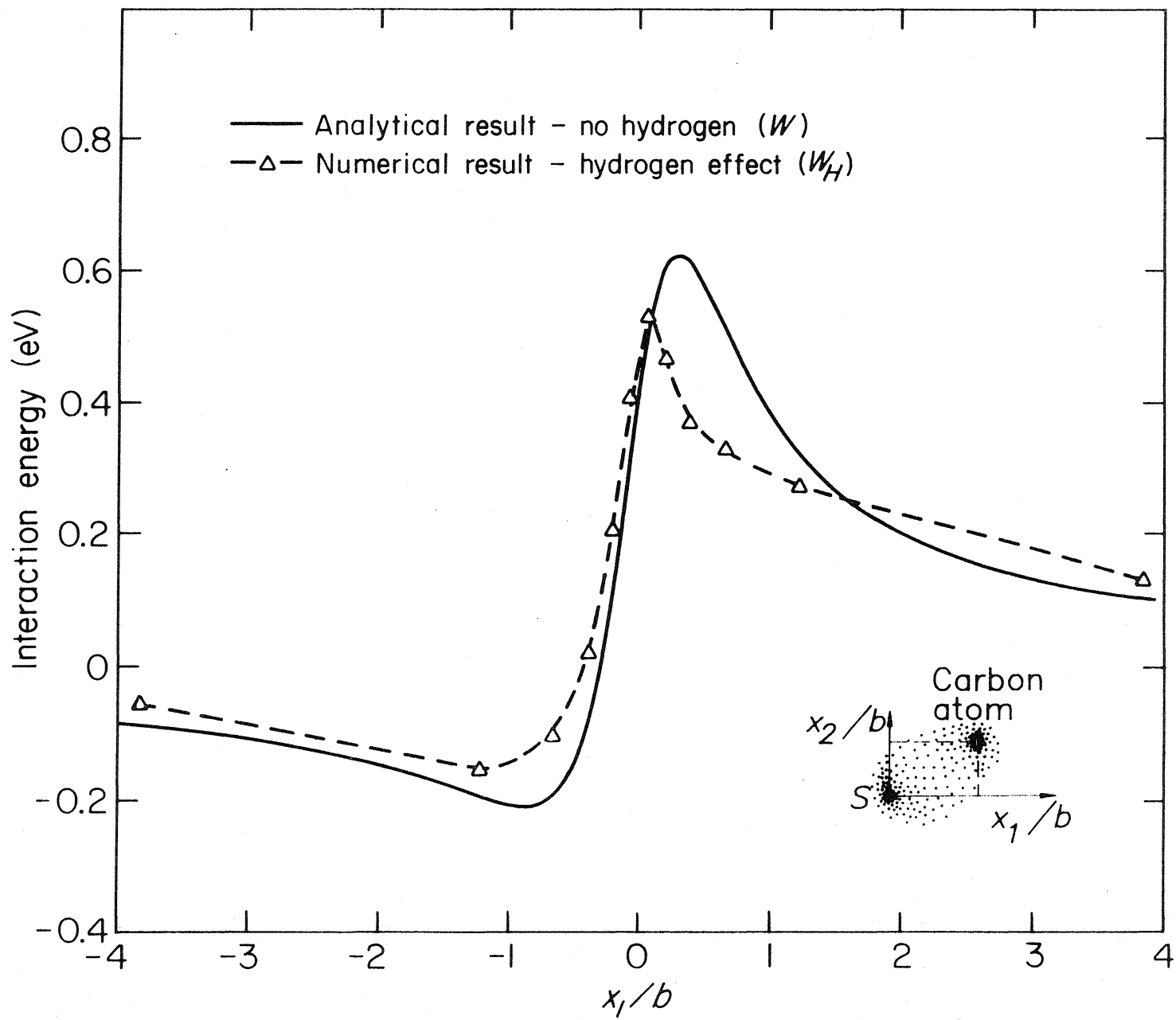
List of Recent TAM Reports

No.	Authors	Title	Date
702	Greening, L. E., P. J. Joyce, S. G. Martensen, M. D. Morley, J. M. Ockers, M. D. Taylor, and P. J. Walsh	Twenty-ninth student symposium on engineering mechanics, J. W. Phillips, coord. (1992)	May 1992
703	Kuah, H. T., and D. N. Riahi	Instabilities and transition to chaos in plane wakes	Nov. 1992
704	Stewart, D. S., K. Prasad, and B. W. Asay	Simplified modeling of transition to detonation in porous energetic materials	Nov. 1992
705	Stewart, D. S., and J. B. Bdzil	Asymptotics and multi-scale simulation in a numerical combustion laboratory	Jan. 1993
706	Hsia, K. J., Y.-B. Xin, and L. Lin	Numerical simulation of semi-crystalline Nylon 6: Elastic constants of crystalline and amorphous parts	Jan. 1993
707	Hsia, K. J., and J. Q. Huang	Curvature effects on compressive failure strength of long fiber composite laminates	Jan. 1993
708	Jog, C. S., R. B. Haber, and M. P. Bendsoe	Topology design with optimized, self-adaptive materials	Mar. 1993
709	Barkey, M. E., D. F. Socie, and K. J. Hsia	A yield surface approach to the estimation of notch strains for proportional and nonproportional cyclic loading	Apr. 1993
710	Feldsien, T. M., A. D. Friend, G. S. Gehner, T. D. McCoy, K. V. Remmert, D. L. Riedl, P. L. Scheiberle, and J. W. Wu	Thirtieth student symposium on engineering mechanics, J. W. Phillips, coord. (1993)	Apr. 1993
711	Weaver, R. L.	Anderson localization in the time domain: Numerical studies of waves in two-dimensional disordered media	Apr. 1993
712	Cherukuri, H. P., and T. G. Shawki	An energy-based localization theory: Part I—Basic framework	Apr. 1993
713	Manring, N. D., and R. E. Johnson	Modeling a variable-displacement pump	June 1993
714	Birnbaum, H. K., and P. Sofronis	Hydrogen-enhanced localized plasticity—A mechanism for hydrogen-related fracture	July 1993
715	Balachandar, S., and M. R. Malik	Inviscid instability of streamwise corner flow	July 1993
716	Sofronis, P.	Linearized hydrogen elasticity	July 1993
717	Nitzsche, V. R., and K. J. Hsia	Modelling of dislocation mobility controlled brittle-to-ductile transition	July 1993
718	Hsia, K. J., and A. S. Argon	Experimental study of the mechanisms of brittle-to-ductile transition of cleavage fracture in silicon single crystals	July 1993
719	Cherukuri, H. P., and T. G. Shawki	An energy-based localization theory: Part II—Effects of the diffusion, inertia and dissipation numbers	Aug. 1993
720	Aref, H., and S. W. Jones	Chaotic motion of a solid through ideal fluid	Aug. 1993
721	Stewart, D. S.	Lectures on detonation physics: Introduction to the theory of detonation shock dynamics	Aug. 1993
722	Lawrence, C. J., and R. Mei	Long-time behavior of the drag on a body in impulsive motion	Sept. 1993
723	Mei, R., J. F. Klausner, and C. J. Lawrence	A note on the history force on a spherical bubble at finite Reynolds number	Sept. 1993
724	Qi, Q., R. E. Johnson, and J. G. Harris	A re-examination of the boundary layer attenuation and acoustic streaming accompanying plane wave propagation in a circular tube	Sept. 1993
725	Turner, J. A., and R. L. Weaver	Radiative transfer of ultrasound	Sept. 1993
726	Yogeswaren, E. K., and J. G. Harris	A model of a confocal ultrasonic inspection system for interfaces	Sept. 1993
727	Yao, J., and D. S. Stewart	On the normal detonation shock velocity–curvature relationship for materials with large activation energy	Sept. 1993
728	Qi, Q.	Attenuated leaky Rayleigh waves	Oct. 1993
729	Sofronis, P., and H. K. Birnbaum	Mechanics of hydrogen–dislocation–impurity interactions: Part I—Increasing shear modulus	Oct. 1993